Investigating the role of the Chromosomal Passenger Complex and putative interactors in *Drosophila* spindle and central spindle formation

Submitted by Sarah Anne Campbell to the University of Exeter

as a thesis for the degree of

Masters by Research in Biosciences

in August 2014

I certify that all material in this thesis which is not my own work has been identified and that no material has previously been submitted and approved for the award of a degree by this or any other University.

(Signature) ……

Acknowledgements

There are many people, who without their endless help and support, completion of this project would not have been possible.

I would first like to thank all the members of the Wakefield lab. To my supervisor Dr. James G. Wakefield for giving me this great opportunity, for his guidance throughout the year, for all that I have learnt from him and for providing doughnuts in the weekly lab meetings!

I would especially like to thank Daniel Hayward, Jack Chen and Pete Jones who took me under their wing and really made me feel part of the team. They gave me so much help and put up with all my questions! Thank you also to all of Lab 211, for the friendships that were made and for making it such a welcoming place where it was enjoyable to come into the lab each day.

Thank you to my sister, my housemates and all my wonderful friends, especially to Holly and Fi for the chats, their understanding and support. For all the times I told my housemates I would be home at a certain time to then get caught up in the lab but to them still being there when I did get back with a mug of tea!

Lastly, but by no means least, I would like to thank my parents and grandparents for their encouragement, the hugs, the endless supply of biscuits during my write-up and for their unwavering faith in all that I do.

Abstract

Mitosis and meiosis, cellular processes leading to the production of diploid and haploid daughter cells respectively, are tightly regulated to ensure faithful chromosome segregation is coupled to cytokinesis. Defects in these processes can lead to many diseases, including the promotion of tumourogenesis and sterility. The Chromosomal Passenger Complex (CPC) orchestrates mitosis and meiosis through regulating the activity of many cellular proteins, including those involved in kinetochore-microtubule interactions and in central spindle formation.

There are four known members of the CPC; the kinase Aurora B, Borealin, Survivin (Deterin) and the inner centromere protein, INCENP. All four subunits show the same localisation throughout the cell cycle; associating with chromatin during interphase and the centromeres during metaphase before transferring to the central spindle mid-zone and equatorial cortex during anaphase. An additional CPC interactor, TD60, has been described in humans. However, the mechanism by which the CPC facilitates cytokinesis and the potential role of TD60 as a CPC component has not been fully explored. The purpose of this research project was twofold: (i) to investigate the role of the CPC in central spindle formation and cytokinesis and (ii) to investigate the function of TD60, in the model organism *Drosophila melanogaster*.

I show that although the CPC is not required for the microtubule (MT) association of two proteins, Pavarotti and Polo - a kinesin-like protein and kinase, respectively - during anaphase, it is required for the accumulation of Pavarotti to the plus ends of these microtubules (MTs). This work therefore sheds light on the relationship between key cytokinetic proteins. Through the

purification and injection of interfering antibodies raised against TD60, I also demonstrate an essential role for this protein in regulating the length of the metaphase mitotic spindle, kinetochore-MT interactions, chromosome segregation and mitotic exit timing, possibly through regulating the localisation of the CPC.

Together, the work in this thesis advances our understanding of these important effectors of cell division, raising further questions as to their cellular roles and relationships to each other.

Table of Contents

List of Figures

List of Tables

List of Supplementary Material

List of Abbreviations

CPC	Chromosomal Passenger Complex
GFP	Green Fluorescent Protein
IP	Immunoprecipitation
kMT	kinetochore Microtubule
LSM	Laser Scanning confocal Microscope
MAP	Microtubule Associated Protein
MBP	Maltose Binding Protein
MT	Microtubule
MTOC	Microtubule Organising Centre
NEB	Nuclear Envelope Breakdown
NER	Nuclear Envelope Reform
PAGE	Polyacrylamide Gel Electrophoresis
PBS	Phosphate Buffered Saline
PCM	Pericentriolar Material
SAC	Spindle Assembly Checkpoint
SAFs	Spindle Assembly Factors
TD60	Telophase Disk 60

1. Introduction

Non-disjunction, a term used to describe failures in chromosome segregation, and unsuccessful cytokinesis of the cell can contribute to the formation of a variety of cancers (Li *et al.,* 2006). Defects in cytokinesis can lead to the production of tetraploid cells observed in the early stages of many cancers including the promotion of tumorigenesis (Fujiwara *et al.,* 2005).

Expanding the knowledge of the mechanisms and the protein pathways involved in cell division will provide a greater understanding into how they participate in the progression of cancer. This information could be used in the advancement of future therapies.

1.1. Cell division and microtubules

There are five main stages of cell division: prophase, prometaphase, metaphase, anaphase and telophase (Fig. 1-1); with interphase (the main growth period) occurring before the cell enters prophase. During somatic cell divisions, DNA replication occurs during interphase, specified as S phase. However, during meiosis, these five cell division stages occur twice, with an intervening interphase devoid of S phase. This leads to the production of four haploid daughter cells.

During cell division two sub-cellular structures - the bipolar spindle and the central spindle - are required for correct chromosome segregation (karyokinesis) and successful cytokinesis of the two daughter cells respectively (Bonaccorsi *et al.,* 1998). The bipolar spindle begins to be generated in prophase and is fully formed by the start of metaphase

chromosome alignment, whereas central spindle formation occurs during anaphase. The bipolar spindle has the ability to organise chromosomes while the central spindle's main role is to organise the cleavage furrow.

Both structures are composed of MTs. MTs are polymers of two related proteins, α and β-Tubulin, which each bind to GTP and form stable heterodimers. These heterodimers polymerise longitudinally to form protofilaments, while protofilaments are able to form lateral interactions with each other, resulting in the formation of hollow cylindrical tubes of 13 or 14 protofilaments (Kerssemakers *et al.,* 2006). MTs have distinct polarity with the α-Tubulin exposed at the slow growing minus ends and β-Tubulin at the fast growing plus ends. This polarity is important in MT polymerisation as GTP bound to the α-Tubulin stabilises as it cannot be hydrolysed and therefore plays a structural role. GTP bound to the β-Tubulin can be broken down to GDP, which results in the phenomenon known as dynamic instability (Mitchison *et al.,* 1984).

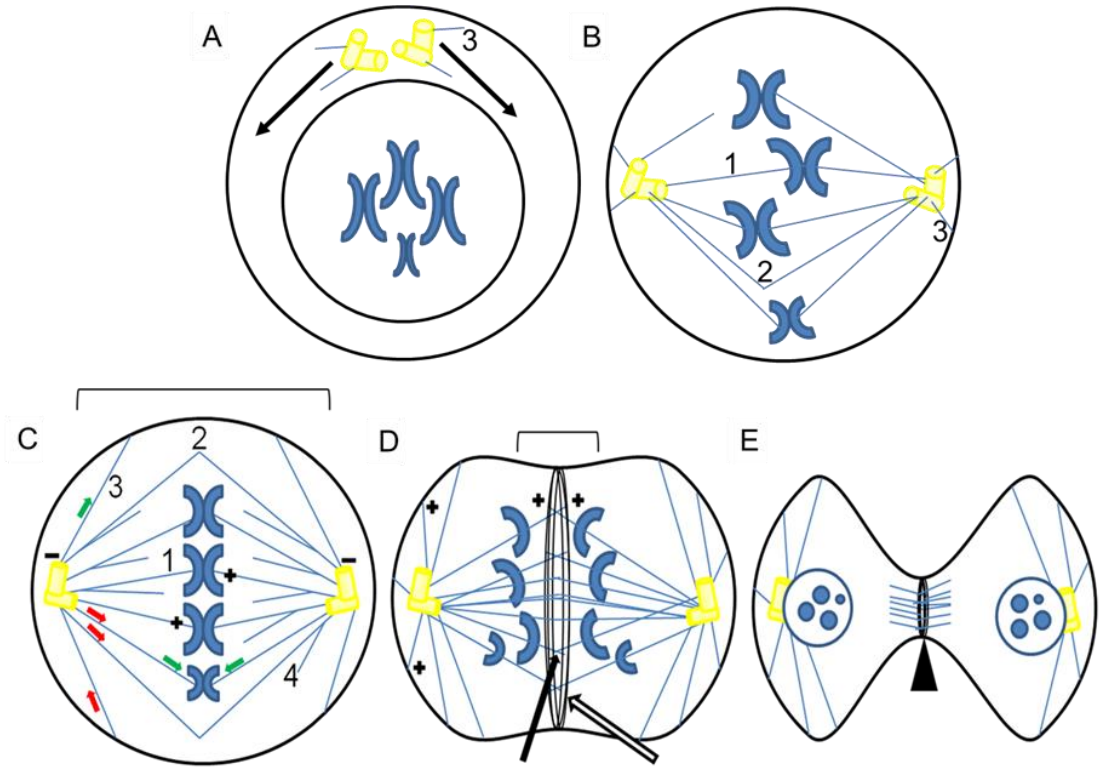

Figure 1-1. Populations of MTs in various stages of cell division (A) Cell in prophase; centrosomes have duplicated and are in the process of moving to opposite poles (indicated by arrows). The nuclear envelope is still intact and chromatin is condensing into chromosomes. **(B)** Cell in prometaphase; the centrosomes have reached the opposite poles and the nuclear envelope has broken down to allow the kinetochore MTs (1) to attach to the kinetochores **(C)** Cell in metaphase; bracelet indicates the bipolar spindles. The chromosomes are aligned to the centre of the cell. There are at least four main subpopulations of MTs: kinetochore MTs (1), interpolar MTs (2), astral MTs (3) and Augmin-generated MTs (4). Dynamic instability occurs within the spindle; the MTs are able to grow (green arrows) and shrink (red arrows). **(D)** Cell in anaphase; the chromosomes move to the poles, bracelet refers the developing spindle midzone. Block arrow points to the central spindle; open arrow to the contractile ring. **(E)** Cell in telophase; triangle indicates to the formation of the midbody, a dense structure of central spindles created when the contractile ring forms a furrow. Figures adapted from Wittmann *et al.* (2001) and Glotzer (2009).

1.1.1. Dynamic instability

This is a term used to describe the growing and shrinking behaviour that takes place at the ends of MTs. The rate of Tubulin addition relative to the rate of GTP hydrolysis determines whether a MT will grow or shrink. If the rate of GTP hydrolysis is less than the amount of GTP-β-Tubulin added, then the MT will continue to polymerise. If the opposite occurs and the rate of GTP hydrolysis is faster than the addition of GTP-β-Tubulin then MT depolymerisation will occur. The transitions between growth and shrinkage are termed “rescue” - when transiting from shrinkage to growth, and “catastrophe” - when transiting from growth to shrinkage. This continual turnover of MT is needed in the cell to allow for reorganisation of the MT cytoskeleton as its role during the various stages of cell division changes.

1.1.2. MT nucleation

New MTs are continually nucleated during cell division. A third Tubulin subunit; γ-Tubulin promotes MT nucleation and is regarded as the primary pathway for nucleating MTs (Job *et al.,* 2003). γ-Tubulin combines with several other proteins to form the γ-Tubulin Ring Complex (γ-TuRC), which provides a template upon which the Tubulin heterodimers can to begin polymerise. The γ-TuRC also acts as the cap of the minus end, providing directional growth at the MT plus end.

1.2. MT generation and formation of the bipolar spindle

The centrosome, the main MT organising centre (MTOC) in animal cells, consists of two MT-based structures termed centrioles, surrounded by

pericentriolar material (PCM). The PCM contains many proteins which lead to the accumulation of γ-TuRC, and has historically been considered to be the main organiser for regulated MT nucleation during spindle formation. However, through mutating the genes involved in centriole formation, it has been shown that the centrosomes are not essential for spindle assembly (Fig. 1-2a), and that other pathways of MT generation exist (see below).

Critical to the success of the pathways mentioned above are a class of proteins termed MT associated proteins (MAPs). These bind to MTs to alter their dynamic properties. There are also many other proteins necessary for bipolar spindle formation, as evidenced by genome-wide RNAi screens (e.g. Goshima *et al.,* 2007).

The centrosome-nucleated pathway requires MAPs such as γ-Tubulin (MandelKow *et al.,* 1995) and Centrosomin (Cnn) with another core centriolar protein Spd-2 required for the recruitment of these two proteins to the centrioles (Giansanti *et al.,* 2008). Chromatin-directed MT generation (Fig. 1-2b) requires the small GTPase Ran, which is dependent upon the generation of a Ran guanosine triphosphate (RanGTP) gradient. This requires the action of the Ran guanine nucleotide exchange factor (RanGEF) RCC1 to convert RanGDP to RanGTP in the area of chromatin. When Ran is in its GTP state, it is able to release spindle assembly factors (SAFs) such as the MAPs TPX2 and HURP/Mars from importins (nuclear transport proteins that import other proteins into the nucleus) thereby activating these SAFs (Gruss *et al.,* 2001). Through recent studies, TPX2 and HURP have been found to be

responsible for spindle growth and correct chromosome segregation (e.g. Hayward *et al.,* 2014). Kinetochores are able to initiate MT polymerisation in what is thought to be similar to that seen in chromatin-directed MT generation through the RanGTP gradient; depleting TPX2 blocked kinetochores-associated MTs from forming (Tulu *et al.*, 2006).

MT-dependent MT generation during spindle formation uses the hetero-octomeric protein complex, Augmin (Goshima *et al.,* 2007; Hughes *et al.*, 2008; Goshima *et al.*, 2008) (Fig. 1-2c). This 8 subunit complex has been proposed increases overall MT density by targeting γ-TuRC to pre-existing spindle MTs (Goshima *et al.,* 2008; Uehara *et al.,* 2009).

These pathways give rise to at least four sub-populations of MTs in the bipolar spindle (Fig. 1-1). The Augmin generated MTs increase spindle density, while the kinetochore MTs are responsible for attaching the kinetochores of the sister chromatids to the spindle poles. There are also interpolar MTs, anti-parallel bundles of MTs crossing the spindle equator, which stabilise the force generation between opposing halves of the spindle; and the astral MTs which are able to interact with the cell cortex, helping in the positioning, stability and growth of the spindle (Wittmann *et al.,* 2001) (Fig. 1-2d).

It is clear that MT generation is a complex process that requires multiple pathways that can either work independently or in cohort to ensure a robust bipolar spindle is assembled (Fig. 1-2e).

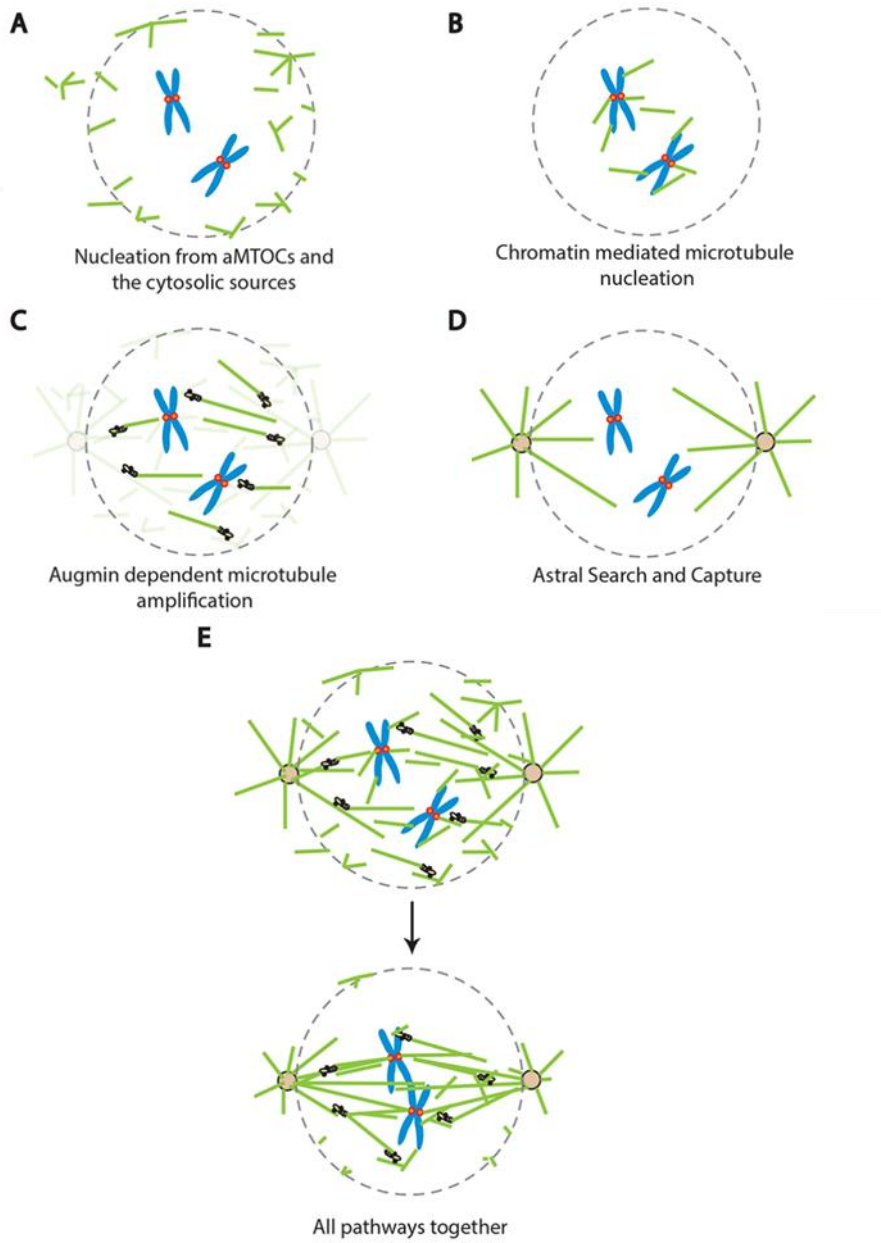

Figure 1-2. Schematic showing the multiple pathways of microtubule generation **A** MTs are nucleated within the cytosol without the need for centrosomes. **B** Chromatin-directed MT generation which requires the small GTPase Ran and is dependent upon the generation of a RanGTP gradient. **C** Microtubules are generated through the help of the Augmin complex. **D** Astral MT search-and-capture MTs increasing the growth and stability of MTs within the cell. **E** MT generation from all the pathways together. Reproduced with permission (Hayward 2014).

1.3. The central spindle

The central spindle, like the bipolar spindle, is composed of MTs, but is found between the two complements of segregating chromosomes in anaphase and telophase. Also termed the spindle midzone, it has been shown in many systems to be required for cytokinesis (Fig. 1-1d,e) (Gatti *et al.,* 2000; Glotzer 2009). The central spindle starts forming in anaphase after the start of chromosome segregation, which occurs due to the shortening of the kinetochores MTs. Several proteins have been shown to be involved in central spindle assembly, re-localising from other cellular locations to instigate the bundling of anti-parallel plus ends of MTs (Glotzer 2009). The acto-myosin contractile ring, a structure containing Actin and Myosin II filaments which forms round the cell cortex at late anaphase/telophase provides the force needed for membrane invagination during cytokinesis. There is evidence that points to cooperative interactions between the central spindle and the contractile ring; in mutants of genes important in the formation of either the central spindle or the contractile ring it led to disruption in the assembly of both structures (Giansanti *et al.,* 1998). This was seen for example in *Drosophila* embryonic cells of *pavarotti* mutants (Adams *et al.,* 1998) and in *Drosophila* spermatocyte *polo* mutants (Carmena *et al.,* 1998). It has also been shown that the central spindle can control the position of the contractile ring, providing a spatial cue its stable assembly (Glotzer 2009).

1.3.1. Central spindle formation

In contrast to spindle formation, there is a much less known about the pathways and proteins that are responsible for contributing to the formation of the central spindle.

There is some evidence that points to the central spindle emerging from reorganisation of the interpolar MTs generated during bipolar spindle formation. However, it has also been found that in the absence of a bipolar spindle, the central spindle is still able to assemble (Glotzer 2009). Augmin has been reported to be involved in central spindle formation as depletion of this protein complex results in, not only problems with bipolar spindle formation, but also defects in central spindle formation (Uehara *et al.,* 2009; Wakefield lab). Augmin could be acting indirectly; it could be that through mutating Augmin this mutation then prevents γ-TuRC from carrying out its role in central spindle assembly.

1.3.2. Differences in MT stability

The dynamics of the MTs constituting the bipolar spindle and the central spindle differ. Fluorescence Recovery After Photobleaching (FRAP) experiments have demonstrated a much faster turnover of MTs within bipolar spindles in metaphase compared to that of central spindles in anaphase; the average half life of MTs of the mammalian bipolar spindle is between 10 and 20 seconds (Salmon *et al.,* 1984; Saxton *et al.,* 1984) and over 2 minutes for MTs of the central spindle (Saxton *et al.,* 1987). The stability of the central spindle probably contributes to its function in specifying the cleavage plane, though analysis of MT dynamics in this

structure, through monitoring EB1-GFP comets, suggests at least a proportion of central spindle MTs continually grow and shrink (Wakefield lab, unpublished).

1.3.3. Central spindle formation in *Drosophila* male meiosis

In general, the molecular components required for cell division are conserved. Since the *Drosophila* genome was sequenced (Adams *et al.,* 2000), 178 out of 287 human disease genes have been found to have homologues in *Drosophila* (Fortini *et al.,* 2000). Results from *Drosophila* studies are therefore largely transferable to humans making it an excellent model organism.

There are three main features found in *Drosophila* male meiosis that make it a particularly advantageous system for investigating central spindle formation; these are outlined below.

One advantage is the large size of the central spindles. The size and robustness of the spindles make analysis of its formation easier and if potential defects in central spindle development are being examined, it allows for more information of the nature of the defect to be obtained (Giansanti *et al.,* 2001). Due to the unique structure found at the end of meiosis in insect spermatids, studying male meiosis in *Drosophila* presents a clear way for identifying mutations in chromosome segregation and cytokinesis (Giansanti *et al.,* 2001). *Drosophila* spermatogenesis starts with the primary gonial cells undergoing four rounds of mitosis to produce a cyst of 16 primary spermatocytes. Following this, the spermatocytes undergo two rounds of meiosis which gives rise to a 64 haploid spermatid cyst. At the end of each meiotic

division, mitochondria line up in the centre of the cell after chromosome segregation. They are equally separated between the two daughter cells before individual mitochondria fuse, to form a structure called the Nebenkern (Giansanti *et al.,* 2001). Therefore, at the end of meiosis, or as it is known insects; the “onion stage” (so called due to the onion appearance of a cross section when viewed under a transmission electron microscope), each spermatid contains one phase light nucleus associated with one phase dark Nebenkern of equal size and shape (Giansanti *et al.,* 2001, Giansanti *et al.,* 2004) (Fig. 1-3). However, if problems in chromosome segregation occur during meiosis, different sized nuclei are seen at the onion stage. If there are failures in cytokinesis of meiosis I and II, the mitochondria are not separated a single large Nebenkern is present in a single cell, surrounded by four nuclei of equal size. If problems occur in both chromosome segregation and cytokinesis, the post-meiotic cysts show a mixed phenotype with nuclei of different sizes surrounded by a large Nebenkern (Giansanti *et al.,* 2001).

The third main advantage is the absence of a strong spindle assembly checkpoint. Male *Drosophila* meiotic cells possess only a weak spindle assembly checkpoint, allowing the cell to progress to the later stages of cell division, even if spindle formation is compromised. This enables one to determine whether a gene product which is important in bipolar spindle formation is also of importance in the latter stages of cell division, such as in the formation of the central spindle (Giansanti *et al.,* 2001).

Figure 1-3. Schematic of Nebenkern formation in a wildtype spermatid. To the far left it shows mitochondrial aggregation with the nucleus above. The next diagram along shows the onion stage spermatid with one phase light nucleus to one phase dark Nebenkern of the same size and shape. The last two on the right represent early elongation and mid-elongation of the spermatid respectively. Diagram from Hales and Fuller 1997.

1.4. Chromosomal Passenger Complex (CPC)

The CPC, composed of the proteins Aurora B (Terada *et al.,* 1998), Borealin (Gassmann *et al.,* 2004), Survivin (Deterin) and Inner Centromere Protein (INCENP) (Adams *et al.,* 2000), has essential roles in regulating kinetochore-MT attachments, control of the spindle assembly checkpoint and in central spindle formation and cytokinesis (Adams *et al.,* 2000; Kallio *et al.,* 2002; Gassmann *et al.,* 2004). There is also evidence to suggest it has a role in chromatin-induced MT stabilization in *Xenopus* egg extracts, through controlling the activity of the MT depolymerising kinesin MCAK by phosphorylating it to reduce its activity (Sampath *et al.,* 2004).

All four subunits of the CPC show the same localisation throughout the cell cycle; associating with chromatin during interphase, the centromeres during metaphase before transferring to the central spindle mid-zone and equatorial cortex during anaphase (Vagnarelli *et al.,* 2004). As well as localising to the same parts during cell division, if one component of the CPC is perturbed then it inhibits the functioning and localisation of the other three subunits (Gao *et al.,* 2008).

Telophase Disk 60 or TD60 is a protein that potentially has a role as a chromosomal passenger protein with the initial reported distribution of TD60 corresponding to that of the CPC (Andreassen *et al.,* 1991) (see page 34).

1.4.1. CPC in MT-kinetochore attachment and the SAC

The spindle assembly checkpoint (SAC) ensures correct MT attachment to the kinetochores for equal chromosome segregation. The CPC, specifically Aurora B, has a role in the SAC in preventing syntely - where either the MTs from the same pole attach to both kinetochores, or merotely - where MTs from opposing poles attach to the same kinetochore (Fig. 1-4). The CPC functions by destabilising the MT attachments to the kinetochores to ensure the chromosomes are correctly bi-orientated. Aurora B phosphorylates the protein HEC1 (Highly Expressed in Cancer 1 or also known as Ndc80), which is found at the kinetochores as part of the KMN complex; a complex essential for MT binding by the kinetochores (Cheeseman *et al.,* 2006). Studies suggest that, by Aurora B phosphorylating HEC1/Ndc80, it allows for the kinetochores to release the MT if it is incorrectly attached (Cheeseman *et al.,* 2006).

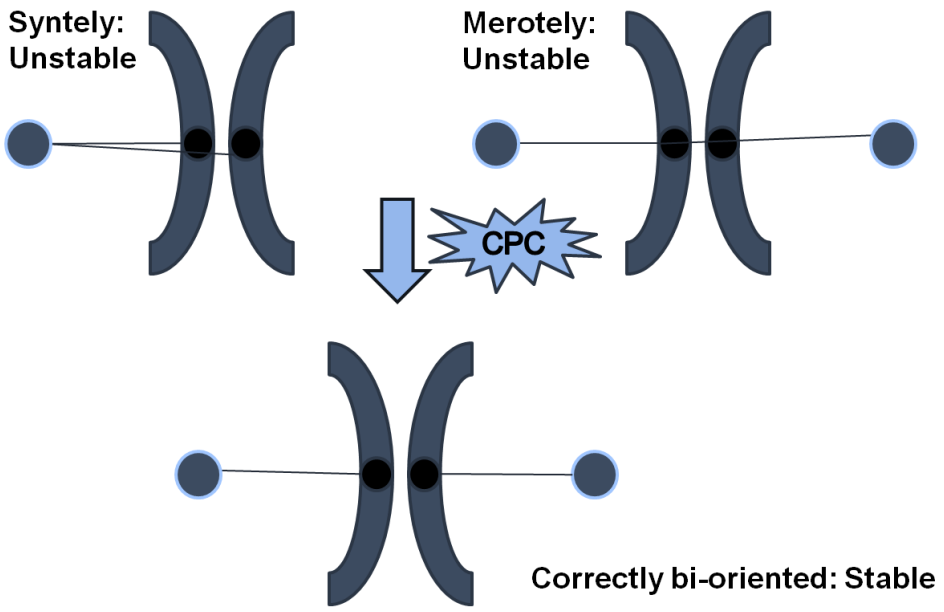

Figure 1-4. Correct MT-kinetochore attachments are required by the CPC to prevent chromosome mis-segregation. Top left diagram shows a syntelic attachment where MTs from the same pole attach to both kinetochores. Top right demonstrates a merotelic attachment where MT from different poles attach to the same kinetochore. Bottom diagram shows, that from the help of the CPC it can create a correctly bi-oriented chromosome with MTs attaching to kinetochores from opposing poles. Diagram adapted from Ruchaud *et al.* (2007).

1.4.2. CPC in central spindle formation & cytokinesis

Most research into the CPC has concentrated on its role in monitoring the former two roles as mentioned in Section 1.4.1. In contrast, the mechanism by which it facilitates cytokinesis is not fully understood. Recognizing that defects in cytokinesis can lead to various cancers it is important to extend the knowledge of the CPC at this end stage of cell division.

It is known that, for correct central spindle formation, the CPC has to migrate to the midzone MTs early in anaphase. Translocation and subsequent localisation of the CPC to these MTs, seen in HeLa cells, is dependent on the kinesin MKLP2/Subito which interacts with both Aurora B and INCENP and vice versa (Gruneberg *et al.,* 2004). Other proteins important in central spindle formation are the centralspindlin complex, which consists of MKLP1/Pavarotti (Pav) and the RhoGEF ECT2, with Aurora B responsible for phosphorylation of these proteins (Douglas *et al.,* 2010) (Fig. 1-5a).

The function of the CPC at anaphase has been further addressed in *Xenopus* tissue culture cells. INCENP function was blocked by microinjection of an INCENP antibody in Xeno S3 cells. It was noted that anaphase spindles, and therefore the distance between the poles, was shorter than in their control counterpart but the astral MT spindles in anaphase were longer. The number of MT bundles found in the midzone was also significantly reduced in the injected cell (Ahonen *et al.,* 2009).

During cytokinesis, when the CPC is localised to the central spindle, Aurora B continues to function if there is a chromosomal bridge present.

By remaining in its active state, Aurora B helps to prevent the development of a tetraploid cell and/or chromosomal damage caused by the cytokinetic furrow. This is undertaken by its activity on MKLP1/Pav; by phosophorylating MKLP1/Pav it leads to stabilization of the intercellular canal, which in turn delays abscission until the chromatin has been cleared from the cleavage site (Steigemann *et al.,* 2009) (Fig. 1-5b).

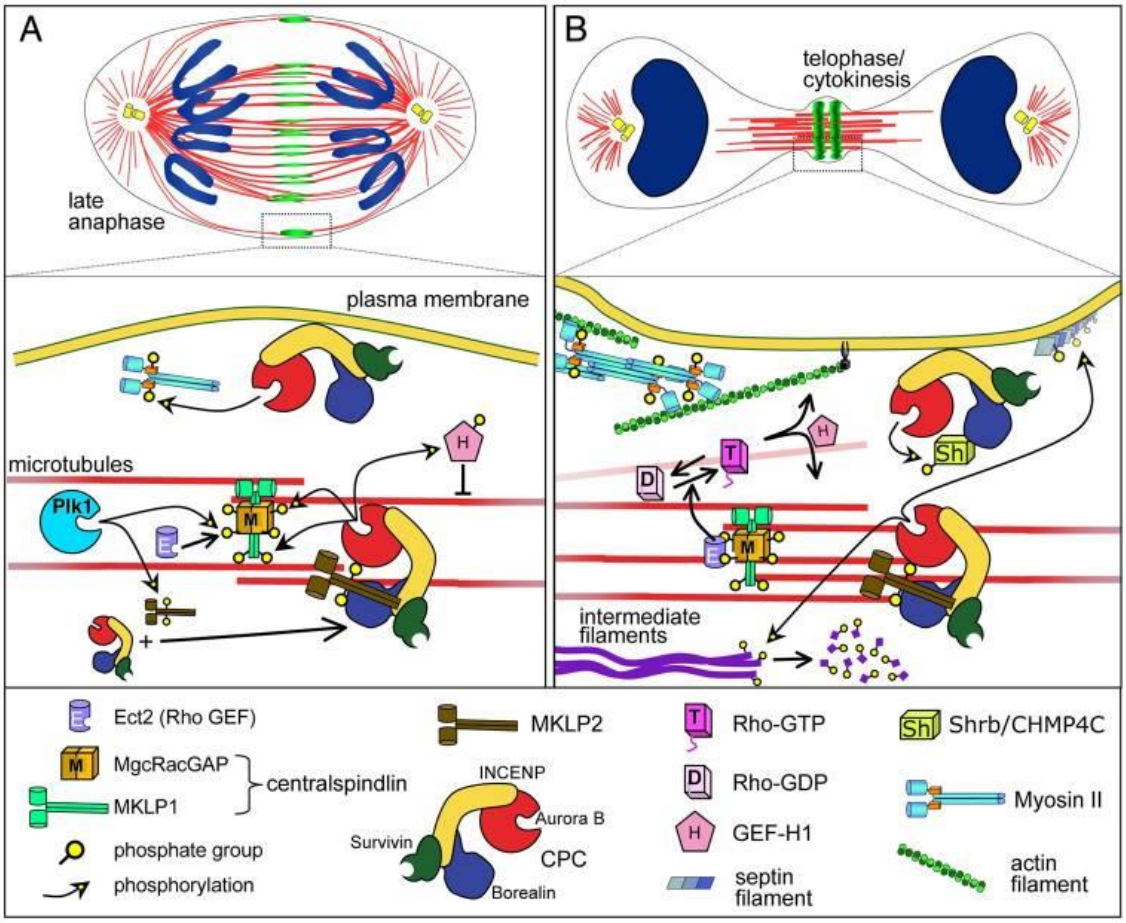

Figure 1-5. Relocalisation of the CPC and its function during the latter stages of cell division (A) During anaphase, the CPC migrates to the midzone MTs. Aurora B is responsible for the phosphorylation of a number of important proteins including the centralspindlin complex which helps to stabilize the midzone. **(B)** During telophase, one of the main roles of the CPC and in particular Aurora B is in the prevention of a tetraploid cell and/or chromosomal damage caused by the cytokinetic furrow. To prevent this, Aurora B phosphorylates MKLP1/Pav thereby stabilizing the intercellular canal which delays abscission until the chromatin has been cleared from the cleavage site. (Image taken from Carmena *et al.,* 2012b).

1.4.3. Australin in *Drosophila* male meiosis

In the model organism *Drosophila melanogaster*, null mutations or knockouts of any of the other CPC components lead to embryonic lethality and therefore observing the function of the CPC in somatic cell divisions is complicated. However, *Drosophila* possess two paralogues of the Borealin subunit of the CPC; borealin-related (borr) which has a role in all the mitotic divisions and in female meiosis, and australin (aust); only present in male meiosis where it specifically replaces Borr (Gao *et al.,* 2008). Pre-meiotic mitoses in *australin* mutants therefore occur normally, allowing the specific disruption of CPC function at the start of meiosis.

The presence of a weak spindle assembly checkpoint in *Drosophila* male meiosis allows for observations post-metaphase, and therefore the contribution of the CPC to cytokinesis can be studied. Previous work in the lab has shown that, in absence of Australin, the central spindle fails to form and equatorial constriction does not occur (Gao *et al.,* 2008).

1.5. MKLP1/Pavarotti and MKLP2/Subito

MKLP1 (mitotic kinesin-like protein-1)/Pavarotti and MKLP2 (mitotic kinesin-like protein-2)/Subito, hereafter referred to as Pavarotti and Subito respectively, are MT motor proteins with roles in organisation of the central spindle (Adams *et al.,* 1998; Guse *et al.,* 2005; Jang *et al.,* 2005).

Subito is known to localise to the central spindle in *Drosophila* oocytes (Jang *et al.,* 2005), in embryos and brain cells (Cesario *et al.,* 2006) and

is required for the localisation of INCENP and Aurora B (Jang *et al.*, 2005; Cesario *et al.*, 2006). The Wakefield laboratory has previously reported that Pavarotti fails to not localise to the central spindle and cell cortex during anaphase in fixed *aust* spermatocytes, unlike in wild type spermatocytes (Gao *et al.,* 2008). In addition, previous research has found that Survivin and INCENP are essential for the localisation of Pavarotti to the midzone (Zhu *et al.,* 2005; Szafer-Glusman *et al.,* 2011). Therefore the precise relationship between Pavarotti, Subito and the CPC during anaphase remains to be addressed.

1.6. Polo

Polo is an essential protein kinase, with important roles throughout cell division. Polo works alongside Aurora B at the kinetochores to ensure correct MT-kinetochore attachments; however, while Aurora B destabilises the MT attachments, Polo promotes stable MT attachments. It is through the phosphorylation of Polo by Aurora B and INCENP that Polo becomes activated at the kinetochores (Carmena *et al.,* 2012a). Pavarotti is also responsible for Polo localisation. It has also been shown through mutations in Pavarotti that Polo kinase fails to localise correctly which gives rise to the formation of a defective central spindle resulting in cytokinesis abnormalities (Adams *et al.,* 1998).

1.7. TD60

As mentioned earlier in the introduction, TD60 potentially has a role as a Chromosomal Passenger protein. The distribution of human TD60 throughout mitosis complements that of the CPC proteins; (Andreassen *et al.,* 1991; Martineau-Thuillier *et al.,* 1998). As seen with the CPC,

TD60 was shown to associate with the centromeres of metaphase chromosomes and to transfer to the equatorial plane in anaphase/telophase (Martineau-Thuillier *et al.,* 1998). In addition, studies have reported both that human TD60 could be co-precipitated by the CPC component Borealin (Gassmann *et al.,* 2004), and that TD60 is required for full Aurora B activation (Rosasco-Nitcher *et al.,* 2008).

TD60 is encoded by the RCC2 gene and shows some structural similarity to the RanGEF, RCC1 (regulator of chromosome condensation 1), and has possible GEF activity on the small GTPase Rac1 (Mollinari *et al.,* 2003). TD60 has also been found to be essential for mitotic progression; RNAi in HeLa cells exhibited a prometaphase arrest (Mollinari *et al.,* 2003).

1.8. Aims of this Masters by Research project

The aim of this project was to further establish the mechanism by which the CPC organises the central spindle. It focused on the examination of Pavarotti, Subito and Polo that, due to recent research, have either been found to be of importance in CPC localisation or in the regulation of protein localisation by the CPC during cytokinesis.

As central spindle formation is a dynamic process, one central aim was to establish a live imaging technique that would allow the localisation of these proteins to be studied in real-time in both wild-type and null *aust* spermatocytes. This was undertaken to specifically answer whether the localisation of these proteins is directly regulated by the CPC and to ascertain in greater detail how the CPC functions in cytokinesis.

This thesis also hoped to elucidate the role of TD60 to explore its function in both spindle and central spindle formation as a possible CPC member. This was investigated through various experiments; RNAi in both *Drosophila* embryos and spermatocytes, microinjection of TD60 antibody using embryos with various GFP-fusion proteins and through attempting to identify TD60 interacting proteins, through biochemical purification of the protein, followed by mass spectrometry.

2. Materials & methods

2.1. Resources used in this thesis

Fly Stock	**Reference**	**Comments**
Tft/*CyO* (II)	Bloomington	Balancer Stock
Ubi Pavarotti-GFP (II)	D Glover	GFP
Bam-GAL4 (III)	H White-Cooper	Transgenic Transposon/Driver
Ubi Polo-GFP (II)	C Sunkel	GFP
MKRS^{Sb}/TM6B^{Tb} (III)	Bloomington Stock Center	GFP
pUASp-Anillin-GFP (III)	A Wilde	GFP
pUASp-Subito-GFP/TM3^{Sb} (III)	K McKim	GFP
pUASp-Subito-GFP/TM6B^{Tb} (III)	This thesis	GFP
Maternal α-Tubulin-GAL4 (II) and (III)	J Raff	Transgenic Transposon/Driver
Sna^{Sco}/*CyO.Tb* (II)	Bloomington	Marker/Balancer
pUAS Aurora B-GFP/*CyO* (II)	Wakefield lab (S Li)	GFP
pUAS Aurora B-GFP;Bam-GAL4	This thesis	GFP
Sp/*CyO*; MKRS^{Sb}/TM6B^{TbDr}	Bloomington	Marker/Balancer
TD60-RNAi/CG9135 (II)	Genome-wide bank, Vienna	RNAi
australin^{1}.β-Tubulin-GFP/*CyO*	Gatti lab	GFP
australin$^{1.4}$/*CyO.Tb* (II) & *australin*$^{1.22}$/*CyO.Tb* (II)	This thesis	Point Mutation

UAS Dicer (I)	Vienna	Transgene
Tubulin-GFP; Histone-RFP	Wakefield lab (D Hayward)	GFP
TD60-GFP; Maternal α-Tubulin GAL4	This thesis	GFP
Tft/*CyO*; MKRS^{Sb}/TM6B^{Tb}	Bloomington	Marker/Balancer
Tft/*CyO*; pUASp Deterin-GFP/TM6B^{Tb}	This thesis	GFP
australin$^{1.4}$/*CyO.Tb*; pUASp Anillin-GFP	This thesis	GFP
australin$^{1.4}$/*CyO.Tb*; Bam-GAL4/MKRS^{Sb}	This thesis	Balancer
australin$^{1.4}$/*CyO.Tb*; pUASp Deterin-GFP	This thesis	GFP
australin$^{1.4}$/*CyO.Tb*; Bam-GAL4/Bam-GAL4	This thesis	Driver
australin$^{1.4}$.Pavarotti-GFP ^{9} /*CyO.Tb*	This thesis	GFP
australin$^{1.22}$.Polo-GFP ^{5} /CyO.Tb	This thesis	GFP
Subito^{1}/*CyO* (II)	Bloomington 5117	Point mutation

Table 1. Fly stocks

Antibody	**Type**	**Conc.**	**Reference**
α-Tubulin, DM1A	Mouse monoclonal	1:1000	Sigma
TD60	Rabbit polyclonal	1:1000	Wakefield lab (T Duncan)
Donkey anti-mouse IgG Alexa-488	Donkey polyclonal	1:1000	Invitrogen
Rabbit anti-mouse IgG-HRP	Rabbit monoclonal	1:10000	Sigma
Goat anti-rabbit IgG-HRP	Goat monoclonal	1:10000	Sigma
Rabbit IgG	Rabbit polyclonal	Variety of conc. used	Sigma

Table 2. Antibodies used

2.2. Fly stocks

2.2.1. Keeping fly stocks

Flies were maintained on standard culture medium in either vials or bottles plugged with flugs - bonded dense weave cellulose acetate plugs (Dutscher Scientific). Dissections were carried out at room temperature and main stocks were kept at 25°C as standard. If it was necessary to slow down development they were kept at 18°C, or at 28°C if there was the need to drive greater expression of the RNAi driver/Dicer combinations. Adult flies were transferred to fresh vials every other day and distilled water and dried yeast was added to the vials when deemed necessary. Most fly pushing techniques were carried out as described by Greenspan (2004).

2.2.2. Creating richer media

To obtain the information needed from the various GFP-fusion lines, the spermatocytes needed to be undergoing meiosis when imaging. Acquiring spermatocytes in meiosis proved difficult, partially due to the lack of larvae emerging from the food and partially due to the small window of opportunity where the cells are naturally in this stage. Primary spermatocytes have a growth phase lasting approximately 80-90 hours with meiosis I and II totalling approximately 4.5 hours (McKee *et al.,* 2012). To optimise the number of third instar larvae/early pupae needed for spermatocyte dissections a new, richer culture medium was tried. This was made using the recipe kindly provided by Maurizio Gatti's lab in the hope this would create healthier lines to, in turn increase the chances of getting cells in the later stages of meiosis (i.e. from early metaphase-

late telophase) when viewing spermatocyte cells. Efficacy of both media was tested, keeping variables consistent; ensuring both media were made on the same day and the same volume and numbers of male and female flies from the same line added to each vial. Observing the vials, there are more larvae ascending when using the new recipe thereby increasing the chances of dissecting a testis with spermatocytes undergoing meiosis.

2.2.3. Collecting flies for crosses

Virgin female flies were collected twice per day, and kept at 25°C between the two collections. Between 4:30pm and 10am the next day the cultures were placed at 18°C to slow down development (Greenspan, 2004). Virgin females were recognisable by their meconium, which indicates their recent emergence from the pupae and therefore their inability to mate.

2.2.4. Collecting embryos

Flies were placed in embryo collection chambers secured with apple juice agar plates and left to lay at 25°C (or at 28°C when collecting TD60 RNAi embryos alongside wildtype embryos to act as a control. TD60 levels in the embryo should be knocked down to a greater extent at 28°C than at 25°C). From these plates the embryos were harvested/collected so they were between 0-3 hours old if needed for immunoprecipitation (IP) or between 1-2 hours if using embryos for fixed/live imaging and microinjection work.

2.2.5. Genetic crosses and recombination

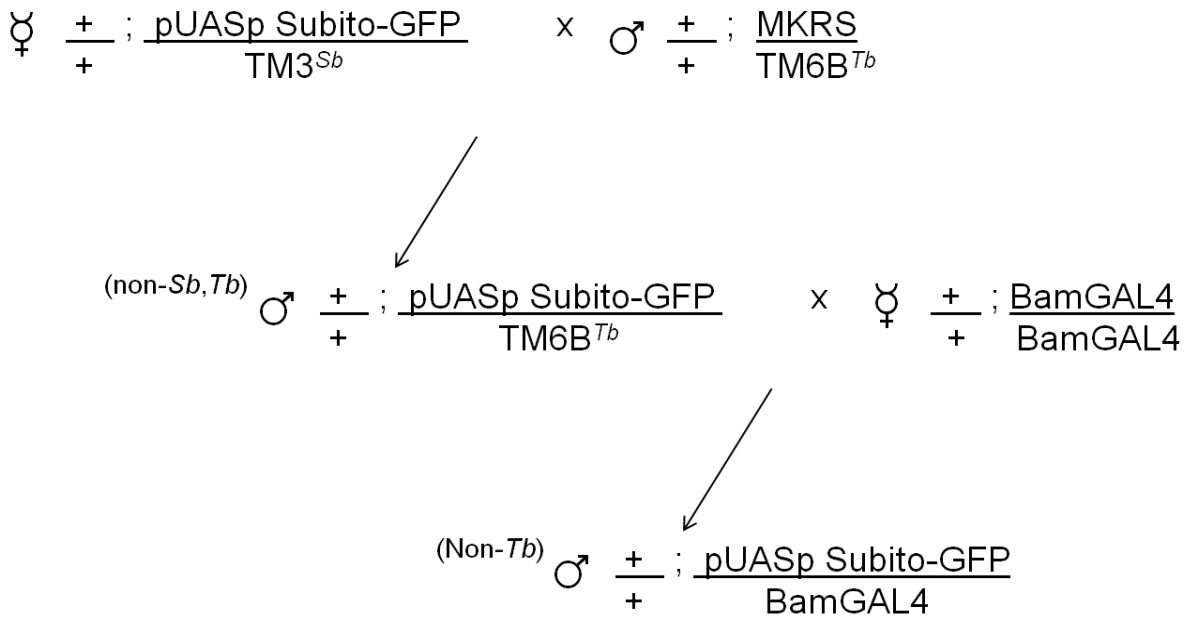

Figure 2-1. Cross set up to create a fly with the marker *Tubby (Tb)* carried on the balancer *TM6B*, instead of *Stubble* (*Sb*) carried on the balancer *MKRS*. *Sb* is a marker only visible in adult flies whereas *Tb* presents itself from larval stage. The second cross was to allow expression of Subito-GFP in spermatocytes using the testes-specific driver Bam-GAL4.

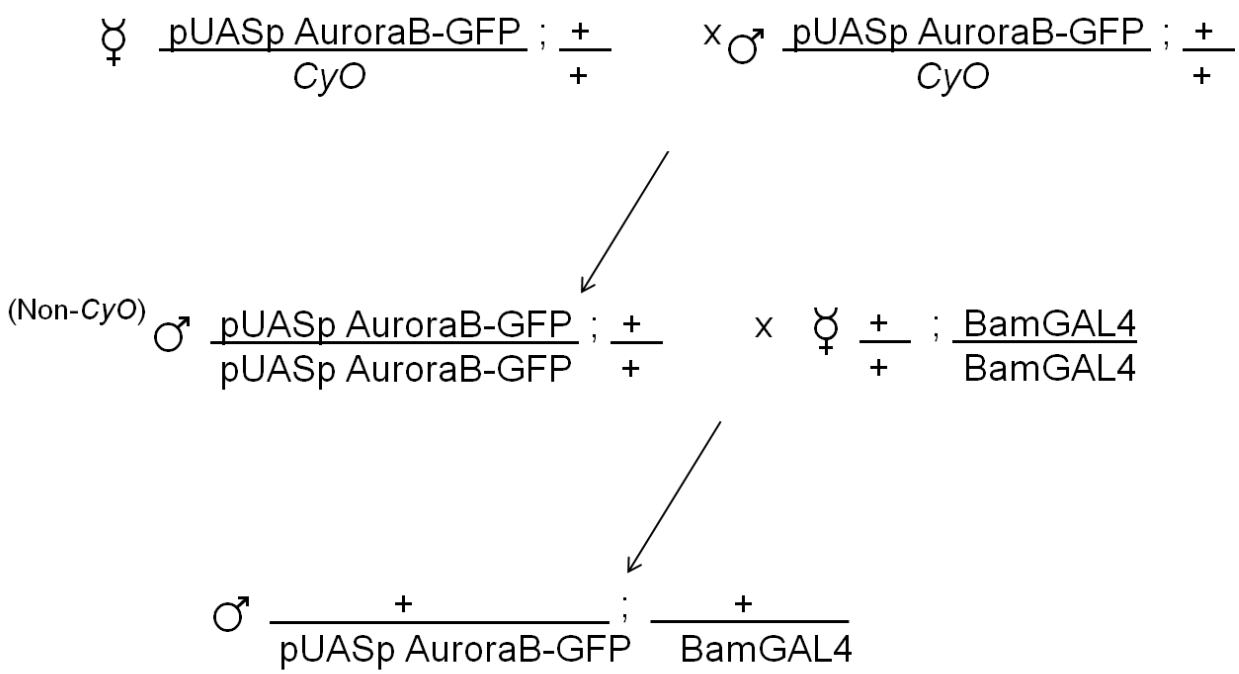

Figure 2-2. Cross to express Aurora B-GFP in spermatocytes using the driver Bam-GAL4.

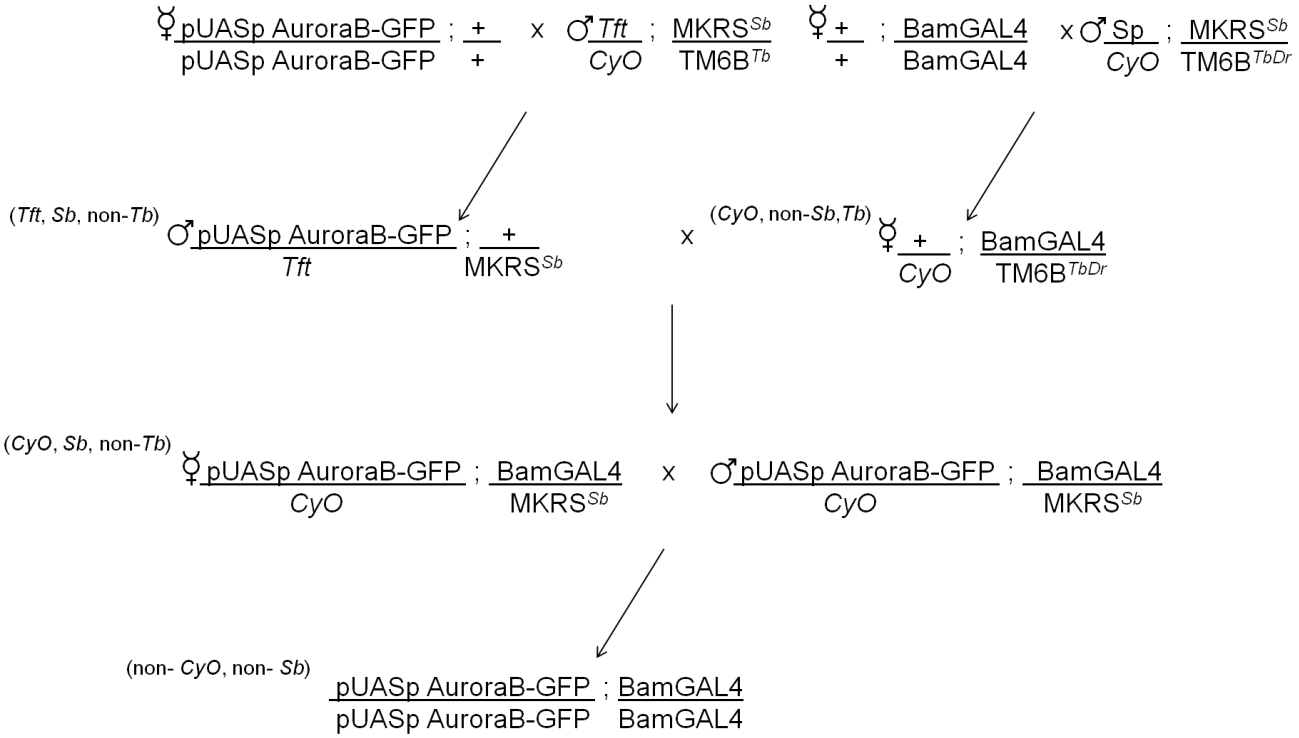

Figure 2-3. Cross to create a fly homozygous for Aurora B-GFP and the driver Bam-GAL4 to give greater GFP expression and less bleaching when imaging in spermatocytes.

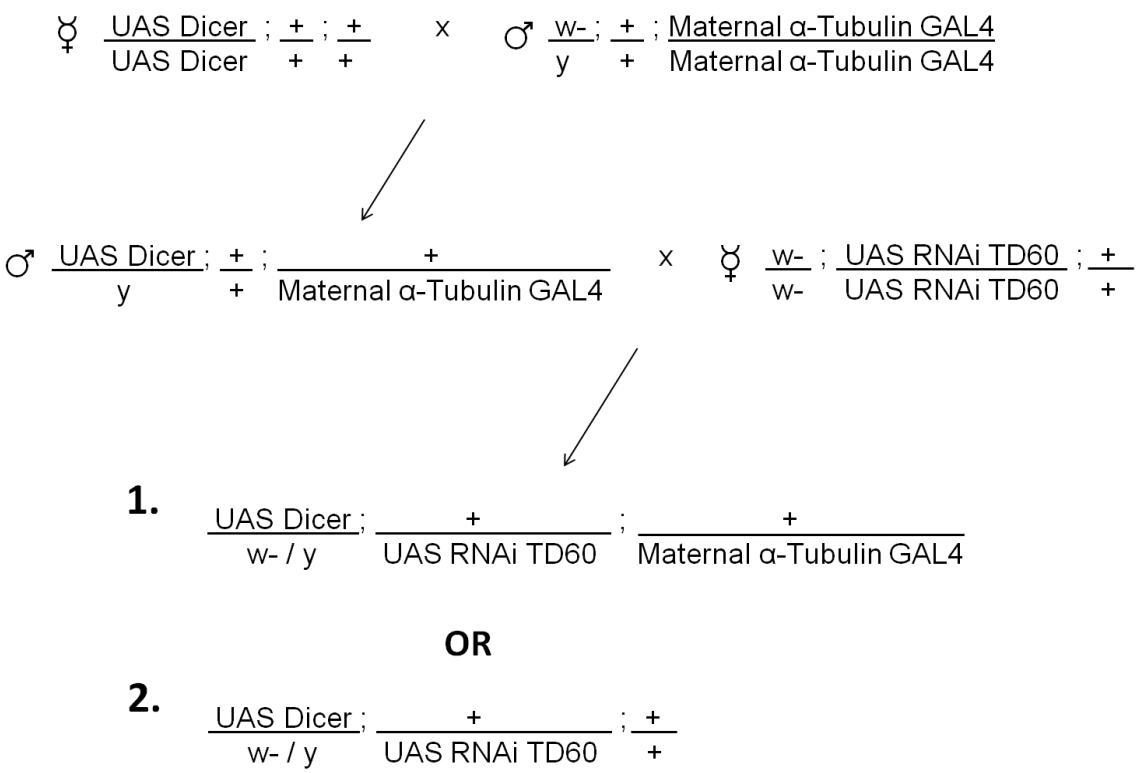

Figure 2-4. Cross set up to knock down TD60 levels in the embryo. There are two possible final outcomes to the cross; **1.** The embryo will possess a copy of all the genes needed for knock down of TD60 levels in the embryo; or **2.** The embryo will lack the driver that is needed to drive expression of the Dicer protein that in turn is needed for knock down of TD60 levels in the embryo. Therefore there is a 50% chance that the embryo visualised has TD60 levels reduced.

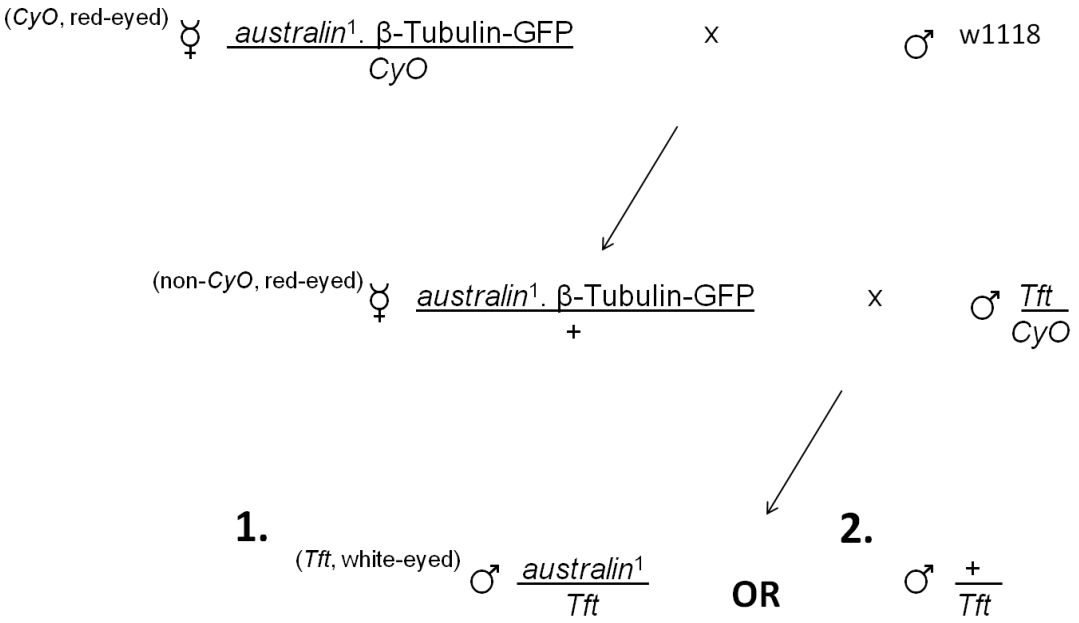

Figure 2-5a. Cross set up to recombine the β-Tubulin-GFP gene out of the second chromosome that also has the *australin* mutation gene. Selecting flies with white eyes (the GFP carries a mini-white gene which gives rise to red eyed flies) will lead to two possible final outcomes to the cross; **1.** Recombination would have been successful; the β-Tubulin-GFP gene would have been recombined out of the chromosome leaving only the *australin* mutation gene; or **2.** The fly selected only has white eyes due to no changes made to one of its copies of the second chromosome and therefore has no *australin* mutation gene.

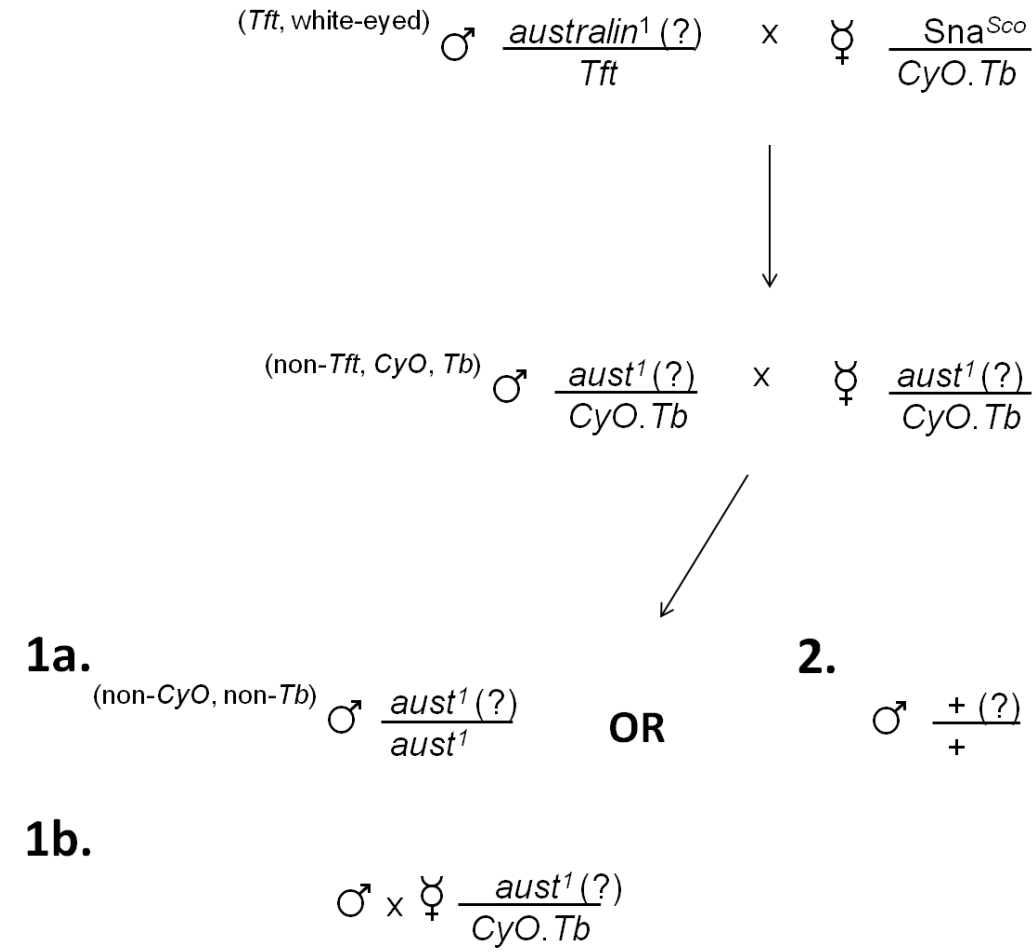

Figure 2-5b. Cross set up to determine whether the recombination crosses from 2-5a were selected for/had been successful 1a. If successful the male flies would be sterile (shown through lack of offspring when mated with virgin females) due to possessing two copies of the *australin* mutation gene; **1b.** A stable stock could be set up once it had been shown that the males were sterile; or **2**. Flies didn't possess the *australin* mutation gene and are therefore not sterile.

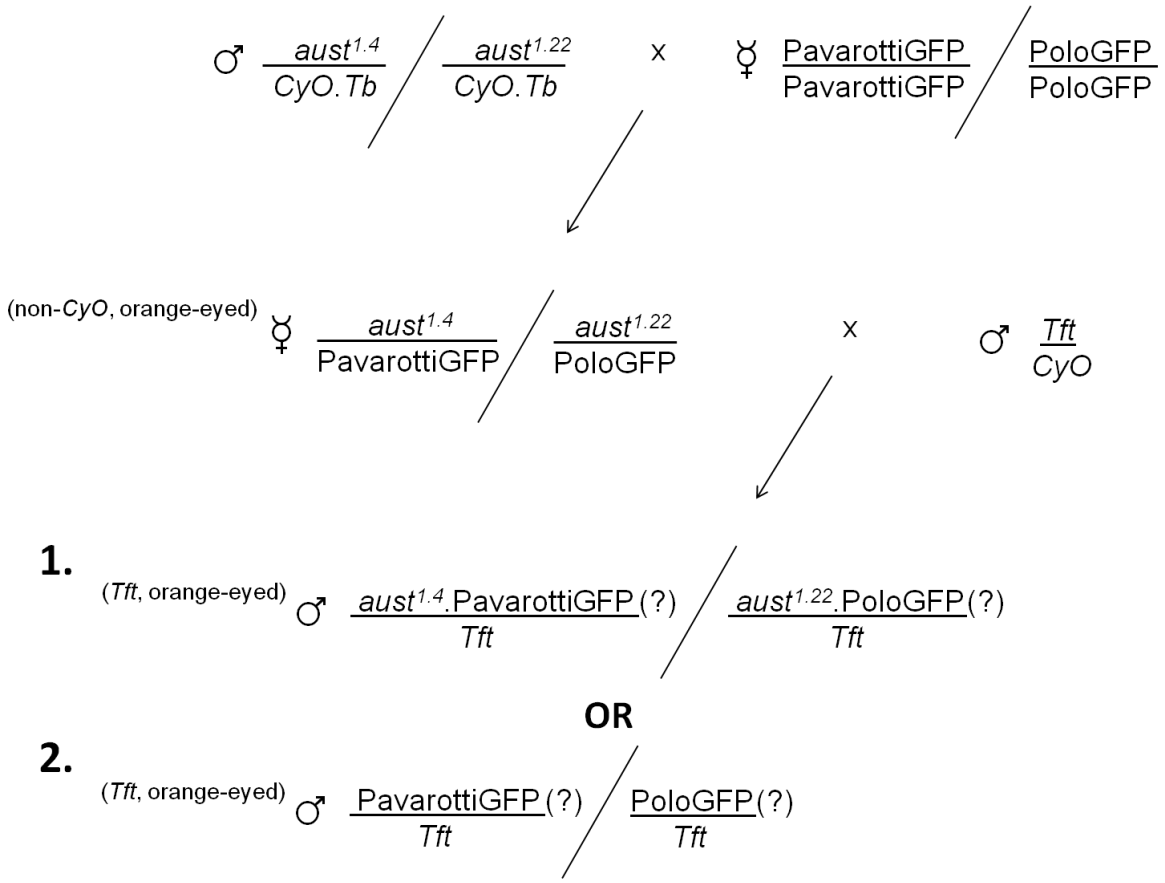

Figure 2-6a. Cross set up to recombine the gene for Pavarotti-GFP/Polo-GFP onto the same chromosome with the *australin* mutation gene. Selecting flies with red eyes will lead to two possible final outcomes to the cross; **1.** Recombination would have been successful; the gene for Pavarotti-GFP/Polo-GFP would have been recombined onto the chromosome containing the *australin* mutation gene; or **2.** The fly selected only has red eyes due to the presence of the GFP and there has been no recombination.

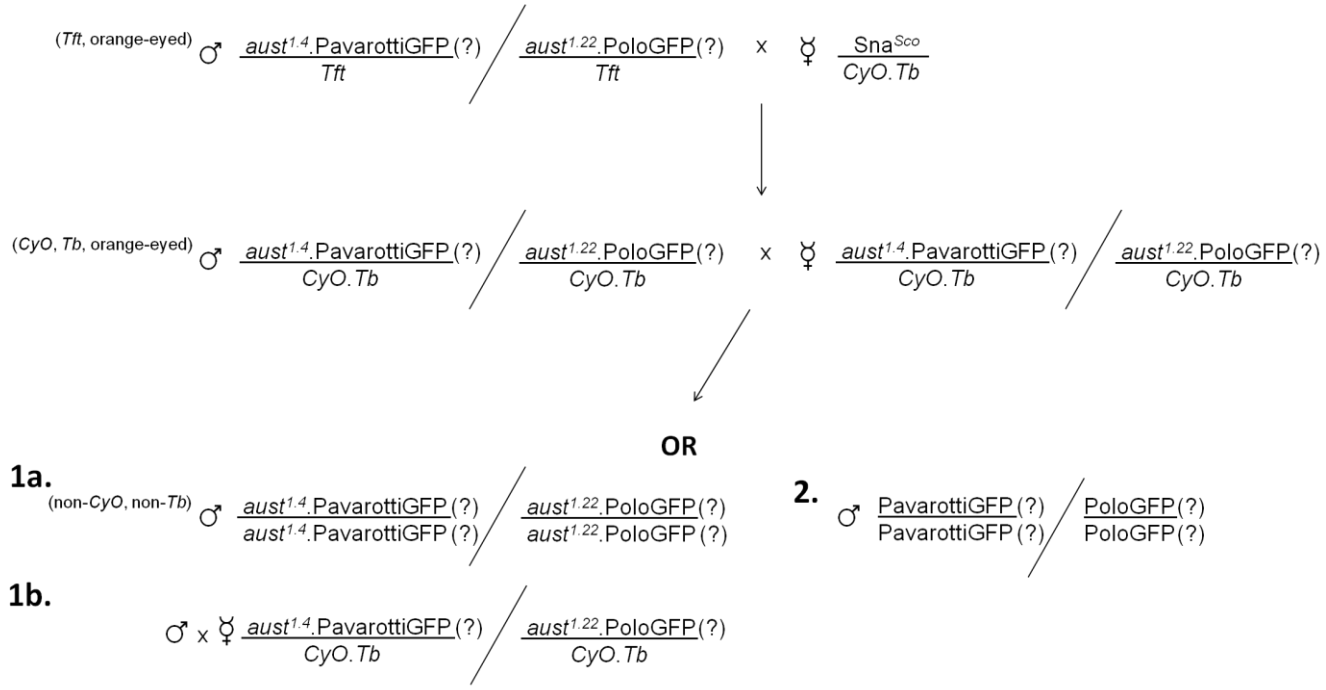

Figure 2-6b. Cross set up to determine whether the recombination crosses from 2-6a had been successful 1a. If successful the male flies would be sterile due to possessing two copies of the *australin* mutation gene and fluorescence from the GFP would be detected under UV light; **1b.** A stable stock could be set up once it had been shown that the males were sterile; or **2.** Flies didn't possess the *australin* mutation gene and are therefore not sterile. Male *aust*$^{1.4}$.Pav-GFP/*Tft* or *aust*$^{1.22}$.Polo-GFP/*Tft* flies were taken to cross with female Sna^{Sco}/*CyO.Tb* flies. If females from that line had been taken to cross with male Sna^{Sco}/*CyO.Tb* the *australin* mutation could have recombined out of the chromosome and it would have not be known from the outward phenotype whether this has occurred or not.

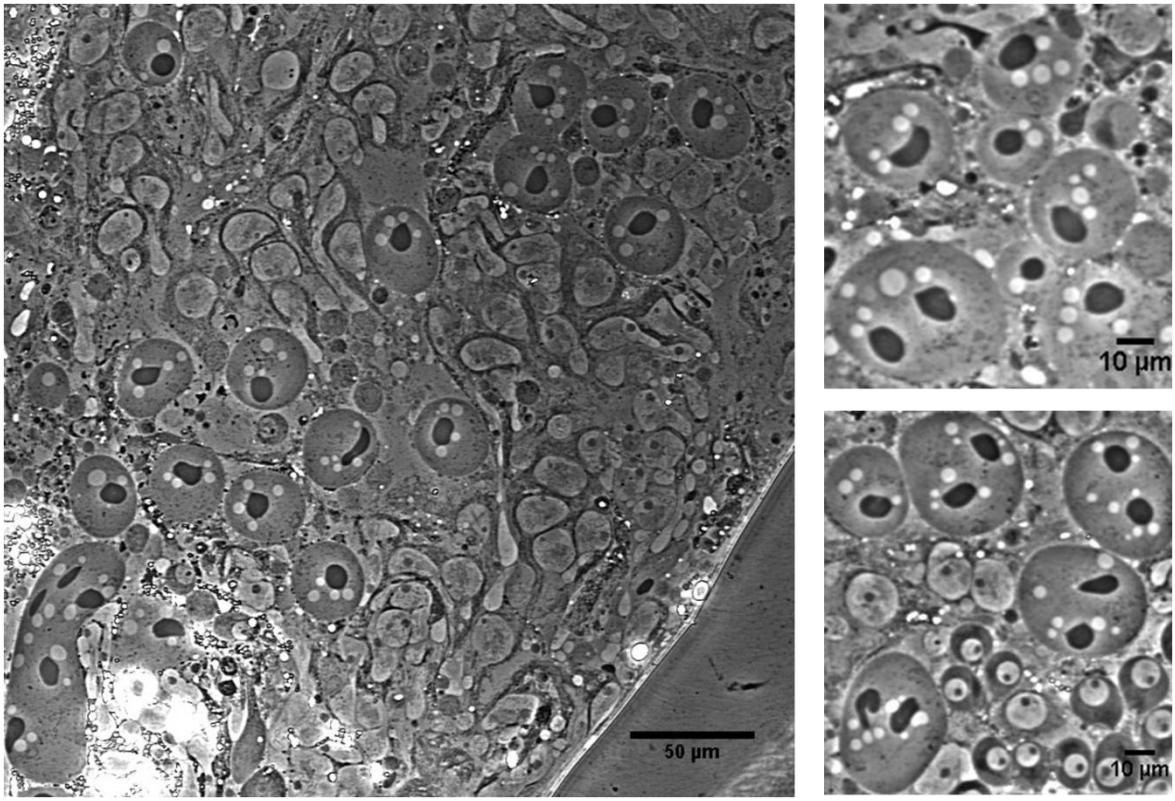

Figure 2-7a. Recombination success: Phase contrast images showing evidence of complete failures in cell division and cytokinesis.

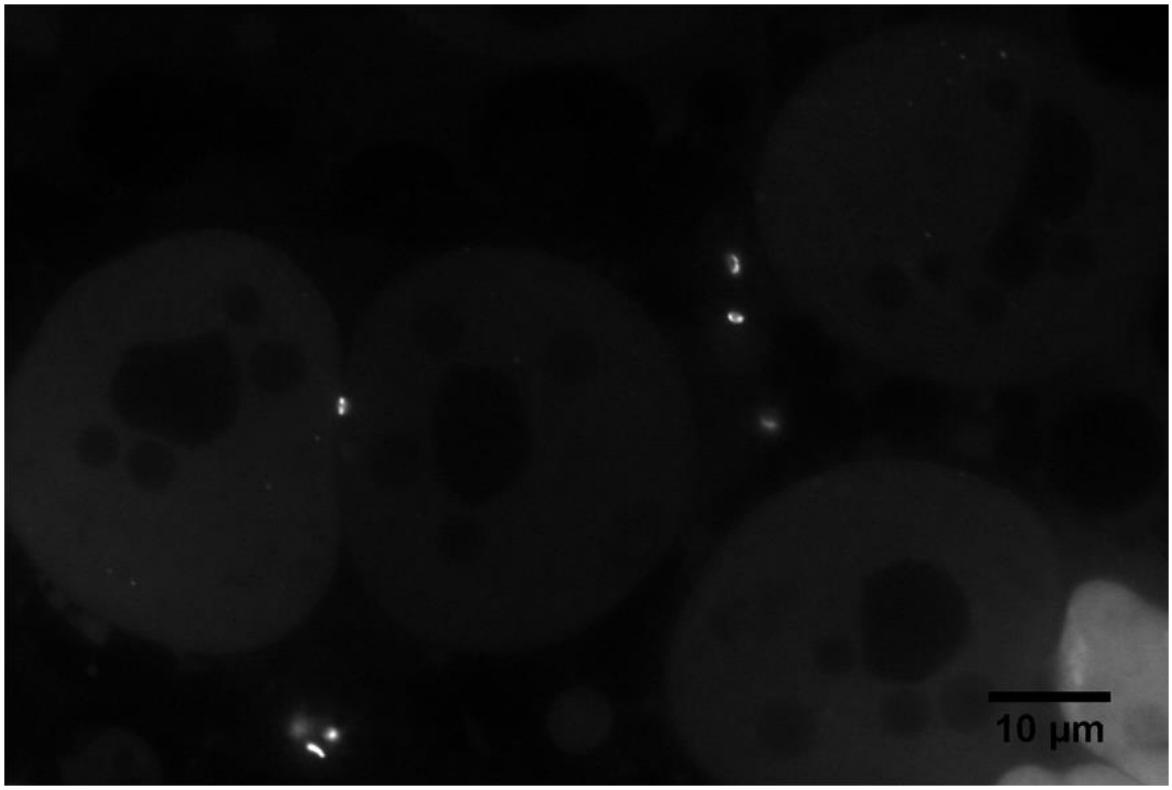

Figure 2-7b. Recombination success: Fluorescence image showing ring canals backing up the previous evidence seen in Figure 2-7a. that recombination of the Pavarotti-GFP gene onto the gene with the *australin* mutation was a success.

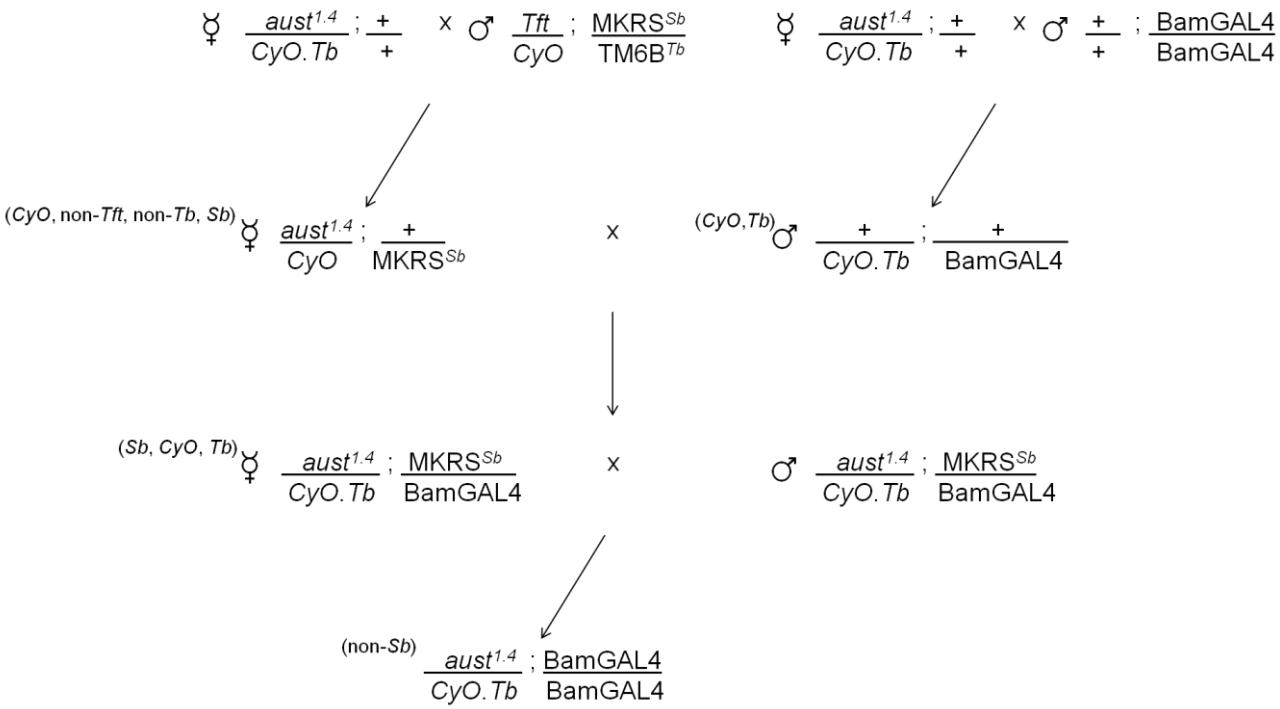

Figure 2-8a. Cross set up to create a stable stock with the gene for the *australin* mutation on the second chromosome and the gene for the driver Bam-GAL4 located on both copies of the third chromosome.

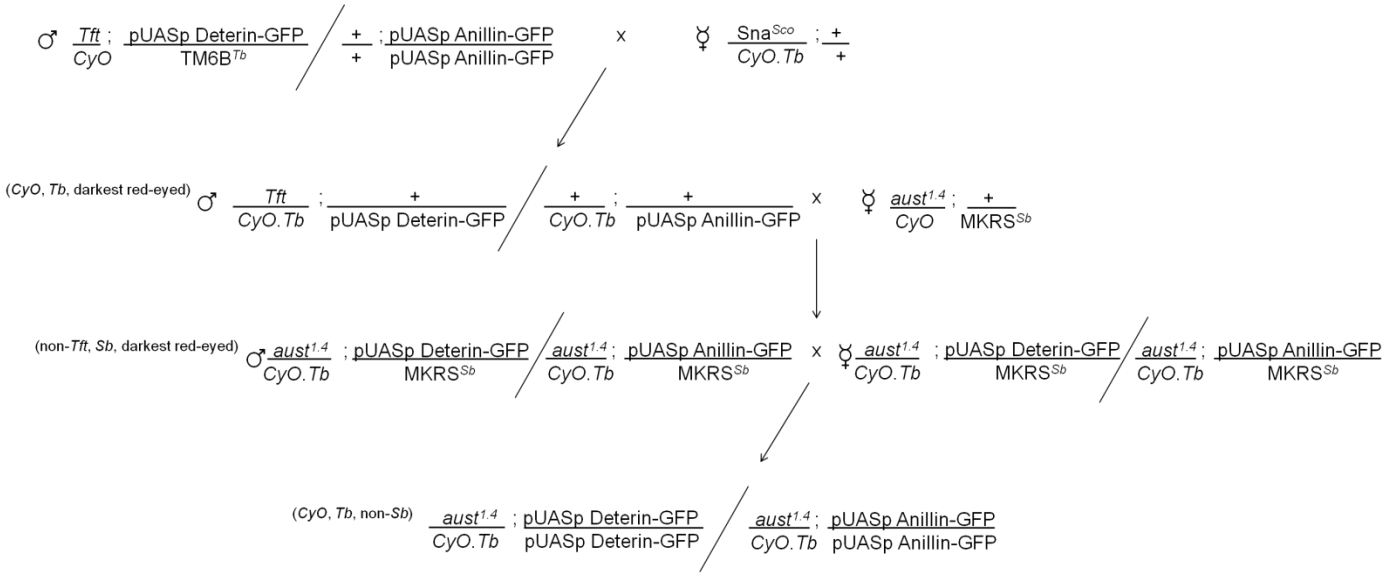

Figure 2-8b. Cross set up to create a stable stock with the *australin* mutation gene on the second chromosome and the gene for Deterin-GFP/Anillin-GFP located on both copies of the third chromosome.

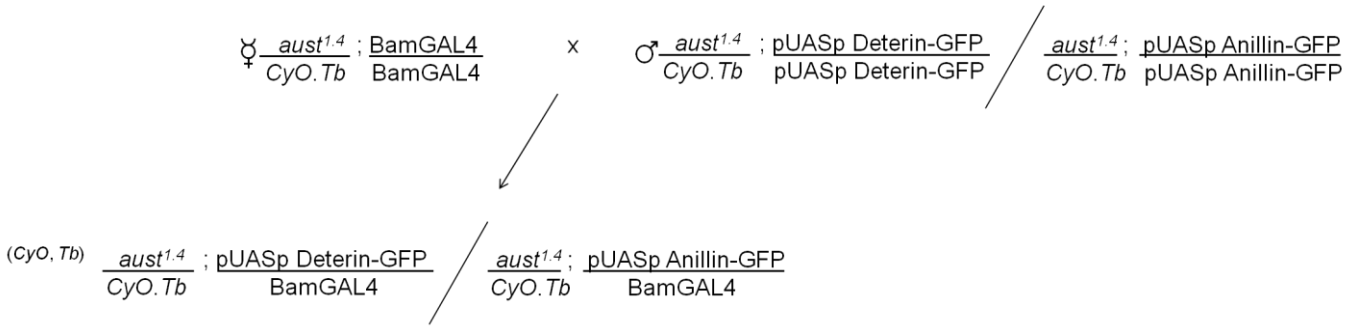

Figure 2-8c. Cross set up to create a line with the *australin* mutation gene on the second chromosome and the gene for Deterin-GFP/Anillin-GFP and the driver Bam-GAL4 on the third chromosome. This was carried out so it was possible to visualise the GFP in the *australin* mutant background. However, due to time constraints it was not possible to examine the localisation of Deterin-GFP and Anillin-GFP in control or *aust* spermatocytes.

2.2.6. Fertility testing

Due to the nature of the mutation, male flies homozygous for the null *australin* allele are sterile. To check the validity of this genetic cross (Fig. 2-5b) fertility testing was carried out. At least two virgin females were added to a vial containing a single male suspected to be sterile. After three days the presence of larvae was noted and if any were present the vial was discarded.

2.3. Biochemistry

2.3.1. Gel electrophoresis

SDS Polyacrylamide gel electrophoresis (SDS-PAGE) was undertaken to analyse various protein samples. Protein samples were prepared using x6 Protein Sample Buffer (88% PSB: 12% Dithiothreitol (DTT) 1 M); 1 µl added to every 5 µl of sample and then placed in heat block at ~95°C for 5-10 minutes. Samples were loaded on 10% gels and run at 150 V (constant) for 60 minutes at room temperature. Gels were then prepared for staining for protein with coomassie blue dye or for Western blotting

2.3.2. Western blotting

After running the protein sample through the gel, it was transferred onto a nitrocellulose membrane for 90 minutes at 150 mA (constant) at 4°C. The membrane was then blocked in 5% milk in TTBS (0.1% Tween-20 and 1X Tris-Buffered Saline) for a minimum of 30 minutes. The appropriate 1° antibody in block was then added and the membrane probed, rotating overnight at 4°C. After 3 x 15 minute TTBS washes the appropriate 2° antibody in block was added to the membrane for a minimum of 60

minutes rotating, at room temperature. Again, the membrane was then washed 3 x 15 minutes in TTBS before being transferred into Milli-Q water. Antibody was then detected in the dark room, using ECL Western blotting substrate (Pierce) according to manufacturer's instructions.

2.3.3. Growing MBP and MBP-TD60 expressing bacteria

To create an MBP and an MBP-TD60 purification column, *E. coli* expressing either protein was grown in LB broth + powder ampillicin at 100 mg/ml. 200 ml of bacteria expressing MBP and 2 l of bacteria expressing MBP-TD60 were grown at 37°c for around 2 hours until OD_{600} of between 0.4 - 0.6. Cultures were induced with IPTG F_c: 1mM at 30°C for 2 hours. After induction the media and cells were centrifuged at 6000 g for 15 minutes to create a bacterial pellet. The bacteria expressing TD60-MBP was re-suspended in 30 ml C buffer (50 mM) HEPES pH 7.4, 1 mM MgCl, 1 mM EGTA) + lyzozyme + PhosSTOP Protease Inhibitor Cocktail tablets (Roche) (1 per 15 ml of solution) + 1 mM PMSF while the bacteria expressing MBP were re-suspended in 5 ml C buffer at pH 7.4 + lyzozyme + 1 PIC tablet. Once re-suspended, bacteria were sonicated for 3 x 30 seconds, placing on ice in between and then centrifuged at 8000 rpm for 10 minutes. The supernatant was passed through a 0.22 µm filter using a syringe. The now clarified supernatant was then added to the prepared amylose-resin beads (to prepare; 3 washes in C buffer, centrifuging at 4000 g for 3 minutes between each wash. After the last wash/spin the C buffer was removed and the supernatant added). The MBP/MBP-TD60 supernatant was incubated with 0.5 ml/2 ml of beads, rotating for 60 minutes at 4°C. After incubation they were spun at 4000 g

for 3 minutes and the supernatant discarded. 3 washes in C buffer were then carried out, centrifuging at 4000 g for 3 minutes between each wash.

The protein was eluted off the beads with elution buffer (C buffer + 10 mM maltose). 2 ml/0.5 ml elution buffer to 2 ml/0.5 ml beads (+protein) was added and the sample gently shaken at room temperature for 5 minutes. Beads were spun at 4000 g 4°C for 3 minutes and supernatant taken and saved. The elution protocol was repeated 3 times, each time saving the supernatant. All MBP elutions/MBP-TD60 elutions were pooled if protein was present after testing with Bradford. Each elution was incubated overnight, rotating at 4°C with 1 ml of equilibrated Affigel-15 beads.

2.3.4. Preparation of affinity chromatography columns

The Affigel-15-MBP and -MBP-TD60 bead solutions were loaded onto 1 ml chromatography columns (Pierce) each containing a fret and solution allowed to flow through via gravity. The flow through was tested for protein by Bradford to confirm the MBP/MBP-TD60 had bound to the beads. Columns were washed with 3 x 1 ml C buffer before washing with ~25 ml of 1 M Tris HCl pH 8 to allow any unbound Affigel to react to completion. Columns were then washed with 1 ml ethanol 20% and stored at 4°C in 20% ethanol, ready for use.

2.3.5. Purification of rabbit anti-TD60 antibody

A polyclonal rabbit anti-TD60 antibody was previously generated in the Wakefield lab. Full length TD60 was expressed in bacteria as an MBP fusion purified using Amylose resin and then sent for injection into rabbits by Eurogentec. The serum, containing both MBP and TD60 antibodies, was first passed through the MBP column to remove the unwanted MBP antibodies before running the sera through the MBP-TD60 column to collect the TD60 antibodies, as described below.

Stored columns were washed twice with 1 ml C buffer to remove the 20% ethanol, the sera (20 ml; undiluted) was allowed to pass through the MBP column via gravity flow. The column was then washed twice with 10 ml PBS + 0.5 M KCl prior to elution of antibodies. Acid and basic elutions were then carried out to remove the MBP antibody off the column (Fig. 2-9). At least x 4 acid elutions were carried out, using 0.1 M glycine pH 2.1 (750 µl) into 1 M Tris pH 8.5 (250 µl) to neutralise. 10 µl of each of the 1 ml of elution in 200 µl Bradford was used to determine the concentration of protein in the eluted fractions. This was followed by four basic elutions, using 100 mM ethanolamine pH 10 (750 µl) into 1 M Tris pH 8.5 (250 µl) to neutralise. Testing protein concentrations in each elute was carried out as before. The column was washed extensively with C buffer and the process repeated until the antibody concentration in the elutions was undetectable.

The anti-MBP-depleted serum was then passed through the MBP-TD60 column, repeating the steps as described for the MBP column. A

standard Bradford reagent assay was undertaken to estimate anti-TD60 antibody concentration.

2.3.5.1. Concentrating up the antibody; method 1

A 30 kDa Amicon centrifugal filter (Millipore) was placed inside an eppendorf and ~450 µl of elution was added to the filter before centrifuging for 5 minutes 4°C 13,300 rpm. The flow through was discarded and the above steps repeated until all the elutions had passed through the filter. The concentrated antibody was then buffer exchanged with 5 x 450 µl injection buffer (50 mM K-HEPES pH 7.4, 50 mM KCl, 1 mM MgCl2). 1 µl of this concentrated antibody was taken and the protein concentration measured by Bradford protein assay.

2.3.5.2. Concentrating up the antibody; method 2

Elutions were placed into a “slide-a-lyser” dialysis cassette (Pierce) and incubated with 400 ml of injection buffer overnight at 4°C and then concentrated up using a 30 kDa centrifugal filter as described in Section 2.3.5.1.

After concentrating, the purified anti-TD60 antibody was aliquoted into suitable amounts for use in micro-injection work (1-2 µl) and then stored at -80°C. A 1:1 glycerol stock was also made and then stored at -20°C.

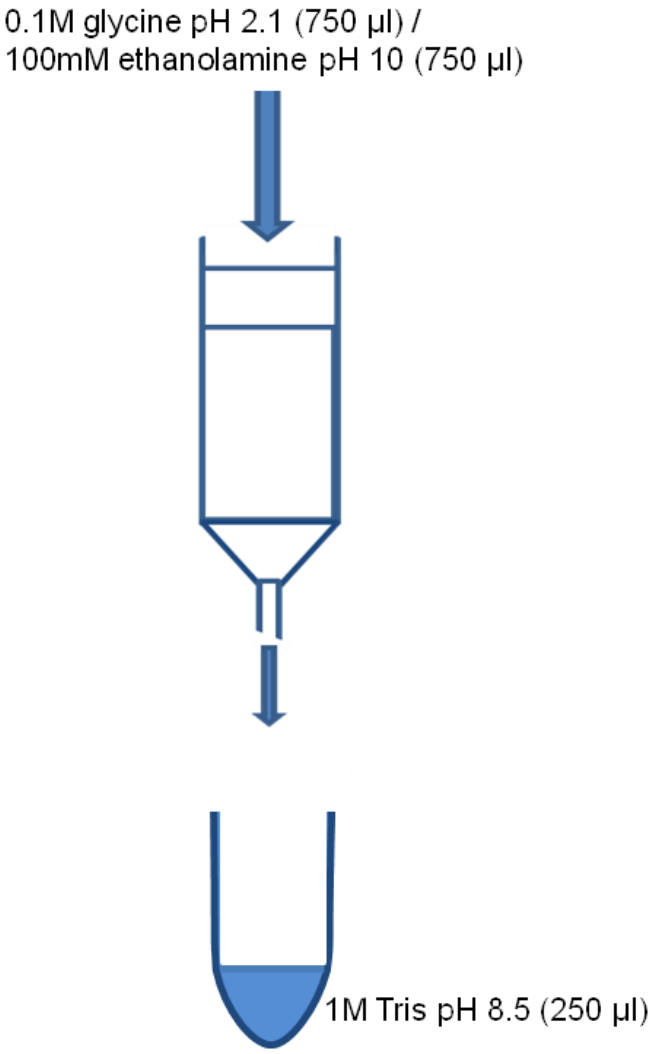

Figure 2-9. How to carry out acid/basic elutions to remove the antibody off the column after sera has been passed through and the column washed x 2 with PBS + 0.5 M KCl 10 ml.

2.3.6. Coupling of antibody to Protein A Sepharose beads

Protein A Sepharose beads (Sigma) were used to couple to TD60 antibody for immunoprecipitation of TD60 interacting proteins. Rabbit IgG antibody was also coupled to the beads to act as a positive control. The beads were prepared by washing 3 x 5 minutes in 1 ml C buffer centrifuging at 2000 g for 30 seconds between each wash. After the final wash, beads were centrifuged again at 2000 g for 1 minute and the C buffer removed. The antibodies were added to the beads at a concentration of 1 µg/µl (TD60 antibody final concentration ~6.5 µg/µl added to 30 µl C buffer therefore 30/6.5 = 4.615 µl of beads used) and incubated for 1 hour at room temperature. After incubation, the antibody-coupled beads were washed 3 x 5 minutes in C buffer, centrifuging at 2000 g for 30 seconds between each wash. The antibody-coupled beads were then stored in C buffer at 4°C until ready for use. The efficiency of the coupling of the antibody to the beads was analysed with SDS-PAGE and Western blotting.

2.3.7. Antibody co-immunoprecipitation

600 mg of 0-3 hour old w1118 embryos were homogenised in 2 ml C buffer with PIC (Roche) 1 mM NaF and Triton 0.1%, using a motor-driven dounce, before centrifuging at 13000 g for 10 minutes at 4°C. The supernatant was removed and then centrifuged at 100000 g for 10 minutes and then 30 minutes at 4°C to further clarify the homogenate.

2.3.7.1. Immunoprecipitation

The Protein A Sepharose beads, bound either with TD60 antibody or Rabbit IgG antibody were incubated with the clarified embryo extract following the protocol described below.

The Protein A Sepharose beads, bound either with TD60 antibody or Rabbit IgG antibody were prepared by washing 3 x 5 minutes in 1 ml C buffer. After the final wash the beads were centrifuged again at 2000 g for 1 minute and the C buffer removed. The clarified embryo extract was divided into two then added to the beads, incubating for 2 hours with rotation at 4°C. Beads were again centrifuged at 2000 g for 1 minute before washing 3 x 10 minutes with 1 ml C buffer. After the final centrifugation, C buffer was removed, the beads flash frozen in liquid nitrogen and stored at -80°C, before being sent off for Mass Spectrometry (Bristol Proteomics Facility). The samples were also analysed by SDS-PAGE and Western blotting to assess purification.

2.4. Cytology

2.4.1. Spermatocyte squashes

Testes squashes were carried out using third instar larvae or early pupae, with dissections performed under a dissecting microscope as previously described by Bonaccorsi *et al.,* (2000) Protocol 5.1 with minor changes; testes were transferred into 3 µl of PBS + Hoechst (at 5 µg/ml) instead of 2 µl of Testis Buffer.

2.4.2. Preparing spermatocytes using a fibrin clot

The method for preparing *Drosophila* spermatocytes using a fibrin clot was adapted from the method previously described by Forer and Pickett-Heaps (2005), to prepare crane fly spermatocytes. Clotting factor was used to avoid having to squash the cells thereby keeping the cells in shape and immobile but in theory still allowing for continuation of cell division. The testes were removed from third instar larvae or early pupae in Ringer's Solution (0.13 M NaCl, 0.005 M KCl, 0.001 M $CaCl_2$ and 0.003 M KH_2PO_4/Na_2HPO_4 buffer at pH 6.8) under a dissecting microscope. Ringer's Solution was prepared as individual concentrated stock solutions as described in Saul *et al.*, 2004.

Once dissected, the testes were placed on a round coverslip (attached to a small chamber) in 3 µl of fibrinogen, bovine plasma (Merck) at 10 mg/ml. This was prepared daily with Ringer's solution + Hoechst at 5 µg/ml (final concentration). The testes were pierced and spread out in the drop using a needle and the cells were then given time to settle. 3 µl thrombin bovine plasma at 50 units/ml (Sigma) was then added. This was left for ~30 seconds to allow the clot to form. Ringer's solution was placed over the top of the clot to prevent desiccation and the lid to the chamber was then attached. The cells were then imaged.

2.4.3. Imaging spermatocytes squashes

Testes preparations were observed at 25°C with a microscope (Eclipse TE2000-U; Nikon) with a Plan APO VC 60 x 1.4 NA objective (Nikon) and a 1.5 x integrated zoom using a camera (c8484-056; Hamamatsu) equipped with a mercury lamp for immunofluorescence. Using phase

contrast microscopy at x 10 magnification, greyscale digital images of the onion stage cysts were obtained. Fluorescence imaging was carried out at x 60 magnification using an oil emersion lens. For the detection of DNA (Hoechst dye) and of various GFP tagged proteins, ultraviolet light was used. Images were taken using IP Lab Spectrum software 3.6.5. Fluorescence images were taken in greyscale and then pseudocoloured and merged using the Fiji/Image J software. Fiji was also used to adjust the colour balance and for alteration of the brightness/contrast level.

2.4.4. Imaging spermatocytes prepared using a fibrin clot

Spermatocytes were visualised with a Zeiss 510 Axiovert 200M Inverted Meta confocal microscope with environmental chamber using a 60 x oil immersion lens. Images were then processed using LSM Image software.

2.4.5. Fixing embryos

0-3 hour embryos were collected on apple juice agar plates, washed into a buchner flask using embryo wash (distilled water + 0.05% Triton X-100) and dechorionated by incubation in bleach for 2 minutes with gentle agitation, before rinsing in embryo wash (3 x) and drying under vacuum. Embryos were washed directly into an eppendorf containing 37% formaldehyde (0.5 ml) using 0.5 ml heptane. The sample was then immediately gently shaken for 2.5 minutes. Once the embryos had settled, the lower level containing the formaldehyde was removed and replaced by 0.5 ml methanol, before gently shaking for 30 seconds. Once the embryos had settled, all solutions were removed and fresh methanol

added (1 ml). After a further wash in methanol embryos were stored at 4°C.

For methanol fixing, the protocol for formaldehyde fixing was applied except that dechorionated embryos were directly washed into an eppendorf containing 0.5 ml of 100% methanol, instead of formaldehyde, before vigorous shaking for 30 seconds.

2.4.6. Antibody staining of fixed embryos

Stored embryos were rehydrated via 3 x 10 minute washes in PBST (PBS + 0.1% Triton X-100), with rotation. The embryos were then incubated for 30 minutes in Blocking Solution (3% BSA in PBST), rotating at room temperature. 1° antibody (DM1A anti-Tubulin clone, Sigma, or anti-TD60) was added to fresh blocking solution at a final dilution of 1:500 and the embryos incubated at 4°C rotating overnight. Embryos were washed 3 x 10 minutes in PBST before the appropriate 2° antibody in Blocking Solution was added (1:1000). The embryos were incubated for 1-2 hours, rotating at room temperature. After removal of the 2° antibody, embryos were washed in PBST for 3 x 10 minutes, with the second wash containing Hoechst at 1 µg/ml to visualise DNA. The embryos were evenly distributed in 40 µl of mounting media on a cover slip (22x22 mm). A slide was then carefully added on top.

2.4.7. Imaging fixed embryos

Fixed and stained embryos were visualised with a Zeiss 510 Axiovert 200M Inverted Meta confocal microscope with environmental chamber

using a 60 x oil immersion lens. Images were then processed using LSM Image software.

2.4.8. Imaging live embryos

Time-lapse fluorescence microscopy was carried out on 1-2 hour old embryos to view the expression of various GFP-fusion proteins. Embryos were removed from the collection plate using embryo wash and placed on a strip of double sided tape. The embryos were dechorionated using forceps under a dissecting microscope. The dechorionated embryos were placed on a 22x50 mm coverslip coated with a line of heptane glue and then covered with halocarbon oil (Sigma) to prevent desiccation. The embryos were viewed on a Yokogawa CSU-X1 spinning disk confocal microscope. Time series typically consisted of taking 5 stacks (0.5 µm between each focal plane) every 5 seconds for one cycle of mitosis, between the stages 9-12 at x 60 magnification. Movies were then analysed using the Fiji/Image J software.

Using the InjectMan NI 2 (Eppendorf), anti-TD60 antibody (concentration ~6 mg/ml) was injected into 1-2 hour old embryos expressing various GFP-fused transgenes. The antibody was loaded into the needle and stored on ice until needed. Injection was carried out at x 10; the magnification was then changed to x 60 for imaging.

3. Results

3.1. The role of the CPC in male meiotic central spindle formation

The aim of the research undertaken in this chapter was to analyse the effect of removing functional Chromosomal Passenger Complex during *Drosophila* male meiosis, assessing the effects on the dynamic localisation of three proteins known to be important in central spindle formation: the kinesins Subito (MKLP2), and Pavarotti (MKLP1) and the kinase Polo (PLK1).

The methodology undertaken within this chapter progressed from preparing testes squashes, to preparing testes in a fibrin clot. Developing the preparation technique in this manner meant the shape of the spermatocytes was maintained, optimising the visualisation of the meiotic cells. Previous research using this clot methodology as seen in Forer's (1998) research on crane-fly spermatocytes showed progression of the cells through meiosis I and II. The intention was to repeat this to follow the localisation of the GFP-fusion proteins in real time, throughout meiosis I and II, to provide more reliable and enriched data. However, technical limitations meant that this was not possible in the lifetime of the project. However, the visualisation of GFP-fusion proteins in fibrin clots during anaphase provides 3D images that result in an important advance in our understanding of the relationship between the CPC and these proteins.

The work in this chapter suggests that Subito does not function to organise central spindle MTs during male meiosis. The analysis of Polo-GFP in *aust* mutant spermatocytes strongly suggests that its localisation

throughout cell division is independent of the Chromosomal Passenger Complex, while analysis of Pavarotti-GFP demonstrates that, although its binding to MTs during meiotic anaphase and telophase is independent of the CPC, the CPC is required to correctly localise Pavarotti to the plus ends of MTs.

3.1.1. Subito-GFP does not localise to the central spindle

Subito is known to have a function in the assembly and maintenance of the central spindle in *Drosophila*; brain cells and oocytes possessing a mutation in *subito* develop a defective central spindle (Jang *et al.,* 2005; Cesario *et al.,* 2006; Jang *et al.,* 2007) and INCENP and Aurora B show impaired localisation (Cesario *et al.*, 2006). However, Subito localisation has not previously been documented in *Drosophila* spermatocytes in great detail; any results relating to this tissue have not been published (Cesario *et al.*, 2006). Initially the research was to follow the pattern of looking at the localisation of Subito-GFP in control testes before monitoring accumulation of Subito-GFP in *aust* (i.e. CPC mutant) spermatocytes.

Examination of Subito-GFP using fluorescence microscopy demonstrated that, in pre-meiotic cells, Subito-GFP concentrated on the MTs around the karyosome - an accumulation of chromatin filaments in the cell nucleus (Mosby's Medical Dictionary) (Fig. 3-1). This localisation has been documented in *Drosophila* oocytes (Jang *et al.,* 2005). In that publication, Subito staining was localised to one side of the karyosome in the majority of the cells. This can also be seen in male pre-meiotic cells in Fig. 3-1. However, there was no specific staining of MTs in cells

undergoing either meiosis I or II (not shown). Meiotic cells (in particular cells in anaphase and/or telophase) were found by phase contrast microscopy (x 10) (Fig. 3-2); once they had been identified, ultraviolet light was used (x 60) to observe GFP localisation in these cells. As Subito-GFP has previously been shown to localise similarly to endogenous Subito in other tissues, I conclude that Subito does not localise to MTs during male meiosis and, as such, is highly unlikely to play a role in central spindle formation in this tissue (see Discussion).

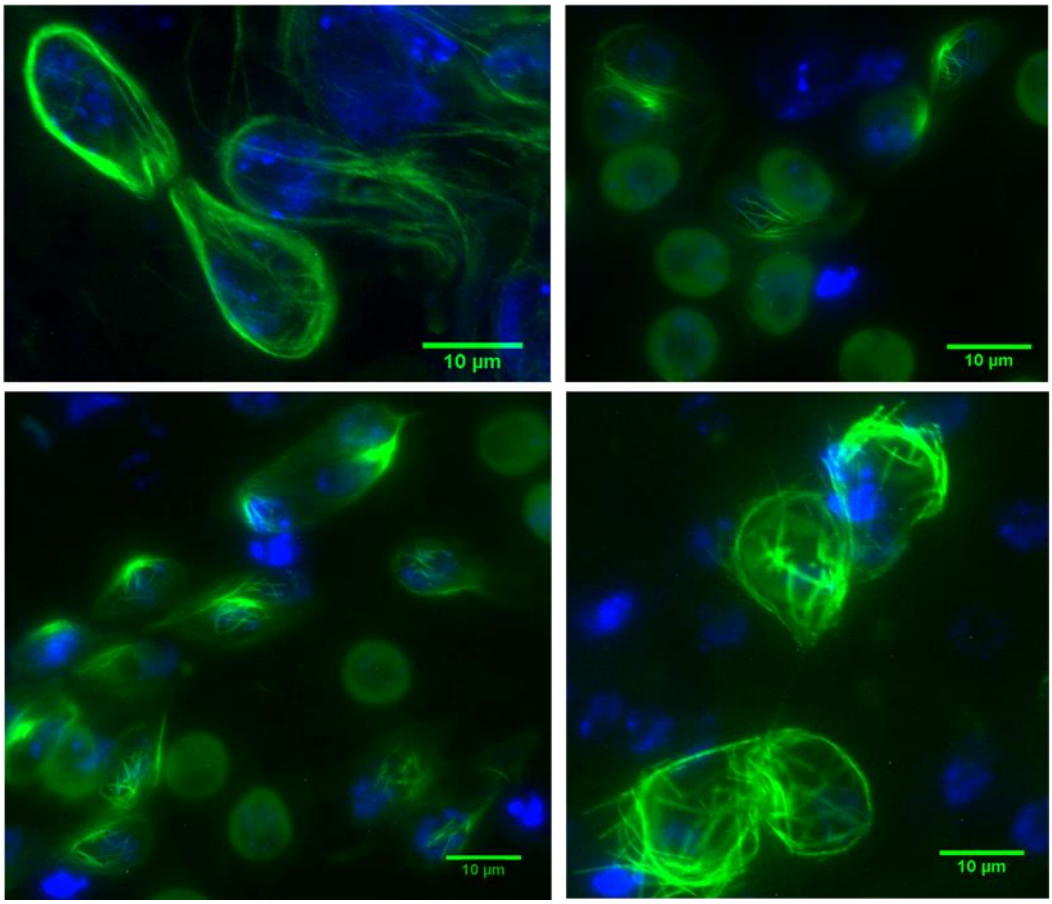

Figure 3-1. Subito-GFP localises on MTs adjacent to the karyosome. Spermatocyte squash observed Subito-GFP localisation on MTs in pre-meiotic cells. Localisation was more prominent on one side of the karyosome (top right and bottom images). Localisation was also seen in early meiosis; interphase/prophase (top left). Subito-GFP in green; DNA stained with Hoechst (5 µg/ml) in blue**.**

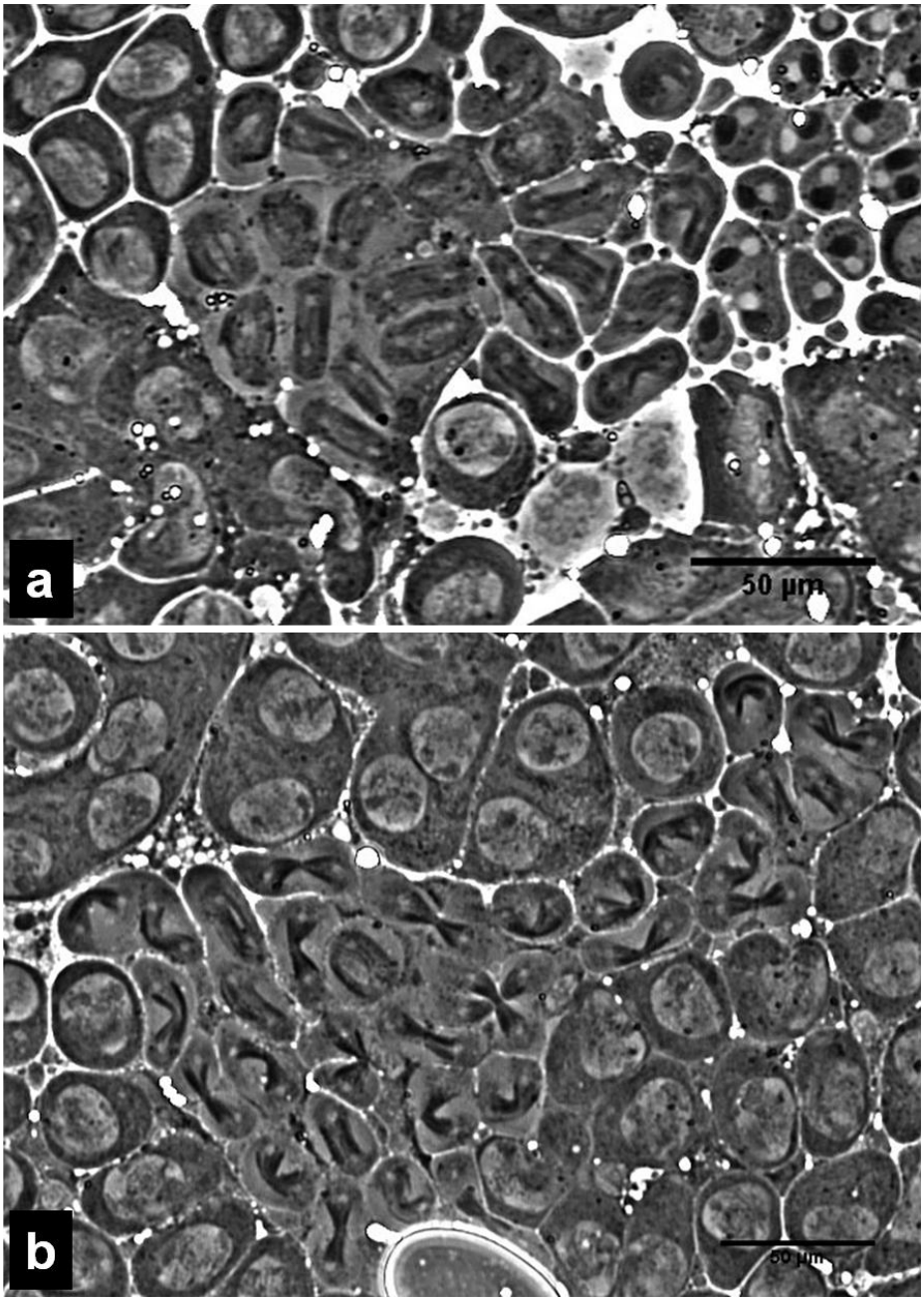

Figure 3-2. Subito-GFP shows no localisation to the central spindle. Phase contrast images were taken of Subito-GFP spermatocytes squashes at x 10 magnification before switching to ultraviolet at x 60 to observe GFP localisation. In all spermatocytes observed in anaphase (as seen in (a)) or telophase (as seen in (b)) there was no fluorescence seen (results not shown).

3.1.2. Pavarotti-GFP localises to the ring canals, the spindle MTs, the equatorial membrane and to the central spindle

Subito (MKLP2) and Pavarotti (MKLP1) are related kinesins with overlapping roles in humans. In contrast to initial studies in *Drosophila* S2 cells, which suggested that the localisation of the kinesin Pavarotti is independent of the CPC (Adams *et al.,* 2001), more recent work has concluded that there is no accumulation of the kinesin Pavarotti around the region of the central spindle in *aust* mutant meiotic anaphase (Gao *et al.,* 2008) Given that Subito failed to localise to MTs during male meiosis, I therefore investigated the localisation of Pavarotti in control and *aust* mutant spermatocytes.

In control spermatocyte squashes, Pavarotti-GFP shows a dynamic localisation. In early anaphase, Pavarotti localises to spindle MTs (Fig. 3-3). As cells progress through anaphase into telophase this localisation becomes restricted to the plus ends of the interdigitating MTs of the central spindle (Fig. 3-3). In addition, a clear accumulation at the equatorial membrane is seen (arrow, Fig. 3-3). As well as localising to the central spindle as clearly shown in Fig. 3-4, Pavarotti-GFP in control cells also localises to the ring canals (Fig. 3-3); structures derived from the contractile ring found in incomplete cytokinesis (which occur during both the mitoses and the meiotic divisions of *Drosophila* spermatogenesis).

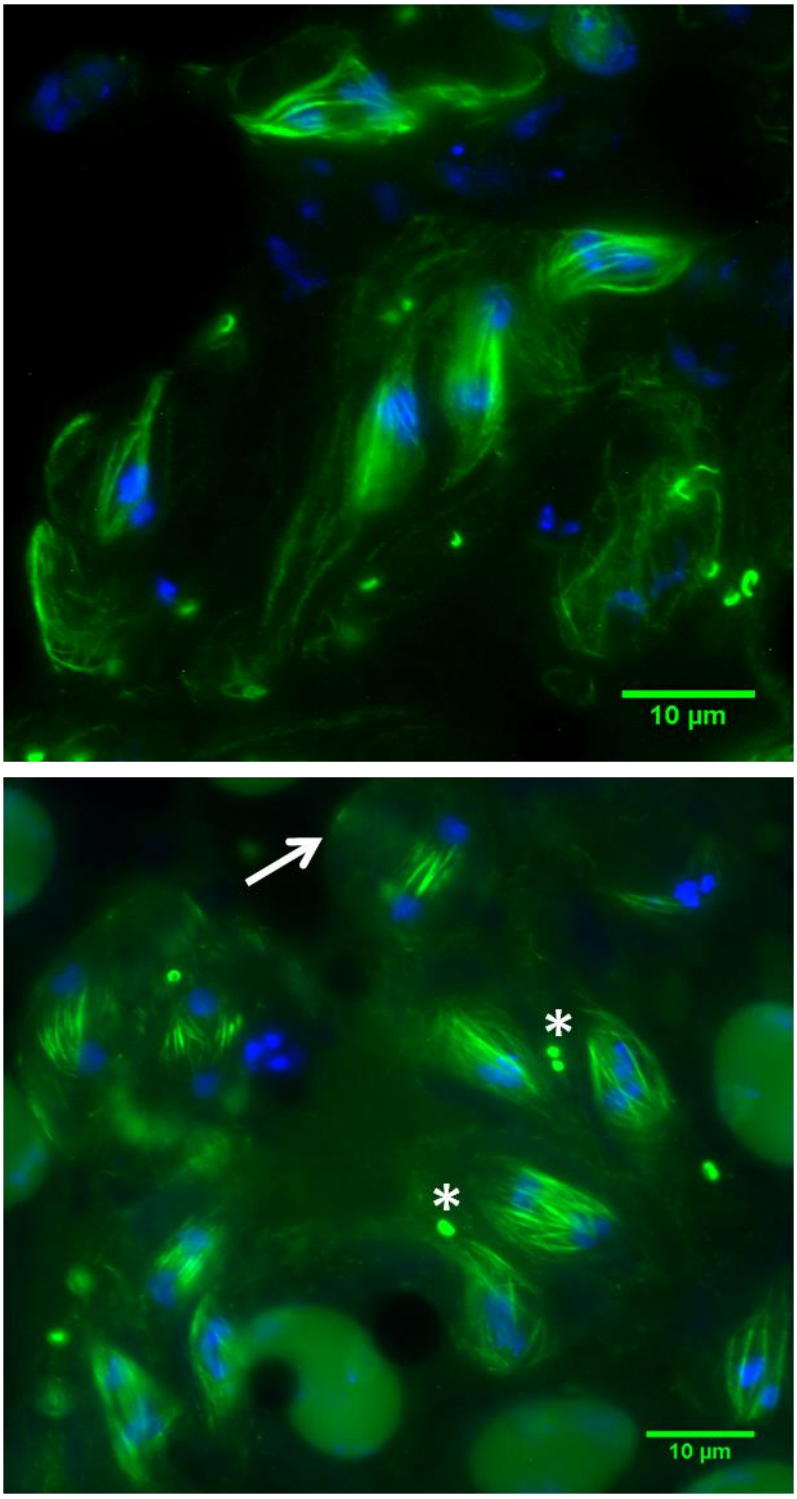

Figure 3-3. Pavarotti-GFP in control spermatocytes localises to spindle MTs, to the equatorial membrane and to interconnecting MT in late anaphase II. Pavarotti-GFP in green; DNA stained with Hoechst (5 µg/ml) in blue. * = Pavarotti-GFP localising to the ring canal (not all have been highlighted) Arrow = Pavarotti-GFP localisation to the equatorial membrane.

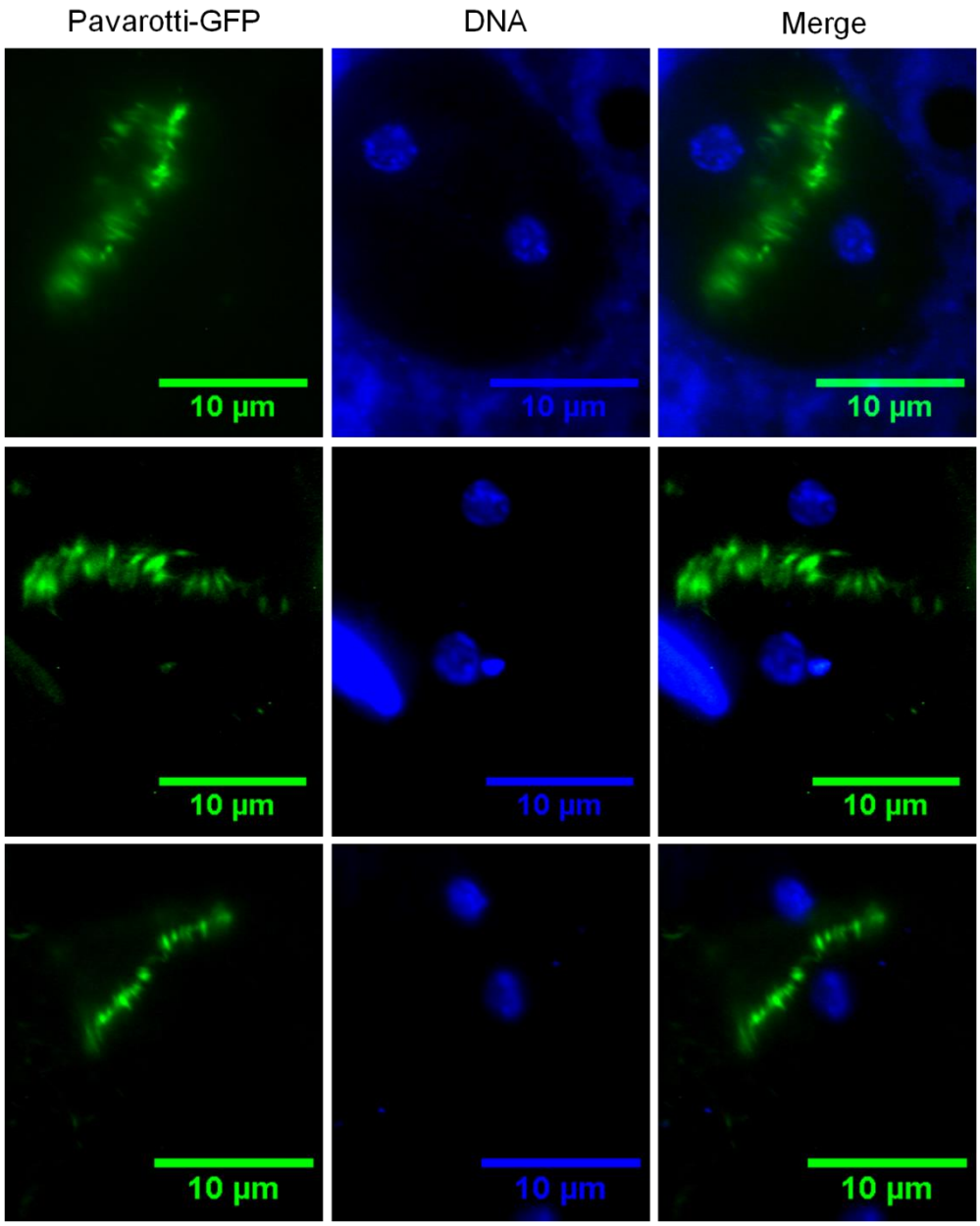

Figure 3-4. Pavarotti-GFP in control spermatocytes localises to the central spindle in telophase II. Pavarotti-GFP in green; DNA stained with Hoechst (5 µg/ml) in blue.

3.1.3. Pavarotti-GFP does not become mis-localised in the *aust*^{1}.Pavarotti-GFP line in anaphase

In order to get more detailed localisation of Pavarotti-GFP during male meiosis, I adapted a fibrin clot visualisation technique based on Forer *et al.*, 1998. Though extensive optimisation was undertaken I found that, under conditions in the lab, cells were unable to continue their development through meiosis even though the methodology undertaken should have allowed for this to occur, as succeeded by Forer *et al.* (1998) and Wong *et al.* (2005) with their research on crane-fly and *Drosophila* spermatocytes respectively. Obtaining larval spermatocytes in meiosis, even with a revised fly food recipe and careful fly husbandry also proved challenging.

However, the technique did allow visualisation of cells without the morphological deformation associated with squashes and other methods. In control spermatocytes (Fig. 3-5a,c,e,g) there was clear localisation of Pavarotti-GFP to ring canals and on the MTs during anaphase and strong accumulation of Pavarotti-GFP on the central spindle/spindle midzone, corresponding to the plus ends of the anti-parallel overlapping MT bundles during late anaphase/early telophase II. In *aust* mutant spermatocytes (Fig. 3-5b,d,f,h), however, although Pavarotti-GFP localised to ring canals and to MTs in anaphase/early telophase, the protein failed to concentrate at the plus ends of MT bundles. One interpretation of this result is that it is a consequence of not forming a correct central spindle; previous research (Gao *et al.,* 2008) and work undertaken in this study demonstrates that Aust is essential for a robust

central spindle with properly ordered MTs. However, Fig. 3-5 f shows clearly that Pavarotti-GFP is present along the length of MTs during anaphase, rather than accumulating at the plus ends. This suggests that CPC function may not be required for initial recruitment of Pavarotti to MTs upon entry into anaphase, but is required for the specific relocalisation to the plus ends of growing central spindle.

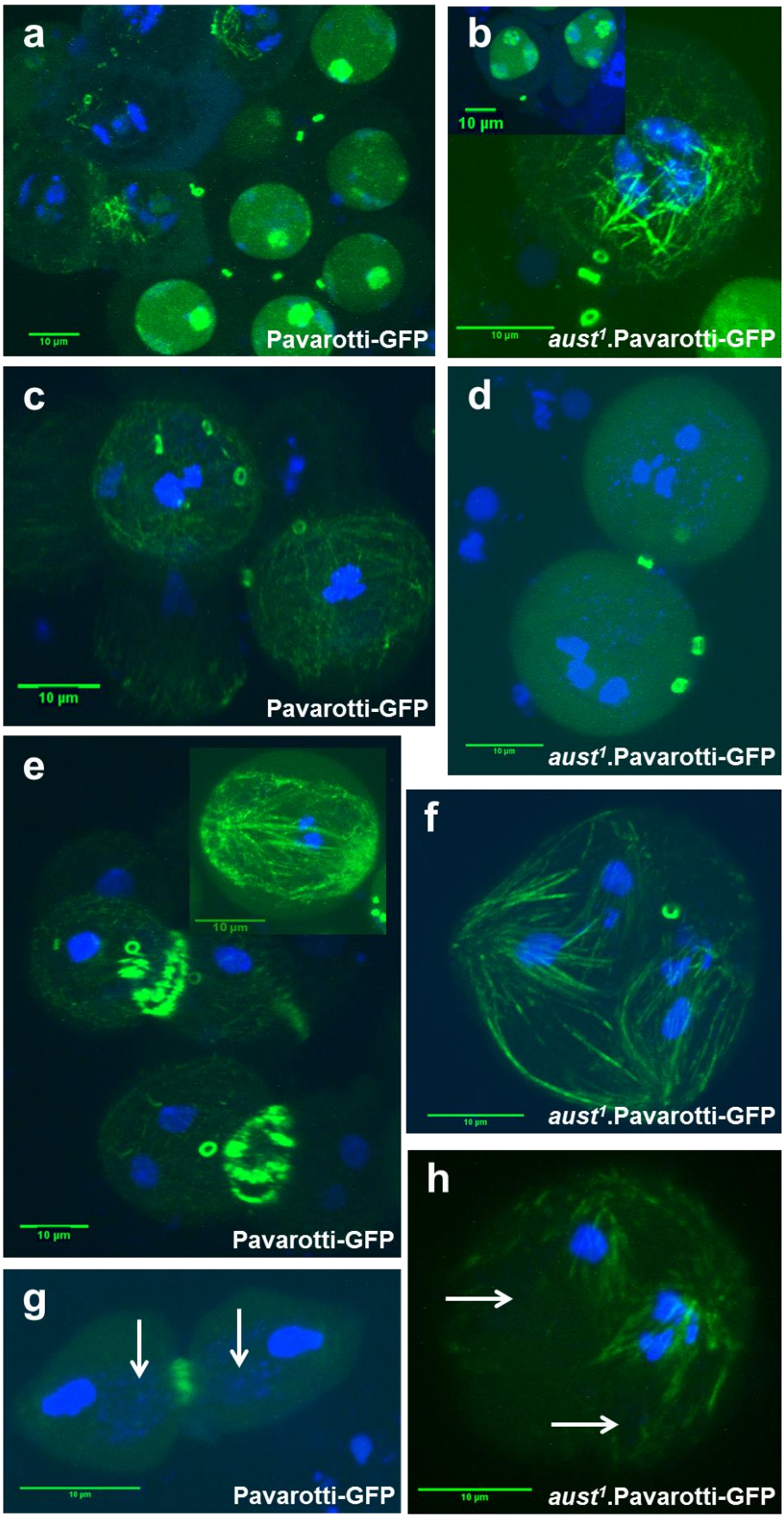

Figure 3-5. Pavarotti-GFP localisation at a variety of stages in control and *aust*^{1}.Pavarotti-GFP spermatocyte cells Pavarotti-GFP in green; DNA stained with Hoechst (5 µg/ml) in blue (see next page for Figure Legend).

Figure 3-5. cont. (a) Control interphase/prophase **(b)** *aust*^{1} interphase/prophase. In interphase, Pavarotti-GFP can be seen localising to the nucleolus in both the control and *australin* mutant background. In early meiosis, Pavarotti-GFP is seen localising to the spindle in both backgrounds. Pavarotti-GFP can also be seen on the ring canals in control and *aust*^{1} spermatcytes, this localisation is to pre-meiotic ring canals.

(c) Control metaphase **(d)** *aust*^{1} metaphase. There is absence of Pavarotti-GFP localisation to the spindle MTs in metaphase of *aust*^{1} mutants**.**

(e) Control anaphase/telophase **(f)** *aust*^{1} anaphase. Pavarotti-GFP localises uniformly to the astral and kinetochore MTs during anaphase in both backgrounds but there is no evidence of localisation to the interlocking MTs as seen in the control ((e) inset) or to the central spindle/spindle midzone (also seen in the control). As well as lack of localisation to the plus ends of the interdigitating MTs in the *aust*^{1} mutant, the DNA has become decondensed showing evidence of mis-segregation.

(g) Control telophase **(h)** *aust*^{1} telophase. Control cell in late telophase II with Pavarotti-GFP localising to the midbody. As well as the DNA, mitochondrial aggregates as shown by the white arrows can be seen separating equally between the two cells which will go on to form the Nebenkern. This can faintly be seen in the *aust*^{1} mutant as also highlighted by the white arrows. DNA in the *aust*^{1} mutant has segregated unevenly and there is no localisation of Pavarotti-GFP to the midbody.

3.1.4. Polo-GFP

Previous research in which the function of the CPC subunit INCENP was perturbed using RNAi demonstrates that, in DMel-2 cells, the CPC is not necessary for Polo localisation to the kinetochores but is required for Polo phosphorylation at the kinetochores (levels of active Polo at the kinetochores was reduced) (Carmena *et al.,* 2012a). This has also been reported in *Drosophila INCENP* mutant larval neuroblasts and HeLa cells (Carmena *et al.,* 2012a). Using *aust* mutant cells, this research aimed to determine whether the CPC affects Polo localisation in *Drosophila* spermatocytes.

As expected, while control Polo-GFP post-meiotic spermatids displayed normal 1:1 ratio of nuclei and Nebenkern, *aust*^{1}.Polo-GFP spermatids showed a single nucleus of ~4 times the size of controls and a large, misshaped Nebenkern (Fig. 3-6), confirming that Aust was indeed mutated in this transgenic combination.

In control spermatocytes undergoing prophase, Polo-GFP localised to the centrosomes, the astral MTs and to a region of condensing DNA (Fig. 3-7; 3-8a). This localisation was not perturbed in *aust*^{1}.Polo-GFP cells, although in late prophase there appeared to be less Polo-GFP localisation to the centrosomes in the mutant line in comparison to the control - with what appeared to be localisation to the centrioles and no localisation to the PCM (Fig. 3-7; 3-8b). Metaphase control cells showed an accumulation of Polo-GFP on the spindle, at centromeres and/or on kinetochores (Fig. 3-8c). Again, *aust* mutant spermatocytes at metaphase displayed a similar localisation demonstrating that the CPC is

not required for Polo to localise either to MTs, centromeres or to kinetochores (Fig. 3-8d). Through anaphase and telophase Polo-GFP maintained its centrosomal localisation but re-distributed clearly to the middle of the central spindle (Fig. 3-8e,g) - similar to the localisation of Pavarotti-GFP described in Section 3.1.3. In contrast, due to the absence of a central spindle in *aust* mutants, there was no clear ring of Polo-GFP staining in the centre of *aust* mutant anaphase or telophase cells (Fig. 3-8f). However, in one case, a weak “interior” spindle staining was observed, with an accumulation of Polo-GFP at the centre of this spindle, presumably correlating to a small population of interdigitating antiparallel MTs (Fig. 3-8h). Overall, these results suggest that Polo-GFP localisation is independent of the CPC.

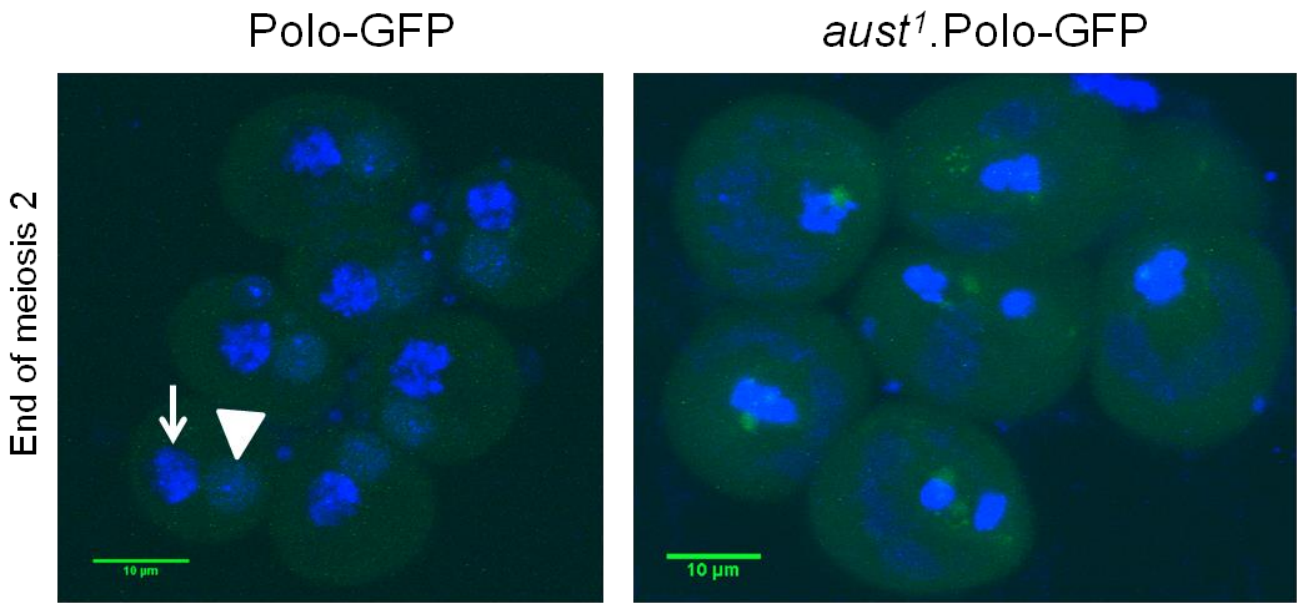

Figure 3-6. *aust*^{1}.Polo-GFP line shows defects in chromosome segregation and cytokinesis. Polo-GFP in green; DNA stained with Hoechst (5 µg/ml) in blue. Onion stage spermatids show one equal sized nuclei (thin arrow) to one equal sized Nebenkern (arrow head) in control line. In *aust*^{1}.Polo-GFP line each spermatid contains multiple nuclei of different sizes with an enlarged Nebenkern.

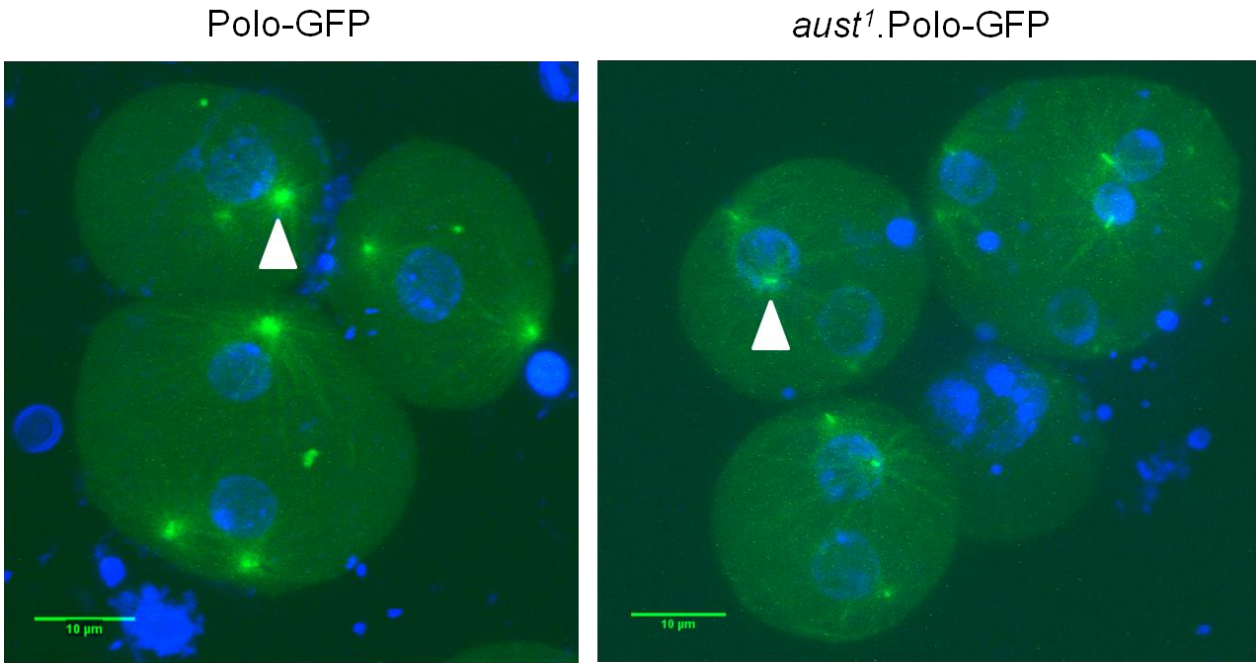

Figure 3-7. Intensity of Polo-GFP localisation is affected in late prophase in the *aust*^{1}.Polo-GFP line. Polo-GFP can be seen localising to the centrosomes in both the control and mutant line as indicated by the arrow heads. In late prophase II there appears to be less Polo-GFP localisation to the centrosomes in the mutant line in comparison to the control. Polo-GFP in green; DNA stained with Hoechst (5 µg/ml) in blue.

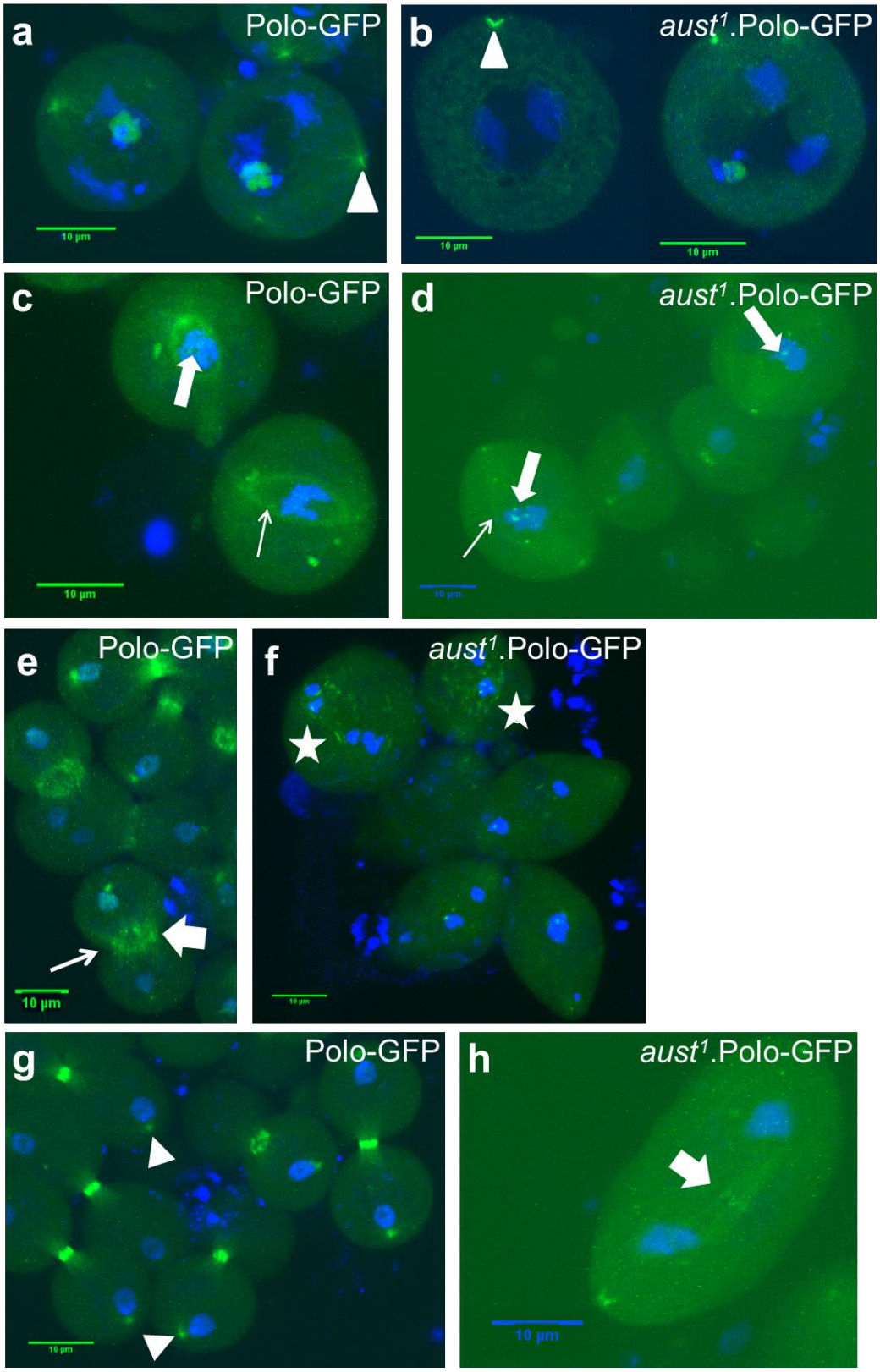

Figure 3-8. Polo-GFP localisation at a variety of stages in control and *aust*^{1}.Polo-GFP spermatocyte cells. (a) control interphase/early prophase **(b)** *aust*^{1} interphase/early prophase **(c)** control metaphase **(d)** *aust*^{1} metaphase **(e)** control anaphase **(f)** *aust*^{1} anaphase **(g)** control telophase **(h)** *aust*^{1} telophase Polo-GFP in green; DNA stained with Hoechst (5 µg/ml) in blue.

Figure 3-8. cont. (a) and (b) Polo-GFP can be seen localising to the centrosomes in both the control and *aust*^{1} mutant as indicated by the arrow heads.

(c) and (d) Thin arrows show Polo-GFP localisation to the astral MTs. Thick arrows show localisation to the kinetochores/centromeres. From these images, there seems to be more spots of Polo-GFP localisation to the kinetochores in the *aust*^{1}.Polo-GFP line but this could be due to the differences in stages between the two images; the stage from *aust*^{1}.Polo-GFP line is slightly later into anaphase than the control line and/or due to the DNA in the control line obstructing the microscope from picking up the Polo-GFP fluorescence.

(e) and (f) Due to lack of the protein Australin, there is no furrow ingression; this is only seen in the control images as indicated by the thin arrow. There is Polo-GFP localisation to the central spindle in the control image as indicated by the thick arrow. In an *australin* mutant, a central spindle is unable to form (Gao *et al.,* 2008) therefore no Polo-GFP localisation to the central spindle is seen in the *aust*^{1}.Polo-GFP line. There is some localisation to the spindles and/or kinetochores (stars) in the *aust*^{1}.Polo-GFP line but the localisation appears irregular. It could be localisation to unattached kinetochores from faulty chromosome segregation; DNA segregation looks not look equal.

(g) and (h) In control cells during telophase and cytokinesis Polo-GFP concentrates on the central spindle midzone. Polo-GFP is also seen back on the centrosomes in late telophase (arrow heads). There does seem to be some localisation to what appears to be a central spindle (block arrow) in the *aust*^{1} mutant.

3.1.5. Discussion

In this part of the Chapter, I have examined the effect of removing the CPC on the dynamic localisation of a number of proteins known to be key regulators of central spindle formation; namely the kinesins Subito and Pavarotti, and the kinase Polo. The work has increased our understanding of the relationship between these proteins in this key model system, suggesting that the CPC is required for the specific accumulation of Pavarotti to the plus ends of central spindle MTs.

By examining the localisation of Subito-GFP in spermatocytes I have found there is no distinctive concentration of Subito to any part of the mid-zone during anaphase and telophase. It was previously found that Subito mutant males are fertile; therefore it is likely that in spermatogenesis Subito is not as important for cell division as seen in other cell types of *Drosophila* (Jang *et al.,* 2005; Cesario *et al.,* 2006). Given the previously reported role of Subito in localising the CPC to the central spindle in, for example, larval brain cells (Cesario *et al.,* 2006); this strongly suggests that another protein is responsible for CPC transportation/accumulation in spermatocytes.

However, this could be disputed. There are a few caveats associated with this result as there is the possibility that the GFP tag, due to its size, is affecting the function and localisation of Subito to the central spindle. Further investigations would need to be undertaken to determine the validity of the line given; this could be undertaken by showing that the Subito-GFP rescues a Subito mutant phenotype. It could also be discovered by using antibodies against Subito that localises to the central

spindle in larval brain cells and then determining whether or not they localise in testes.

Previous research has examined the localisation of Pavarotti in fixed cells; either in *Drosophila aust* spermatocyte cells (Gao *et al.,* 2008) or in cells treated with dsRNA against one or more of the CPC components (Adams *et al.,* 2001; Giet and Glover, 2001). In both cases, in contrast to wild-type cells, it was found that in cells lacking CPC, Pavarotti was absent from the central spindle midzone and equatorial cortex (Gao *et al.,* 2008). Both studies concluded that the CPC is involved in the recruitment of Pavarotti to the cleavage site. In contrast, research by Adams *et al.* (2005) concluded that Pavarotti localisation was distinct to that of the CPC. In Dmel-2 tissue culture cells with depleted levels of Aurora B or INCENP, Pavarotti was consistently detected in midbody structures. However, given this was the result of gene knock down, not a null mutation, it is still possible that some functional CPC was present in this study.

The research carried out in this thesis shows that the CPC is not responsible for Pavarotti's localisation to the astral and kinetochore MTs during metaphase or anaphase, but has a potential role in permitting Pavarotti, as a MT motor protein, to "walk up" and concentrate to the plus ends of the interdigitating MTs in anaphase. It is still to be determined whether this role is a direct consequence of the loss of the CPC or indirectly due to defects in the central spindle itself caused by the lack of the CPC. Guse *et al.* (2005) research indicates that the CPC is responsible for phosphorylating Pavarotti as part of the centralspindlin

complex therefore this suggests it is a direct consequence. Gao *et al.* (2008) concluded that no interdigitating MTs were present in the *australin* mutant spermatocytes, although from observing the movies from their research there is indication that some interdigitation occurs between MTs emanating from opposite centrosomes, albeit only for a brief time. In contrast to my research, they found Pavarotti absent from MTs in anaphase and telophase in the *aust* mutant. Due to their methodology; fixation of cells rather than live cell imaging, and use of antibodies to highlight protein localisation instead of using a GFP-tag, this could potentially explain their results.

It would be of interest to carry out FRAP (fluorescence recovery after photobleaching) to find out whether Pavarotti is able to reaccumulate at the MTs in the *aust* mutant. This could help determine whether the CPC is responsible just for the initial localisation of Pavarotti or if it is needed to maintain an accumulation of Pavarotti on the MTs. In addition, the next logical step would be to look at whether the CPC is responsible for the functioning of Pavarotti. Pavarotti, as part of the centralspindlin complex, controls the localization of the RhoGEF Pebble (Pbl), orthologue of the human protein ECT2) that in turn allows for the activation of Rho. Rho is required for contractile ring assembly and the start of cytokinesis (Zhao *et al.,* 2005). Production of a line with Pbl-GFP or staining using antibodies against Pbl could assist in establishing whether the CPC affects the role of Pavarotti in localising ECT2 to where the furrow would form.

This thesis provides evidence that Polo-GFP localisation throughout cell division is independent of the CPC and therefore suggests Polo acts upstream of the CPC. It is known from previous research that Polo concentrates at centromeres before INCENP (i.e. the CPC) (Carmena *et al.,* 2012a) and it has also been observed that, upon RNAi of Aurora B or INCENP, there is less Polo at the kinetochores (Carmena *et al.,* 2012a). There does also seem to be some localisation to what appears to be a bundle of interdigitating MTs in anaphase in the *aust*$^{1.22}$.Polo-GFP line (see Fig. 3-8 f). This structure is not a central spindle per se - there are very few MTs and these are concentrated to the very interior of the cell so it is unclear what this population represents. Given that these MTs were not highlighted in spermatocytes expressing Pavarotti-GFP, one explanation is that they are a distinct population of MTs, perhaps remnants of the overlapping spindle MTs, which specifically accumulate Polo. Further work is required to precisely define the consistency of this localisation.

Polo is able to localise to the kinetochores without the CPC but subsequent activation of Polo is unlikely (Carmena *et al.*, 2012a). Polo is needed for the stabilisation of kinetochore-MT so without Polo activation it would lead to chromosome mis-segregation which can be seen in Fig. 3-6.

In prophase II of *aust* spermatocytes, the concentration of Polo-GFP to the centrioles appears to be less intense than in control cells and there is no localisation to the surrounding PCM. Quantification of this would need to be undertaken to verify this result but, if consistent, suggests that the

regulation of Polo by the CPC may persist from one meiotic cycle to the next.

In summary, observations of GFP-fusion proteins in 3D, using fibrin clot-based immunofluorescence has provided new and intriguing data relating to the relationship between the CPC and Polo and Pavarotti. However, following Pavarotti-GFP and Polo-GFP live throughout cell division I hoped to accurately define the moment where, in *aust* spermatocytes, the localisation of these proteins becomes abnormal. As I was unable to achieve conditions where spermatocytes progressed normally through meiosis, we are still left with questions surrounding the relationship between these important cytokinesis effectors. Improvement to the live cell imaging technique such that we can follow GFP localisation throughout metaphase, anaphase and telophase should finally allow these questions to be answered.

3.2. Investigation into the function of the proposed CPC component, TD60

TD60 (telophase disc protein of 60 kDa) was originally reported as a protein that associates with the centromeres of metaphase chromosomes and transfers to a cortical ring by telophase (Andreassen *et al.,* 1991). Given this localisation was qualitatively similar to that of the CPC components INCENP, it has been suggested that TD60 is an associated member of the CPC with similar localisation in human cells (Andreassen *et al.,* 1991). This hypothesis is supported by a further study that demonstrated that human TD60 could be co-precipitated by the CPC component Borealin (Gassmann *et al.,* 2004), and that TD60 is required for full Aurora B activation (Rosasco-Nitcher *et al.,* 2008). However, the precise role of TD60 in the cell remains elusive.

The Wakefield lab generated a GFP-transgenic fly line of the *Drosophila* homologue of TD60, in order to investigate its function in mitosis and meiosis. There is no mutant allele of TD60 and previous work in the lab failed to demonstrate a phenotype when TD60 was knocked down using RNAi in S2 tissue culture cells (Duncan and Wakefield, unpublished). However, RNAi was incomplete - with ~5% of TD60 protein remaining after extensive RNAi treatment. In this project, I attempted RNAi *in vivo* - knocking down TD60 in the early embryo and assessing the effect on the fast, synchronous mitotic divisions that take place. As an alternative approach, I purified an antibody raised against full-length TD60 and injected it into embryos, hypothesising that it may interfere with the function of endogenous TD60. By reassessing the localisation of TD60-

GFP in the early embryo, I show that, although TD60-GFP does not localise similarly to the CPC, its localisation is affected by injection of anti-TD60 antibodies, suggesting they do interfere with function. The consequence of injecting these antibodies upon mitosis is severe - I provide evidence that TD60 functions in maintaining mitotic MT organisation, mitotic checkpoint signalling and chromosome segregation.

3.2.1. Anti-TD60 antibody purification

Affinity purified antibodies can be extremely useful tools in investigating protein function. I therefore undertook purification of previously generated rabbit anti-TD60 polyclonal antibodies generated against a bacterially expressed and purified MBP-TD60 fusion protein (Duncan and Wakefield, unpublished). To ensure separation of anti-TD60 and anti-MBP antibodies, DNA constructs to express MBP and MBP-TD60 were transformed into bacteria and expressed protein purified. Both MBP and the MBP-TD60 were covalently attached to Affigel 15 beads and serum sequentially passed through the MBP column until all anti-MBP antibodies had been depleted. The anti-MBP depleted serum was then passed through the MBP-TD60 column, in order to elute anti-TD60 specific antibodies. Fig. 3-9 outlines the purification of the proteins used in this affinity purification technique. Western blotting of *Drosophila* 0-3 hour old embryos (Fig. 3-10) demonstrates that this approach was successful: anti-TD60 antibodies recognise a single band of ~60 kDa. Known quantities of embryo extract were also used to calculate roughly how much TD60 was present in a given amount of extract (Fig. 3-10). ~50 ng of pure MBP-TD60 gave a band of similar intensity to 0.5 µl of

embryo extract. The embryo extract was prepared by homogenising 100 mg of embryos in 400 µl extraction buffer. 0.5 µl was loaded on a gel; this equates to 1/800th of total TD60 present in 100 mg of embryos. Therefore 50 ng x 800 = 40000 ng of TD60 in 100 mg embryo, thus there appears to be roughly 400 ng TD60 in 1 mg of embryos.

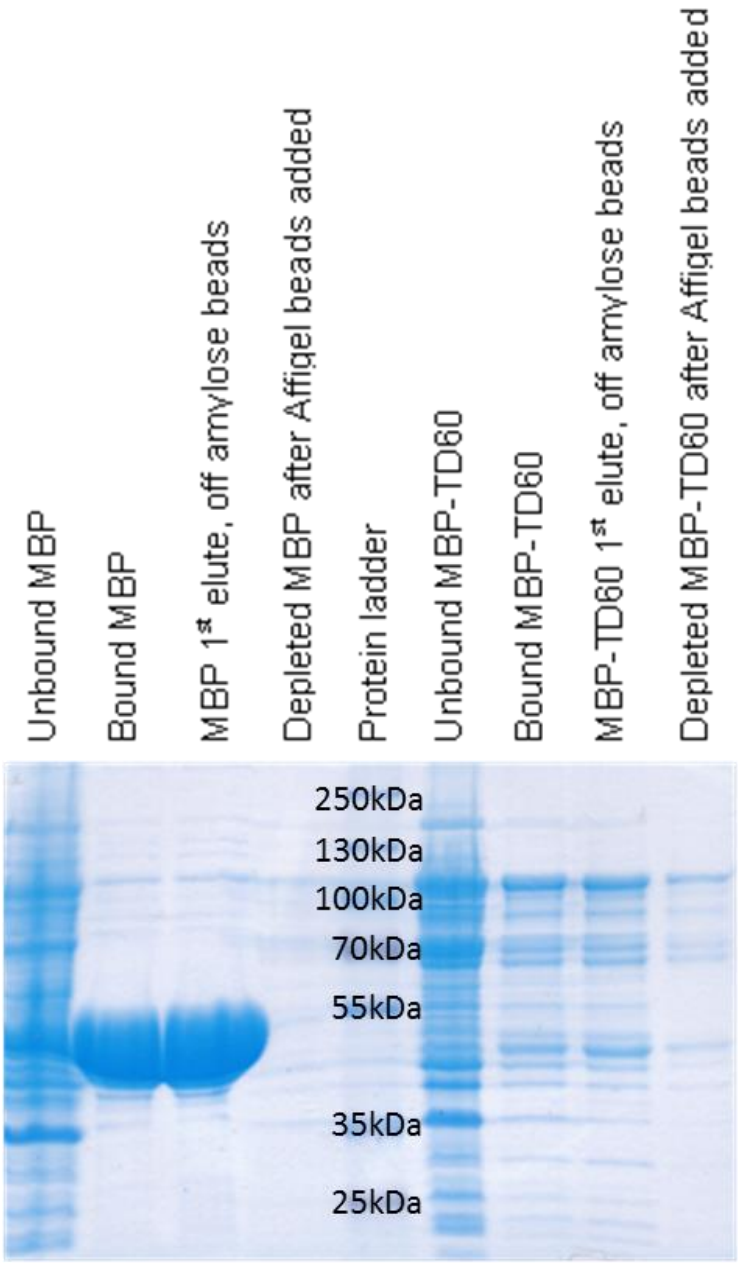

Figure 3-9. Gel showing both MBP and MBP-TD60 protein bound successfully to Affigel 15. *Bound MBP* - the MBP has bound to the amylose resin beads. *MBP 1st elute* - MBP off amylose beads after maltose added; the gel shows this has worked. *Depleted MBP* - the MBP has bound to the Affigel beads. This is also seen for the MBP-TD60 protein. There has been some degradation of the protein and not all the protein has bound to the Affigel beads but the gel shows that some has bound as the depleted well shows a band that is a smaller/weaker than the band from the 1st elution.

3.2.1.1. Checking the validity of the purified antibodies

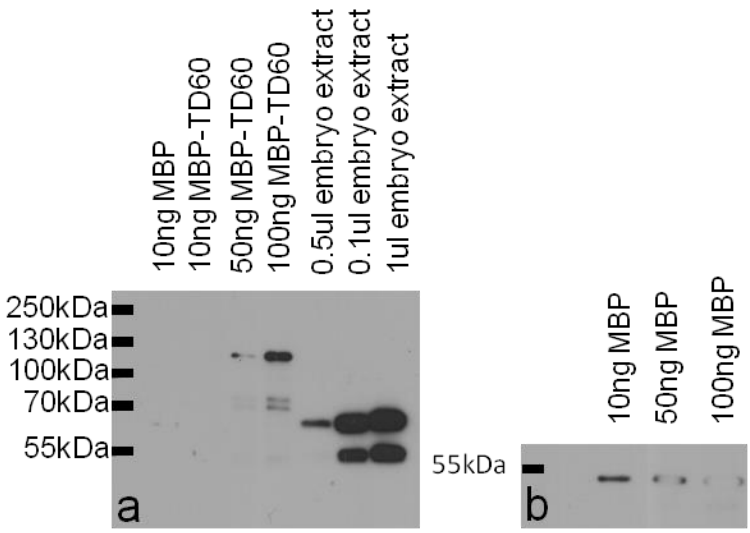

Figure 3-10. Western blot confirming the specificity of the anti-TD60 and anti-MBP antibodies. (a) Western blot of both pure MBP-TD60 and embryo extract incubated with affinity-purified TD60 antibody. A major band of predicted ~100 kDa is seen in the MBP-TD60 lane while a major band of ~60 kDa is seen in extracts. Anti-MBP antibodies have been effectively depleted as no cross-reactivity of affinity purified antibodies is seen in lanes containing MBP alone. (b) Western blot showing the purified anti-MBP antibody (which has a molecular weight of ~42 kDa) has been successfully purified.

3.2.2. TD60 RNAi

3.2.2.1. TD60 embryonic knock down is incomplete and produces no clear mutant phenotype

TD60 RNAi has been carried out in HeLa cells (Mollinari *et al.,* 2003) but due to the presence of the spindle assembly checkpoint the cells arrest at prometaphase. Previous work in the lab has attempted to knock down *Drosophila* TD60 in S2 tissue culture cells and, although no phenotype was observed, ~5-10% of TD60 was still present after RNAi (Duncan and Wakefield, unpublished). To attempt to investigate the function of *Drosophila* TD60, the gene was specifically silenced by expressing dsRNA in embryos. To maximise knock down of the TD60 protein in the embryo, the UAS driven Dicer was used (Handler *et al.,* 2011), and the embryo collection chambers were placed at 28°C to further enhance the efficacy of the *in vivo* RNAi processing pathway.

Following treatment, TD60 protein levels were measured. Western blotting determined that TD60 protein levels had been reduced but substantial TD60 protein remained (Fig. 3-11). One technical ambiguity associated with this results is that, due to the nature of the genetic cross only half the embryos contained the second driver; maternal α-Tubulin-GAL4, which is needed for driving Dicer expression, therefore only half the embryos expressed the TD60 RNAi. Taking into account the embryos that did not have their TD60 levels reduced, the Western blot results cannot discount that a fraction of TD60 is still present in TD60 RNAi embryos.

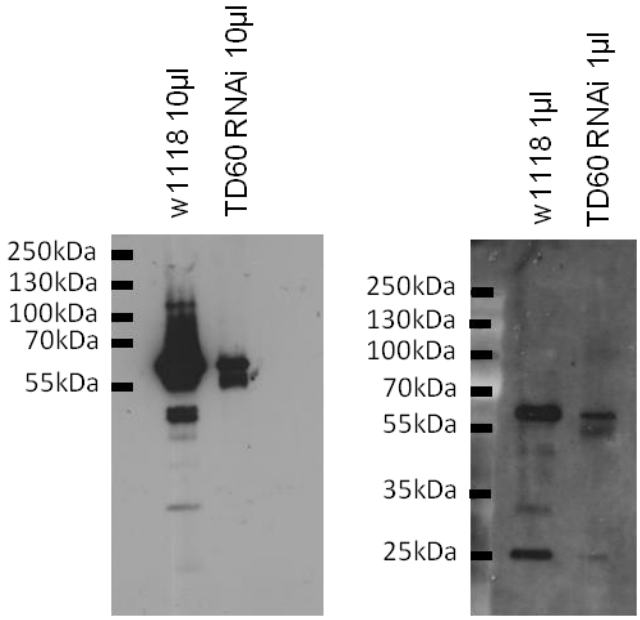

Figure 3-11. TD60 RNAi reduces TD60 protein levels. Embryos were harvested at 28°C and collected from flies possessing both one copy of UAS-driven *in vivo* TD60 dsRNA hairpin construct and one copy of UAS-driven Dicer, with half the embryos collected also under the control of maternal-α-Tubulin-GAL4 (used to drive Dicer/RNAi expression). Western blotting was carried out to determine the extent to which the RNAi had decreased TD60 protein levels in the embryo.

As only half of the embryos collected expressed the TD60 RNAi, it provided an internal control when fixing and staining were undertaken. Around 300 embryos were analysed and no abnormalities in DNA or MT organisation were detected (Fig. 3-12). However, in parallel experiments, undertaken on embryos from the same collection batch, the intensity of TD60 was reduced in approximately 50% of TD60 RNAi embryos (Fig. 3-13). This is consistent both with the results seen from the Western blotting (Fig. 3-11) and the expected frequency of embryos in which TD60 should be reduced via RNAi. As an additional control, post-cellularised RNAi embryos were fixed and stained for anti-TD60. There were no changes in the intensity of TD60 staining when compared to control embryos (Fig. 3-14). This is expected as zygotic transcription (which is not affected by the RNAi driver) occurs at the end of the 13 syncytial mitotic divisions, prior to cellularisation.

In conclusion, although *in vivo* RNAi does result in a reduction of TD60 expression in the early embryo, it is likely that some endogenous TD60 remains, even when Dicer is co-expressed and the UAS driver is enhanced through incubation at 28°C. Therefore, an absence of abnormalities in mitosis in these embryos cannot be used to determine whether TD60 normally functions during mitosis.

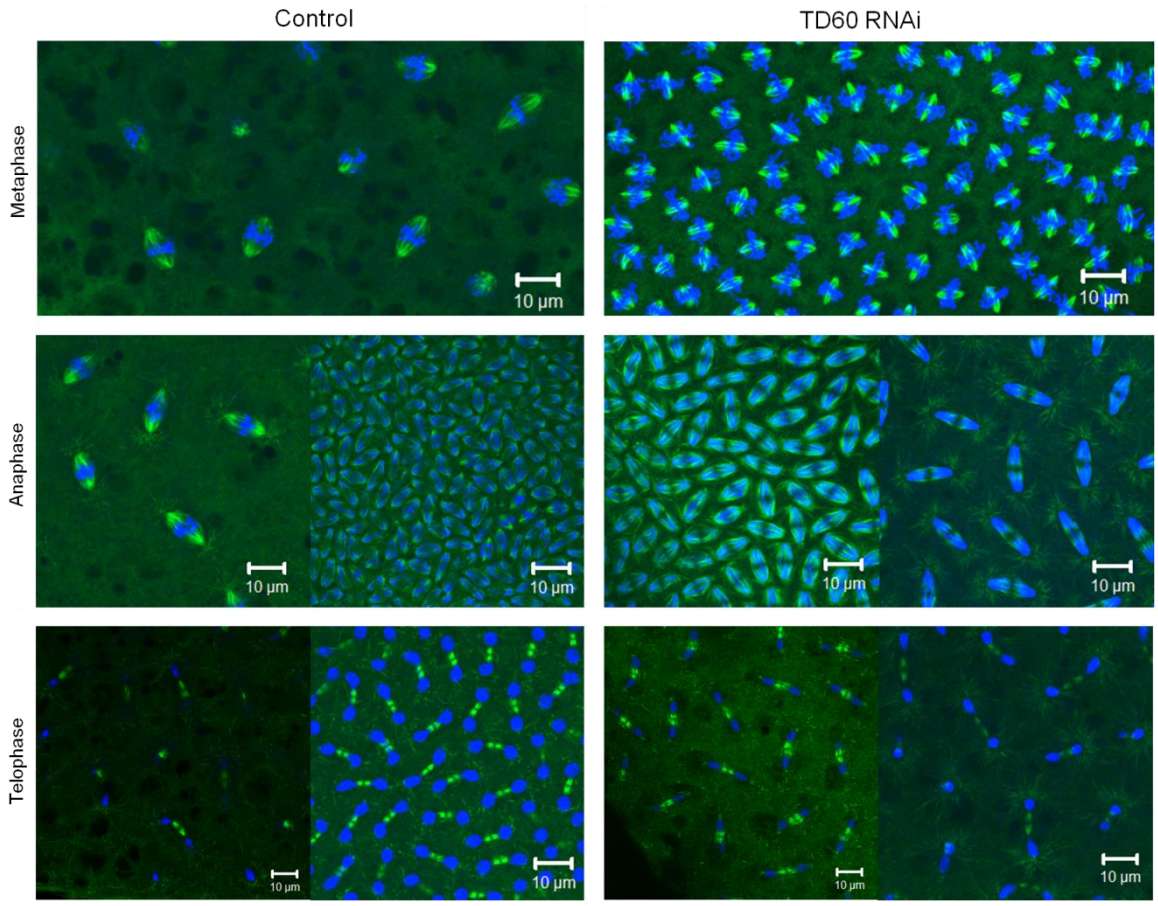

Figure 3-12. No clear phenotype seen in TD60 RNAi embryos. Embryos were harvested at 28°C and collected from flies possessing both one copy of UAS-driven *in vivo* TD60 dsRNA hairpin construct and one copy of UAS-driven Dicer, with half the embryos collected also under the control of maternal-α-Tubulin-GAL4 (used to drive Dicer expression). Embryos were stained using anti-Tubulin (green) and Hoechst (blue). Z stacks were taken using confocal microscopy.

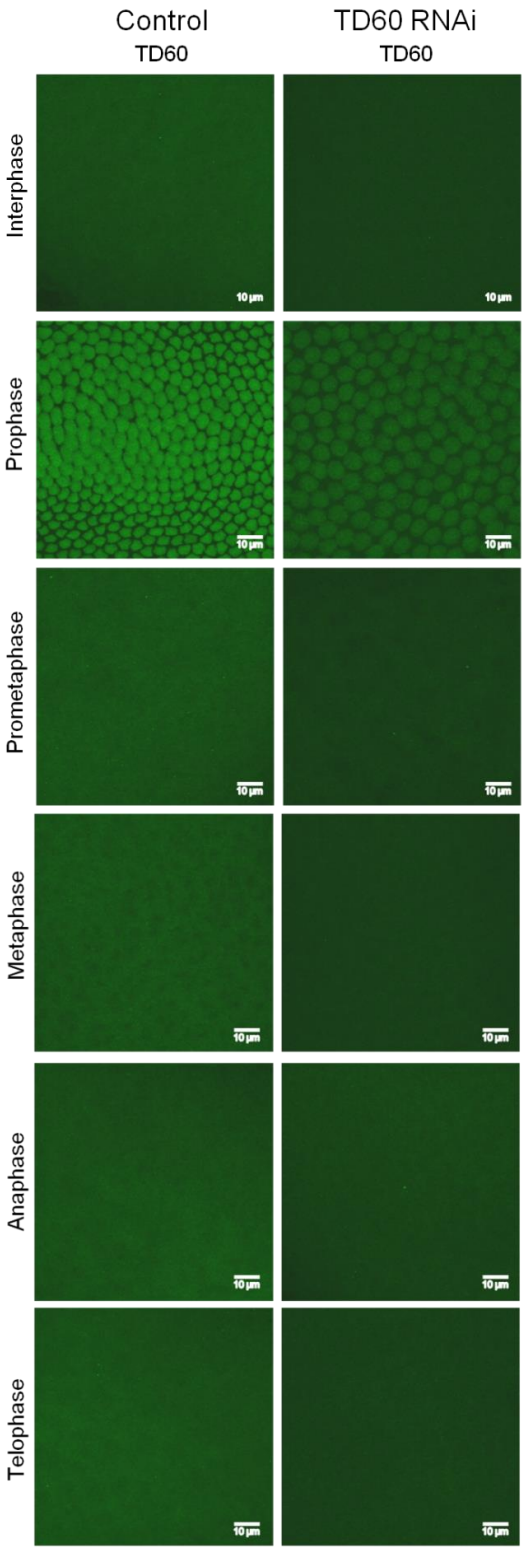

Figure 3-13. TD60 staining intensity is reduced in TD60 RNAi embryos. Taking the images from the previous two figures and placing them side-by-side it is possible to see a slight reduction in TD60 staining throughout cell division in the TD60 RNAi embryo. Embryos were stained using anti-TD60 (green). Z stacks were taken using confocal microscopy.

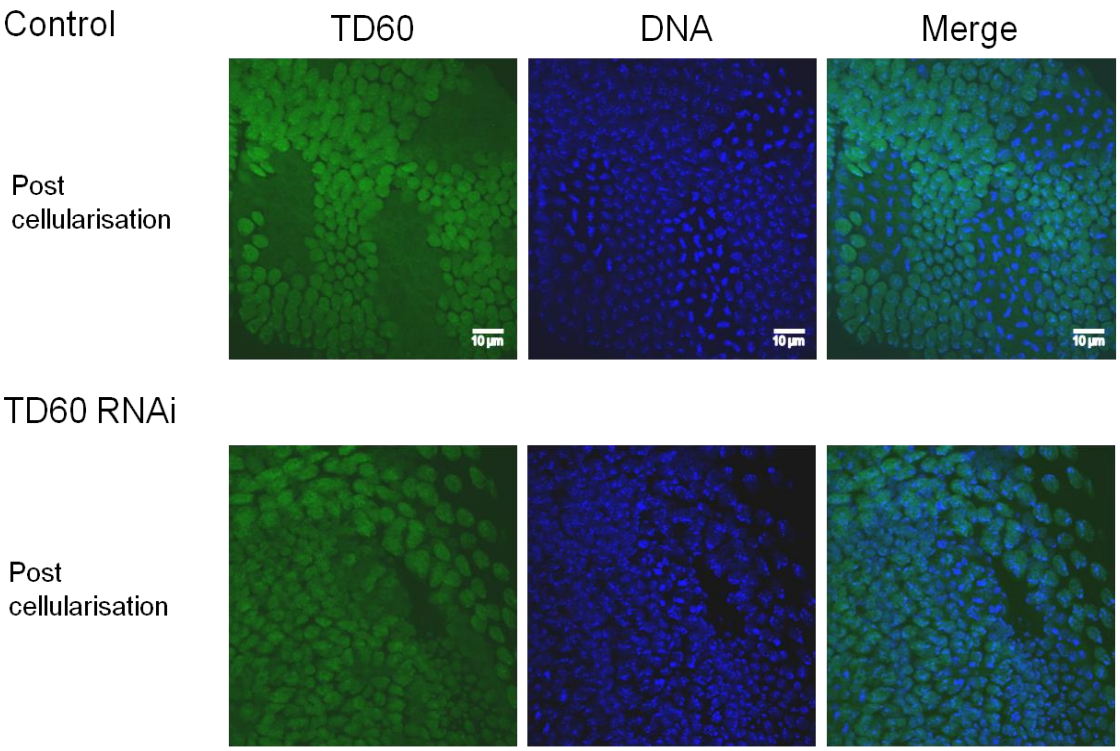

Figure 3-14. No changes in TD60 staining when comparing intensity in post cellularised control and TD60 RNAi embryos. Embryos were stained using anti-TD60 (green) and Hoechst (blue). Z stacks were taken using confocal microscopy.

3.2.3. Injection of affinity purified anti-TD60 antibodies into syncytial embryos affects the localisation of TD60-GFP

As an alternative approach to RNAi, the affinity purified anti-TD60 antibodies (αTD60) were injected into cycle 10-12 syncytial embryos expressing one of a number of GFP-fusion proteins and time-lapse movies acquired. In order to first determine the effect of anti-TD60 on TD60 itself, injections were made into embryos expressing TD60-GFP.

In uninjected *Drosophila* embryos, TD60-GFP is nuclear in interphase, redistributes to the cytosol upon nuclear envelope breakdown (NEB), is weakly visible on condensing chromatin after NEB and on the mitotic spindle at metaphase. During anaphase, TD60-GFP remains both on chromatin and faintly on MTs while, by telophase, TD60-GFP is again nuclear (Fig. 3-15). Unlike the CPC, TD60-GFP does not clearly localise to the embryonic central spindle or to kinetochores. When anti-TD60 antibodies are injected in interphase, the levels of TD60-GFP in the nucleus decrease over time (Fig. 3-16), such that it is excluded from the nucleus by NEB - the presence of cytoplasmic puncta is a clear marker of antibody-antigen aggregation, strongly suggesting the antibody is binding to TD60-GFP (Fig. 3-15). Although, in this instance, mitosis proceeded upon antibody injection, this seems likely to be due to injection of low levels of antibodies.

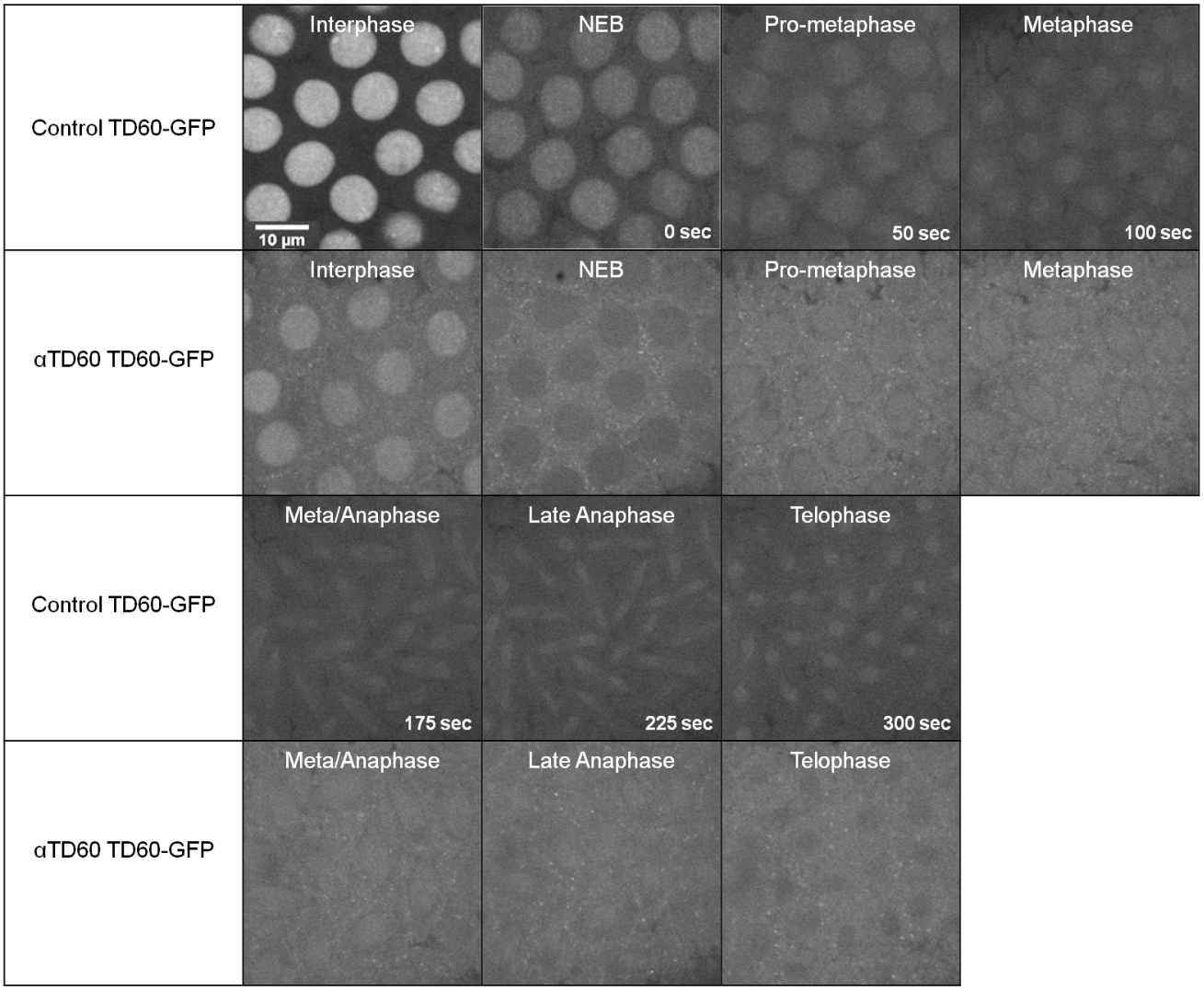

Figure 3-15. Comparison of TD60-GFP localisation throughout a cycle of mitosis in a Control TD60-GFP embryo and an anti-TD60 TD60-GFP injected embryo. Panels were aligned using NEB. While, in control embryos, TD60 accumulates in the nucleus until NEB, at which time it begins to associate with the growing mitotic spindle, in anti-TD60 injected embryos, interphase nuclear localisation is lost over time such that, by the end of NEB/beginning of pro-metaphase, TD60-GFP is excluded from nuclei. Cytoplasmic puncta can clearly be seen from NEB in the anti-TD60 injected embryo.

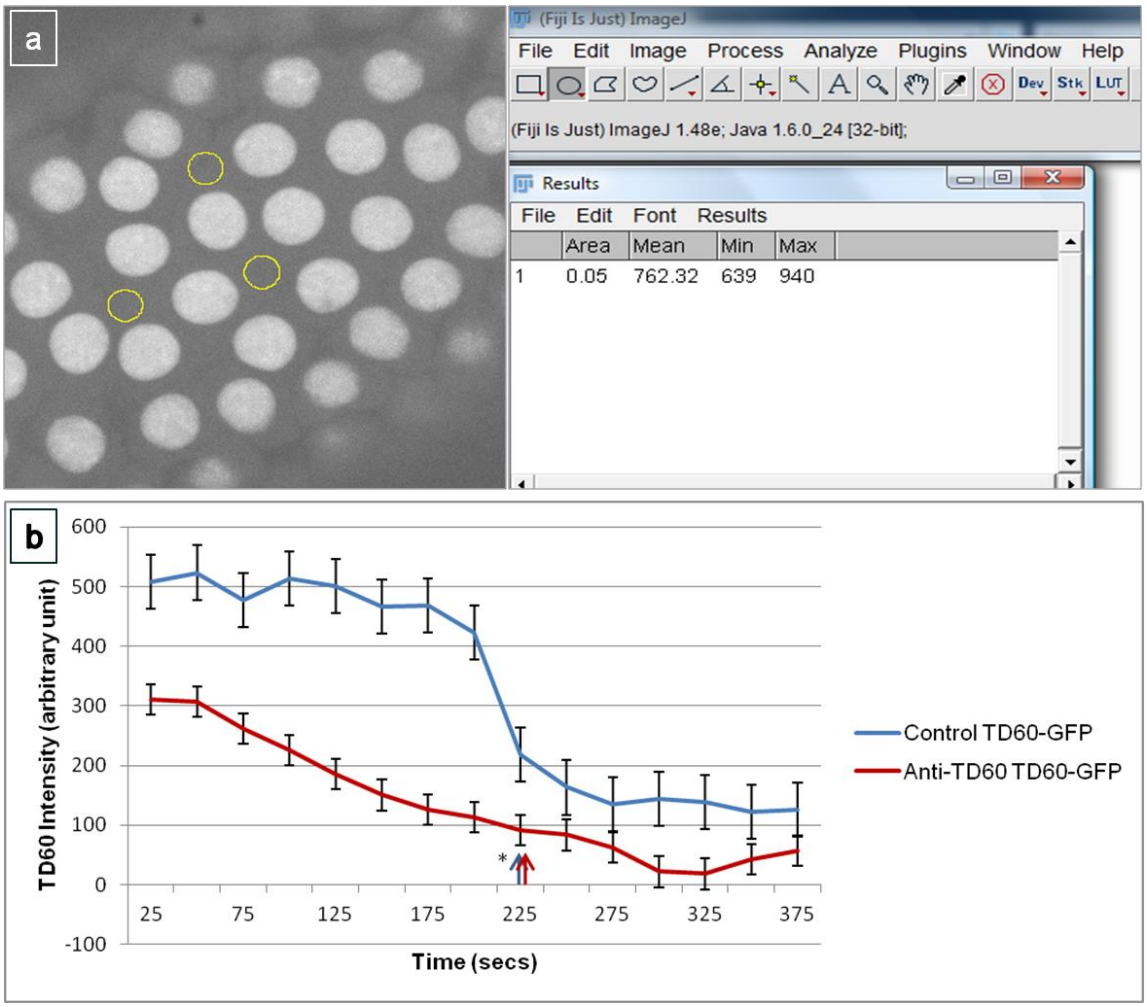

Figure 3-16. TD60-GFP intensity in the nucleus is affected with injection of TD60 antibody (a) Still taken from control TD60-GFP demonstrating how fluorescence levels were normalised. Fluorescence levels were normalised in both the control and the anti-TD60 TD60-GFP background using the image processing programme ImageJ. The mean value points, taken from 3 areas of cytoplasm in each background at t=0, were subtracted from each measurement taken to normalise background fluorescence. To measure TD60-GFP intensity in both backgrounds, circles around each of 3 nuclei, for each background, were drawn and measurements taken (taken every 5 frames) **(b)** Graph of TD60-GFP nuclear intensity over time. In control embryos the nuclear TD60-GFP is rapidly lost at NEB. In contrast, TD60-GFP is gradually lost from nuclei during interphase, following injection of anti TD60 antibodies. * = NEB (arrow colour associated with the line colour).

3.2.3.1. TD60 is required for normal mitotic progression

Injection of anti-TD60 antibodies into Tubulin-GFP; Histone-RFP expressing embryos was undertaken to simultaneously visualise the effect of inactivating TD60 on MT and chromatin dynamics during mitosis (Fig. 3-17). Although anti-TD60 injection had no visible effect on the initial stages of mitotic spindle formation, and no effect on chromosome condensation, mature mitotic spindles around the site of injection partially collapsed, and chromosome alignment failed (see Fig. 3-17 and 'Tub-GFP His-RFP Anti-TD60' movie). In spite of this, embryos uniformly progressed into anaphase with qualitatively normal timing (see S2. in Supplementary material), when compared to control injected embryos. Although some spindle elongation occurred during late anaphase/early telophase, central spindle stability was compromised, and DNA failed to segregate.

The injection of a larger amount of antibody resulted in the embryo arresting at metaphase/anaphase (results not shown).

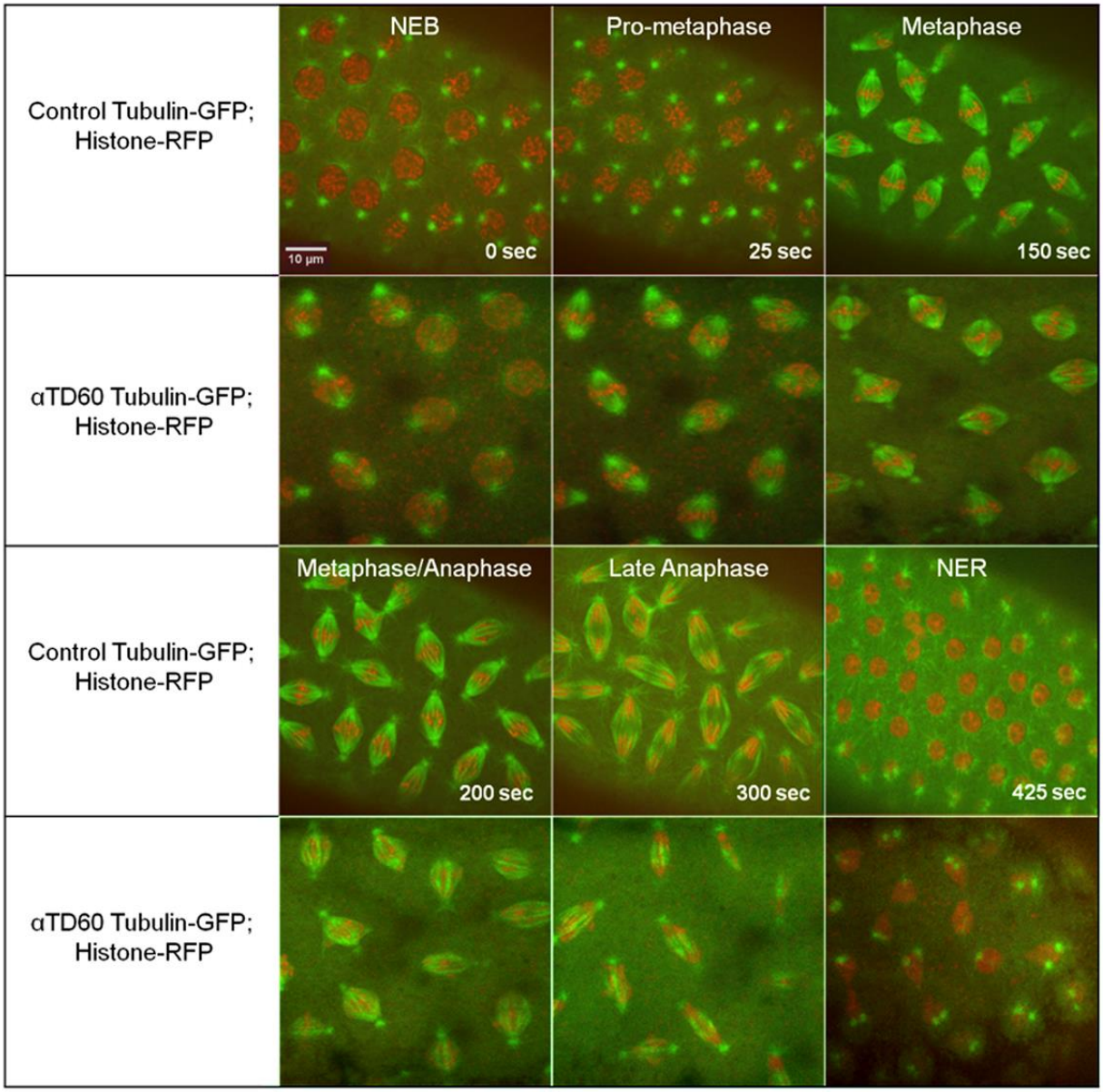

Figure 3-17. Injection of anti-TD60 antibody into Tubulin-GFP (in green); Histone-RFP (in red) embryos highlight problems with spindle stability and DNA segregation. Panels were aligned for NEB and the same time differences are shown between panels when comparing the Control with the anti-TD60 injected embryo.

3.2.3.2. TD60 is required for correct kinetochore MT dynamics, and for maintenance of the spindle assembly checkpoint

Rod (Rough-deal) is part of the RZZ complex, which functions as part of the spindle assembly checkpoint (SAC). This complex is a kinetochore component and comprises three proteins; Rod, Zwilch and Zw10. Similar to one of the roles of the CPC, the RZZ complex prevents progression into anaphase in the presence of incorrectly aligned chromosomes in metaphase, with the help of other proteins including Mad2 and Dynein (Basto *et al.,* 2004; Buffin *et al.,* 2005).

During prophase and prometaphase in control embryos, Rod-GFP associates with kinetochores (Fig. 3-18). Upon stable kinetochore-kMT (kinetochore microtubule) interactions, Rod-GFP streams polewards (see 'Rod-GFP control' movie). This "shedding" has been shown to be dependent on the minus end directed motor complex, Dynein. It is thought that, upon shedding of kinetochore-associated Rod and Mad2, the SAC is satisfied and spindles progress to anaphase. In control anaphase, therefore, two populations of Rod-GFP are visible - a small population remaining on the kinetochores and a population on the anaphase kMTs that decreases as these MTs are depolymerised (see Fig. 3-18 and 'Rod-GFP control' movie). In contrast, after microinjection of TD60 antibody in interphase (see Fig. 3-18 and 'Rod-GFP Anti-TD60' movie), although Rod-GFP associates with kinetochores and kMTs, there are defects with streaming and, instead, Rod-GFP continues to accumulate on this MT population. Interestingly, this abnormal Rod-GFP

streaming does not preclude these spindles from entering anaphase, albeit after a time delay. In these abnormal anaphases Rod-GFP is seen following the depolymerising kMTs towards the spindle poles. However, a fraction of dot-like Rod-GFP remains in the middle of the anaphase spindle. Manual tracing of Rod-GFP during anaphase suggests that these dot-like Rod-GFP structures are kinetochores that have failed to be segregated, presumably due to abnormal anaphase.

These results therefore suggest that injection of anti-TD60 antibodies causes a metaphase defect that leads to either abnormalities in kMT organisation or Rod poleward-streaming and an anaphase defect in which chromosome segregation is inhibited. In addition, the transit into anaphase seen, even in the presence of these severe SAC abnormalities, suggests that TD60 might normally be required to maintain the SAC.

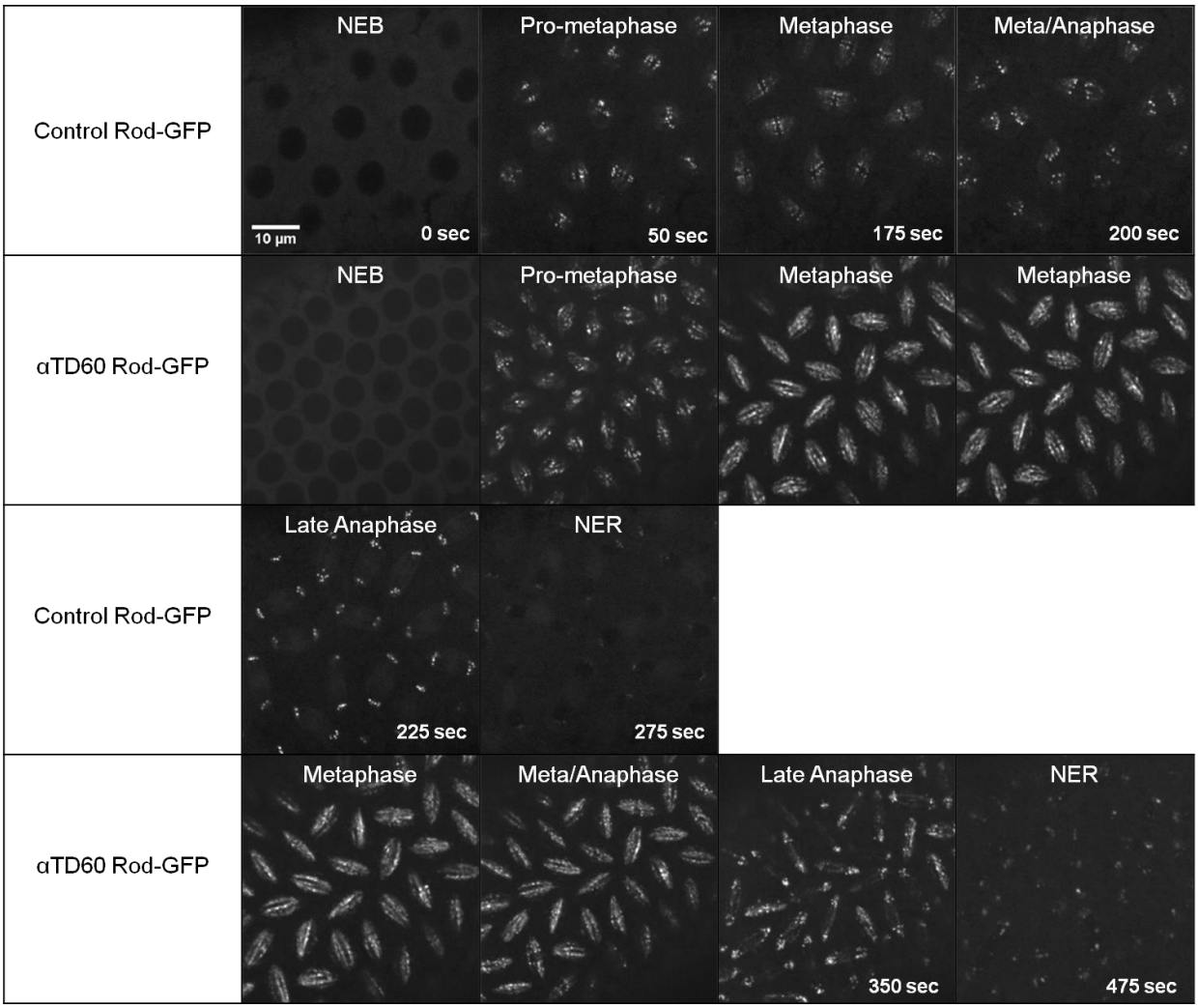

Figure 3-18. Comparison of Rod-GFP localisation throughout a cycle of mitosis in a Control Rod-GFP embryo and an anti-TD60 Rod-GFP embryo. Rod-GFP accumulates on kinetochores in pro-metaphase, and streams along kMTs during metaphase. In control embryos the majority of Rod-GFP is lost prior to anaphase entry. In anti-TD60 injected embryos Rod-GFP remains on kMTs, even through their depolymerisation in "anaphase". Panels were aligned for NEB and the same time differences are shown between panels when comparing the Control with the anti-TD60 injected embryo.

3.2.3.3. Polo-GFP allows quantification of anti-TD60 injection phenotypes

Polo-GFP strongly localises to the centrosomes throughout mitosis. In prophase and through into metaphase it localises to the kinetochores. It then re-distributes during anaphase and telophase, to the central spindle, before becoming nuclear during late telophase (see Fig. 3-19 and 'Polo-GFP Control' movie). This dynamic localisation makes Polo-GFP a very useful background in which to assess centrosome positioning, NEB, kinetochore movement and nuclear envelope reformation. Given the apparent defects in spindle length, kinetochore dynamics, chromosome segregation and mitotic timing in anti-TD60 injected embryos accumulated during the above studies, I therefore analysed Polo-GFP localisation in embryos injected with anti-TD60 antibodies. In anti-TD60 injected embryos, Polo-GFP was still able to localise correctly (see Fig. 3-19 and 'Polo-GFP Anti-TD60' movie). However the dynamics and movements of these sub-cellular structures were altered, in comparison to control embryos.

Firstly, I measured centrosome-centrosome (i.e. pole-pole) distance throughout from NEB to NER, in order to quantify spindle size (Fig. 3-20 b). In control nuclei at NEB, centrosome-centrosome distance is 9.87 µm +- 1.15 µm (SD). As spindle formation proceeds, this distance increases until, at the metaphase anaphase transition, centrosomes lie 15.99 µm +- 0.60 µm apart. As anaphase progresses, centrosome rapidly further separate until, at NER, they are 17.7 µm +- 1.5 µm apart. In the injected embryo, centrosome-centrosome distance is not affected at the start of

mitosis (9.35 µm +- 0.29 µm at NEB) and after an initial lag in the early stages of mitosis, the rate of pole-pole separation (i.e. actual mitotic spindle formation) occurs at the same rate as in controls (the angle of the line is the same, but shifted to reflect the smaller distance; at the metaphase anaphase transition the centrosomes lie 11.90 µm +- 0.66 µm apart). Whereas, in control embryos, centrosomes continue to separate as the spindle elongates through anaphase, the pole-pole distance in anti-TD60 injected spindles actually begins to decrease with centrosomes reaching a maximum of 11.72 µm +- 0.33 µm, signifying partial spindle collapse. Thus, in agreement with the Tubulin-GFP; Histone-RFP analysis, mitotic spindles are shorter in anti-TD60 injected embryos and anaphase B elongation is substantially inhibited.

Next, I determined the time taken to progress from NEB to anaphase A, using the kinetochore-associated Polo-GFP as a marker. In control embryos, the time from first association of Polo-GFP with kinetochores to observable kinetochore-pair separation in anaphase was 150 seconds (see Fig. 3-19 and S3. in Supplementary material). In anti-TD60 injected embryos, this was 300 seconds (see Fig. 3-19 and S3. in Supplementary material). Therefore, in agreement with above data, there is a significant delay in mitotic progression in TD60 inhibited embryos. However, similarly to what was observed in other GFP backgrounds, anaphase did occur - with attempted chromosome segregation, mitotic exit, chromosome decondensation and centrosome duplication all happening within 11 minutes of NEB.

Observation of Polo-GFP dynamics upon anti-TD60 injection also highlighted a number of other interesting points. Firstly, the kinetochore-associated Polo-GFP demonstrated that kinetochore pairs undergo fluctuations between poles similarly to control embryos. However, while paired dots of Polo-GFP only transition into lines at the point of anaphase A in control embryos (Fig. 3-21), kinetochore lines of Polo-GFP are present for extended periods of time, with some persisting throughout the aborted anaphase (Fig. 3-21). Again, this suggests that some aspect of the SAC is incorrectly functioning when TD60 is perturbed.

Finally, it was clear that central spindle formation was inhibited in anti-TD60 injected embryos. Whereas, in control embryos, Polo-GFP localised to antiparallel interdigitating MT bundles in anaphase, no such localisation was seen in anti-TD60 injected embryos (see 'Polo-GFP Anti-TD60' movie). However, whether this is a direct consequence of impaired TD60 function or a secondary consequence of a failure in chromosome segregation remains unclear.

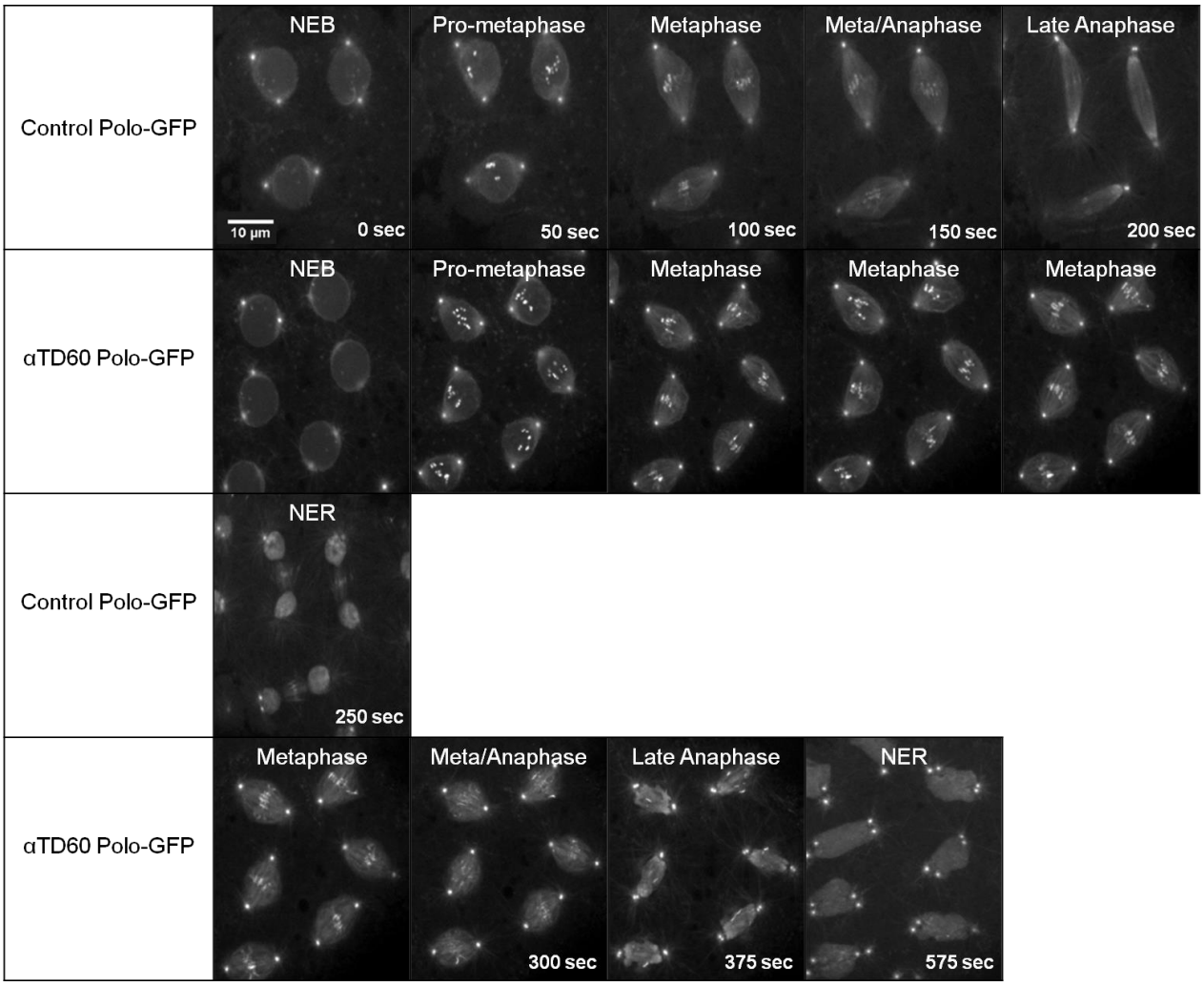

Figure 3-19. Comparison of Polo-GFP localisation throughout a cycle of mitosis in a Control Polo-GFP embryo and an anti-TD60 Polo-GFP embryo. The same time differences were used between panels when comparing the Control with the anti-TD60 injected embryo demonstrating the time delay seen in the injected embryo.

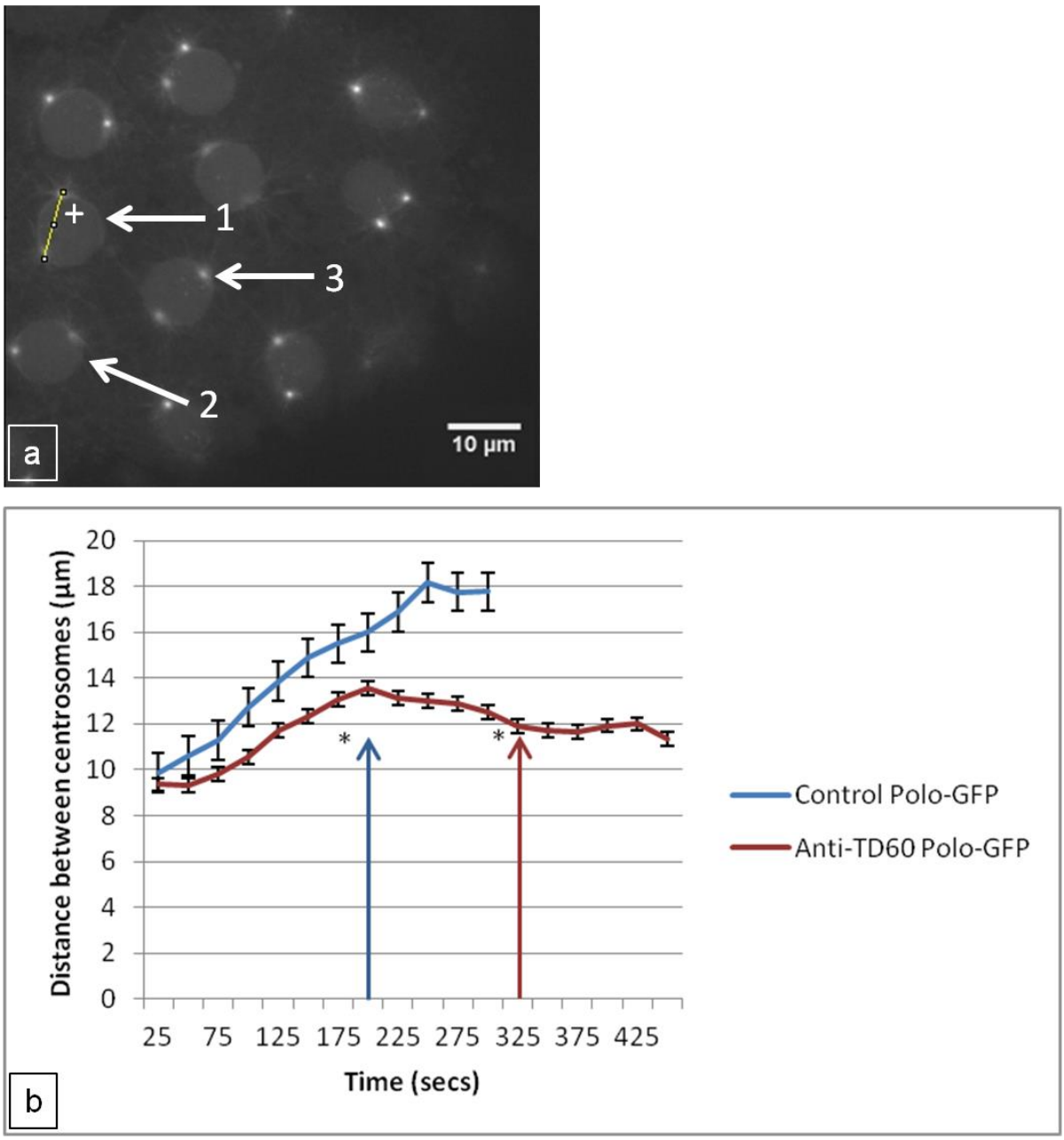

Figure 3-20. Nuclei from a Polo-GFP embryo injected with anti-TD60 antibody show a smaller distance between centrosomes throughout mitosis than seen in a control embryo. (a) Shows an example of how measurements were taken in the background anti-TD60 Polo-GFP at NEB. + = a line was drawn to measure the distance from centrosome to centrosome (undertaken for nuclei 1, 2 and 3) Centrosome distance was measured from NEB (t=0) until NER. This was carried out using the image processing programme ImageJ.

Figure 3-20. cont. (b) Measurements were taken from both backgrounds starting from NEB (t=0). The distance between centrosomes during spindle formation is slower in anti-TD60 injected embryos than in control. In addition, while centrosome-centrosome distance increases again during anaphase B, following chromosome segregation, this increased separation is completely absent in anti-TD60 injected embryos. * = start of Anaphase B (arrow colour associated with the line colour); note the delay in the injected embryo.

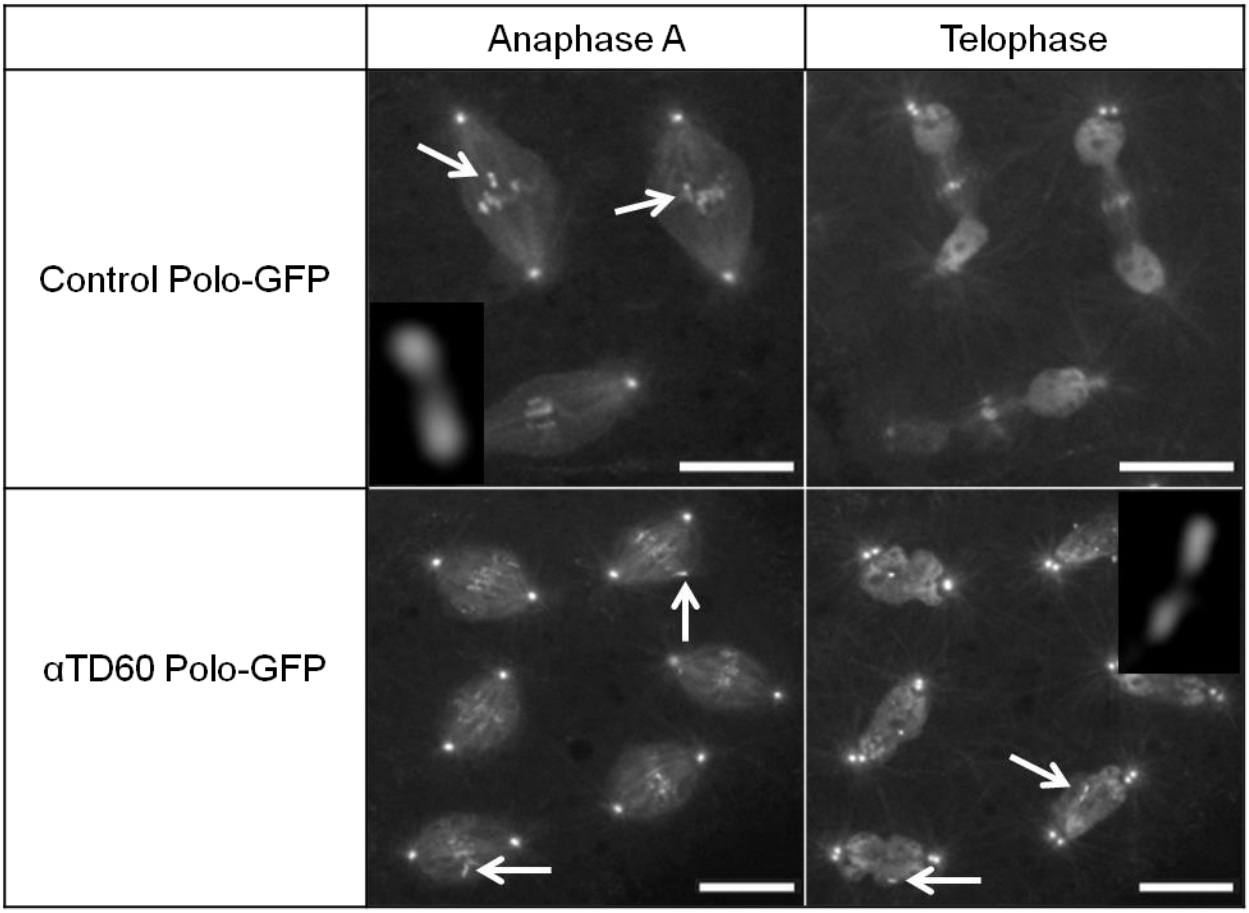

Figure 3-21. Kinetochore lines, indicating incorrect MT-kinetochore attachments, remain in anti-TD60 injected Polo-GFP background. In control embryos, kinetochore pairs are present as dots that move to opposing poles during anaphase. In anti-TD60 injected embryos distinct kinetochore "lines" are present throughout failed anaphase and chromosome decondensation. Arrows = kinetochore lines. The inserted image in the left upper panel and right lower panel show a magnified kinetochore line. Scale bars = 10 µm.

3.2.3.4. Aurora B-GFP

Finally, given the proposed role of human TD60 in regulating the activity of Aurora B, and its apparent association with the CPC, I asked whether Aurora B localisation was affected in embryos in which TD60 function had been perturbed. Aurora B-GFP, like Polo-GFP, has a dynamic localisation during mitosis (Fig. 3-22). In control embryos, Aurora B-GFP is localised to nuclei in interphase. Directly following NEB, it accumulates transiently on condensing chromatin, before concentrating at kinetochores in late pro-metaphase (Fig. 3-22; 3-23). A small population is also present on the mitotic spindle. At anaphase onset, a small fraction of Aurora B-GFP is maintained on kinetochores, moving polewards, while an accumulation of the protein is seen at the forming central spindle. By NER, Aurora B-GFP re-accumulates in the nucleus, with a small dot-like accumulation remaining at the midbody (see Fig. 3-22 and 'Aurora B-GFP Control' movie).

In embryos injected with anti-TD60 antibodies, although initial recruitment to condensing chromatin appears normal, close to the site of injection, there is little or no specific accumulation on the kinetochores (Fig. 3-22). Instead, Aurora B-GFP remains along the length of the chromatin in late pro-metaphase (Fig. 3-22; 3-23). However, as spindles transit into anaphase, there is some concentration of Aurora B at interdigitating MT bundles in spindles that form a central spindle-like structure (see Fig. 3-22 and 'Aurora B-GFP Anti-TD60' movie). These results suggest that TD60 may, indeed, have a function in regulating Aurora B localisation/activity during mitosis, and pave the way for further

experiments aimed at determine the precise relationship between these proteins.

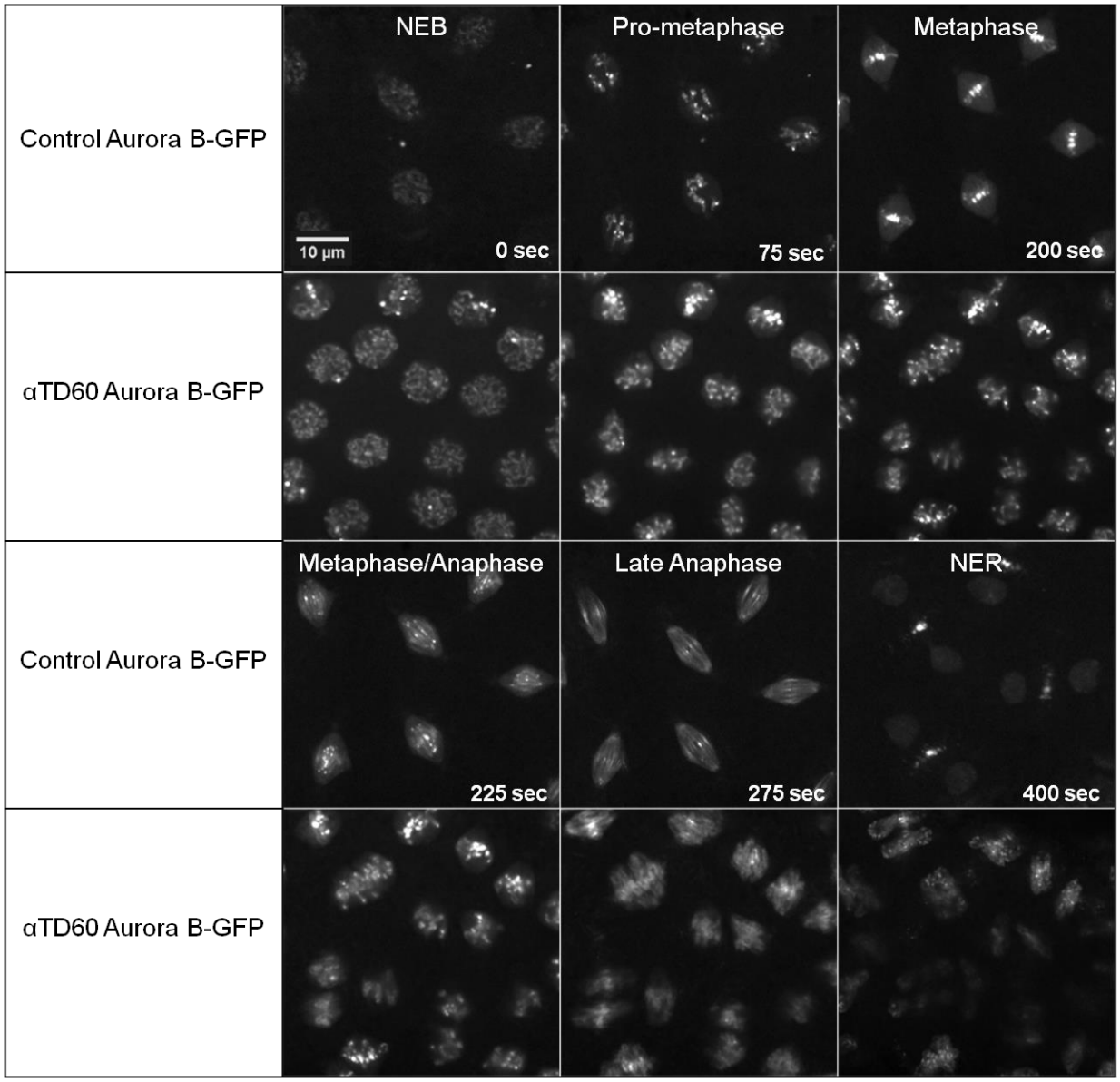

Figure 3-22. Comparison of Aurora B-GFP localisation throughout a cycle of mitosis in a Control Aurora B-GFP embryo and an anti-TD60 Aurora B-GFP embryo. The same time differences were used between panels when comparing the control with the anti-TD60 injected embryo. This particular anti-TD60 injected embryo showed no time delay. Injection of anti-TD60 in another embryo (see S4. in Supplementary material) did show a significant time delay; possibly due to the larger amount of antibody injected in to the embryo.

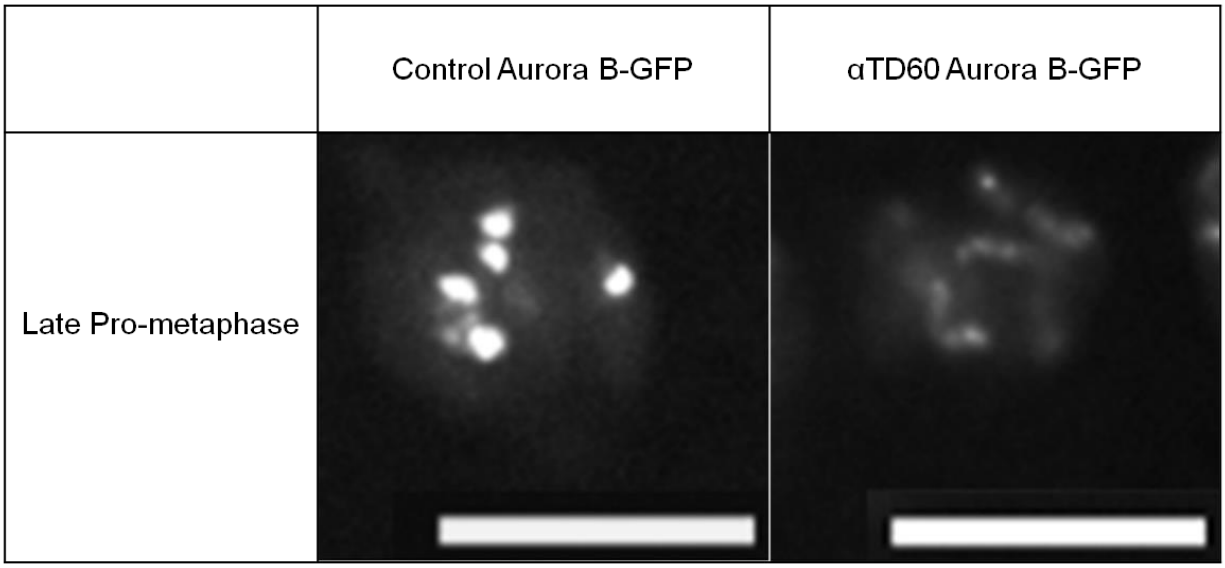

Figure 3-23. Comparison of Aurora B-GFP intensity in late pro-metaphase in a Control Aurora B-GFP embryo and an anti-TD60 Aurora B-GFP embryo. Aurora B-GFP can be seen localising specifically to the kinetochores in the control movie whereas in the Aurora B-GFP anti-TD60 movie, Aurora B-GFP has a more general localisation on the chromatin and not on the kinetochores. Scale bars = 10 µm.

3.2.4. Identification of potential TD60 interacting proteins

Given that proteins rarely act in isolation within the cell, and that human TD60 has been shown to interact biochemically with the CPC, I coupled the affinity-purified anti-TD60 antibodies to Sepharose Protein A beads, in order to perform immunoprecipitation/mass spectrometry (IP/MS), in an attempt to identify potential TD60 interacting partners from *Drosophila* embryo extracts. As a control, I coupled random rabbit IgG to beads (Fig. 3-24 a). From these results, it can be estimated that ~1 µg of IgG antibodies are attached to ~1 µl of beads (Fig. 3-24 b).

A high speed embryo extract was generated from ~0.8 g of 0-3 hour embryos, and equal volumes were incubated with either control or anti-TD60 beads. After extensive washing, samples were sent to the Bristol Proteomics Facility for MS analysis. Figure 3-25, a western blot of the purification procedure, demonstrated that TD60 was present in the anti-TD60 bead sample. Results were compared, with any protein IDs occurring in both control and anti-TD60 beads discarded, unless enriched by >10 fold in the anti-TD60 sample. Table 3 shows a list of specific anti-TD60-Sepharose-Protein A interactors.

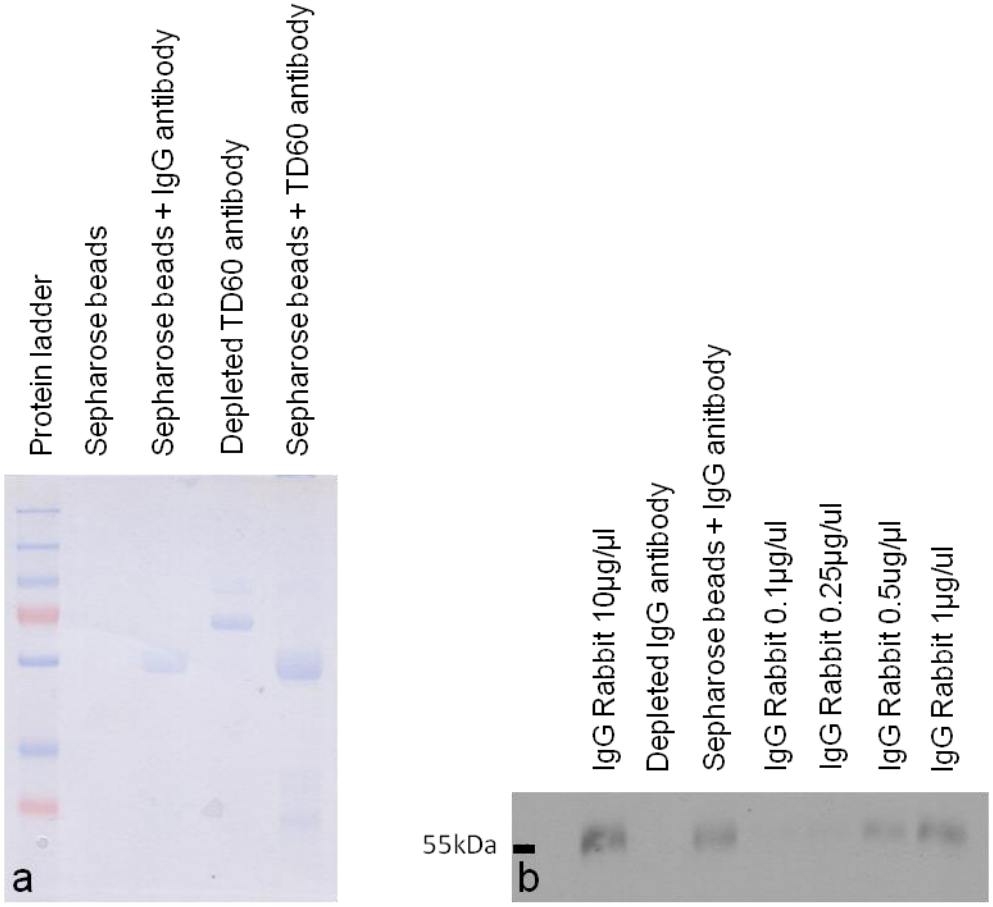

Figure 3-24. TD60 and the control IgG antibodies have both successfully attached to the Protein A Sepharose beads. (a) The gel shows that both the control (IgG antibody) and the TD60 antibody have attached to the Protein A Sepharose beads. The antibodies have separated into the two basic structural units; the heavy chain which is around 50 kDa and the light chain; around 25 kDa (on the protein ladder, the 55 kDa mark is the line under the top red line and the 25 kDa mark is the bottom red line. The light chain is less visible on the gel and can't be seen from the 'Sepharose beads + IgG antibody' sample) **(b)** From the Western blot it can be estimated that ~1 µg of IgG antibodies are attached to ~1 µl of beads. The molecular weight of the antibody also correctly matches that of the antibody as indicated by the controls.

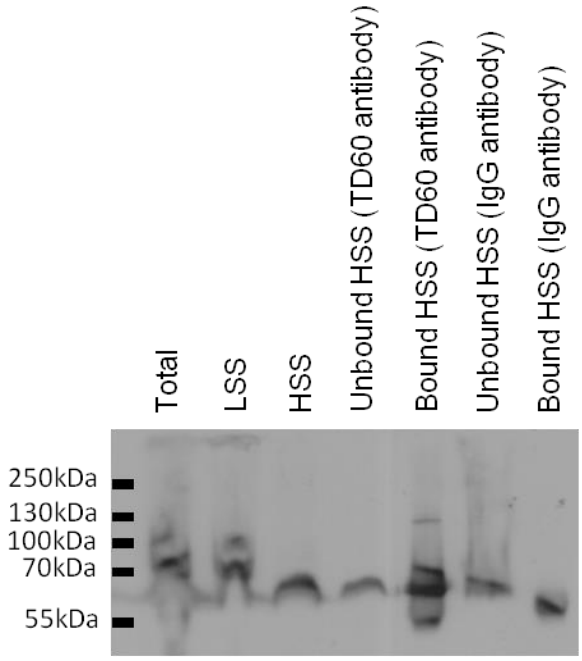

Figure 3-25. Western blot showing TD60 is present on anti-TD60 Protein A Sepharose beads. The blot ran a bit too fast resulting in a shaky blot but the results still clearly show that the TD60 protein has successfully bound to the beads. This is demonstrated by the molecular weight; TD60 has a molecular weight of ~60 kDa. Some TD60 protein remains unbound but the majority has bound to the beads as made apparent by the larger band size in the 'Bound HSS' lane compared to the 'Unbound HSS' lane.

Encouragingly, the most abundant protein identified in the anti-TD60 beads was CG9135/TD60; confirming that the anti-TD60 antibody immunoprecipitates TD60. Eleven other specific interactors were identified; none of which corresponded to CPC members. Of these, Hsp60 might be discounted - as a chaperone the presence of Hsp60 most likely reflects the folding of the TD60, rather than a regulatory function per se. More studies will be required to test whether these proteins are true TD60 interactors; however, it is interesting to note that one, Elav, is listed by Biogrid.org as directly interacting with human TD60. Rok; Rho kinase, is another protein worth investigating, having a known role in regulating Actin cytoskeleton organisation during cytokinesis.

Accession	# AAs	MW [kDa]	Score (IgG control)	Score (anti-TD60)
CG9135	487	53.4	27.38	3694.04
ATPsyn-beta	505	54.1	31.01	736.62
Hsp60	573	60.8	8.95	186.91
CG32104	1215	137.4		123.16
elav	479	50.3		90.15
ms(3)72Dt	622	67.7		78.29
D19B	774	87.8		65.98
CG3995	322	37.4		65.48
rok	1390	160.2		44.44
CG14837	760	83.5		35.61
CG32113	3919	444.8		31.92
BoYb	1059	121.3		30.72

Table 3. Mass spectrometry results from IP of TD60 antibody attached to Protein A Sepharose beads with wildtype embryo extract. This table excludes any protein IDs occurring in both control and anti-TD60 beads unless enriched by >10 fold in the anti-TD60 sample.

3.2.5. Discussion

It is clear that, both in tissue culture cells and in the organism, RNAi of TD60, although resulting in substantial gene expression knock down, does not lead to complete loss of the protein in cells. This is probably due to the high levels of TD60 protein present in these tissues, coupled with a low protein degradation rate. As such, it is difficult to conclude from these experiments what effect completely removing TD60 has upon mitosis. Rather than attempting to optimise *in vivo* RNAi conditions (i.e. exploring different maternal RNAi drivers, driving RNAi in other tissues where TD60 might be less highly expressed) and given these difficulties, I decided instead to explore an alternative method of inactivating TD60 function - antibody injection into syncytial embryos. Polyclonal anti-TD60 antibodies, generated in rabbits, were affinity purified and tested for specificity in the early embryo. A single band of the predicted Mr of TD60, which reduces upon RNAi of the TD60 gene, is recognised, confirming the specificity of the antibodies.

Injection of these antibodies into interphase embryos results in dramatic and reproducible mitotic phenotypes. It is interesting that injection, although completely abolishing the nuclear localisation of TD60, does not give any visible interphase phenotype. As syncytial embryos cycle directly from S to M phase, without intervening gap phases, this suggests that TD60 may not have an essential function in this tissue during S phase.

The first phenotype observed occurs after initial mitotic spindle formation - centrosome separation and initial MT nucleation from centrosomes do

not appear to be affected. Tubulin-GFP; Histone-RFP movies demonstrate that bipolar spindles form relatively normally, but that the steady-state length of the mitotic spindle cannot be maintained, and they at least partially collapse. This points towards a role for TD60 in mitotic MT dynamics, though it is currently unclear how this might be facilitated.

Anti-TD60 injected embryos also exhibit abnormal kMT dynamics (as assessed by Rod-GFP) although kinetochores undergo oscillatory movements suggesting that kinetochore-kMT interactions are formed and are capable of transmitting force. It is possible that the defects seen in Rod streaming reflect a direct role for TD60 in regulating the RZZ complex, or its shedding from kinetochores. The transportation of Rod off the kinetochore is a Dynein dependent process with targeting of Dynein to the kinetochore reliant on the proteins Spindly and Dynactin (Griffis *et al.,* 2007). Loss of TD60 could directly affect Dynein's behaviour or indirectly by disturbing Spindly's activity; to investigate these assumptions the next step could be to look at their localisation in an embryo injected with anti-TD60. However, given the effect on spindle MTs, it is perhaps more likely that the effect on Rod streaming is a consequence of abnormal spindle dynamics. Again, given that CLASP/MAST has been shown to play a role in kinetochore-kMT interactions it will be important to assess its localisation in anti-TD60 injected embryos.

The third consistent phenotype relates to mitotic timing. Embryos injected with low amounts of anti-TD60 antibody show reduced spindle length and abnormal chromosome segregation, but pass from metaphase to

anaphase with qualitatively similar timing. Injection of higher concentrations (as shown in most of the movies associated with this thesis) causes a significant delay in anaphase initiation. Although this could be interpreted as evidence for an active SAC following disruption of TD60, it is important to recognise that all the abnormal spindles DO pass into anaphase co-ordinately. This strongly suggests that aspects of the SAC have been compromised. By way of comparison, it has recently been shown that injection of interfering antibodies against the Augmin complex result in abnormal spindle morphology and abnormal Rod-GFP streaming but that these embryos remain arrested in metaphase, as would be expected when the SAC is unsatisfied. The simplest interpretation of the anti-TD60 injections is therefore that the SAC is compromised and therefore that TD60 plays a role in maintaining the SAC in spindles with incorrectly attached kinetochores.

Anti-TD60 injected embryos also show two distinct phenotypes in anaphase. First, chromosome segregation is dramatically inhibited. The localisation of kinetochore-associated Rod-GFP and Polo-GFP both show numerous examples of chromosomes that do not move polewards in anaphase. The consequence of this is that, upon chromosome decondensation and NEF, a single large nucleus is formed containing both complements of chromosomes. This is especially apparent in the Polo-GFP movie. It is likely that this phenotype is a consequence of incorrect kinetochore-kMT interactions seen earlier in mitosis. Again, as such defects should be monitored by the SAC, it points towards a role for TD60 in checkpoint signalling. The second anaphase phenotype is a defect in central spindle formation. It can be argued that this is merely a

consequence of not segregating chromosomes - the area of the spindle in which the central spindle normally forms is, in anti-TD60 injected embryos, taken up with DNA. In addition, a central spindle is sometimes apparent (see, for example, Aurora B-GFP movie). However, it could also be the case that TD60 is normally required for central spindle formation, or for the maintenance of the spindle MTs in metaphase that will eventually go on to form the central spindle. Injection of anti-TD60 antibodies into embryos expressing the MT minus end-binding protein Asp (Abnormal spindle), may well distinguish between these possibilities.

3.2.5.1. How does TD60 function?

The research presented in this thesis provides compelling evidence for a role for TD60 in mitotic spindle organisation, SAC signalling and chromosome segregation. The IP/MS, although clearly isolating TD60 and a number of specific interacting partners, does not provide clear candidate proteins through which TD60 could facilitate these roles. Perhaps the simplest interpretation is that TD60 does, indeed function through regulating Aurora B activity. Aurora B-GFP embryos injected with anti-TD60 antibodies show correct localisation of the CPC to chromatin in interphase and to anaphase MTs (when they form). However, a notable difference to control embryos was the apparent inability of Aurora B to move from chromosome arms to the kinetochore/centromere in pro-metaphase. Instead of dot-like kinetochores, as in controls, Aurora B-GFP was diffusely present all over chromosomes when TD60 function was inhibited (see Aurora B-GFP movies). If TD60 does function through the CPC, it could provide an explanation for all the associated

phenotypes. The CPC has a clearly demonstrated role in kinetochore-kMT interactions and in maintaining the SAC. HEC1/Ndc80, as part of the KMN complex, is needed for MT binding to the kinetochores. Aurora B is responsible for phosphorylating this protein if there is a lack of tension; by Aurora B targeting Ndc80 it helps in preventing incorrect attachments. Aurora B also phosphorylates Klp10A, a homolog of the depolymerase Kif2a to prevent it from depolymerising the kinetochore MTs if the MT and kinetochore attachments are incorrect. In terms of SAC function, inhibition of Aurora B in human tissue culture cells bypasses the SAC, with cells entering anaphase in the presence of mis-aligned chromosomes (Yang *et al.,* 2007; Hardwicke *et al.,* 2009). The CPC in other systems also has a role in stabilising/generating MTs around chromatin, similarly to the Ran.GTP pathway (Sampath *et al.,* 2004). Reduction of Aurora B activity could therefore theoretically lead to a destabilised, shorter spindle. Finally, the CPC is also required for correct chromosome segregation and central spindle formation. Thus, repetition of the anti-TD60 antibody injections into Aurora B-GFP embryos, and into embryos carrying transgenes to other CPC subunits, is of high priority. It is also possible that TD60 may function independently of the CPC, but still affect Aurora B localisation.

When TD60/RCC2 was entered into the STRING database ('Search Tool for the Retrieval of Interacting Genes/Proteins') (Jensen *et al.,* 2009) to search for known and predicted protein-protein associations, the MAP CLASP (known as Mast in *Drosophila*) was highlighted as having a high confidence interaction (Von Mering *et al.,* 2005) with a score of 0.962. CLASP is a protein that has a known role in spindle length, with

mutations in CLASP leading to the mutant phenotype “short spindles” (Goshima *et al.,* 2007; Reis *et al.,* 2009).

CLASP has other key roles during the latter stages of cell division including the establishment of correct MT-kinetochore attachments (Maiato *et al.,* 2002), localisation of key cytokinetic proteins including Pavarotti, Aurora B, Actin and Anillin and in completion of furrow formation (Inoue *et al.,* 2004). It will therefore be of interest to find out whether CLASP localisation is altered upon injection with anti-TD60 antibodies. In addition to this, replication of the IP and MS should be undertaken, but instead of using TD60 antibody as a means of pull-down, using TD60-GFP embryos (using GFP-Trap A beads). This would help to increase the reliability of the results obtained from the previous mass spectrometry and might pull down other proteins such as CLASP, which, according to the STRING database (Jensen *et al.,* 2009), has a potentially strong interaction with TD60.

4. Conclusion

The work in this thesis advances our understanding of the roles of both the CPC and TD60 during meiosis and mitosis, respectively.

I have shown that although the CPC is not required for the MT association of Pavarotti or Polo during meiotic anaphase, it is required for the accumulation of Pavarotti to the plus ends of these MTs. Through the purification and injection of interfering antibodies raised against TD60, I have also demonstrated an essential role for this protein in regulating the metaphase spindle length, mitotic timing and chromosome segregation.

Although details of the molecular pathways in which TD60 and the CPC function still require further investigation, my work provides an important advance and defines clear routes of study that should lead to a greater understanding of the fundamental process of cell division.

5. Supplementary material

S1. Fly food recipes

I. Gatti lab fly food recipe (2 l)

1. Stir together water (900 ml), baker's yeast (150 g), sugar (100 g) and agar powder (15 g)
2. Boil for 20 minutes
3. Add maize flour (70 g) in 200 ml of water
4. Add an additional 900 ml of water
5. Boil for 40 minutes
6. Add propionic acid (14 ml) and dispense into tubes

II. Wakefield lab fly food recipe (12 l)

1. Heat 10.4 l of water to ~95°C using a hot plate
2. Add 1 l of boiling water to 67.5 g of agar
3. In a 2 l jug, add maize flour (675 g), soya flour (81 g) and baker's yeast (138 g)
4. In another 2 l jug add malt (675 g) and molasses (225 g). Microwave for 3 minutes then make a paste with water (600 ml)
5. Add the flour and malt mixes to the 10.4 l of water
6. Heat for 1 hour stirring every 10-15 minutes
7. Cool to ~70°C
8. Add propionic acid (50 ml), orthophosphoric acid (3.1 ml) and nipagin (100 ml) and dispense into tubes

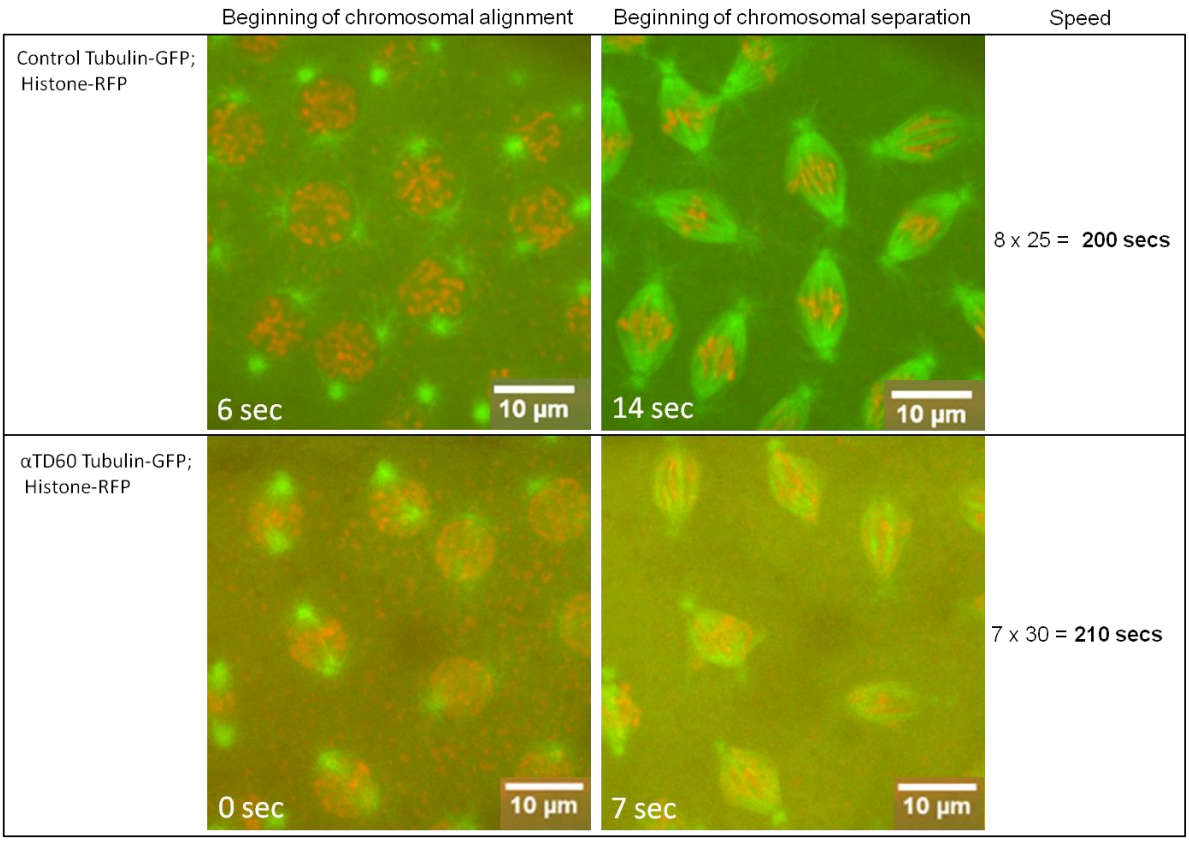

S2. Tubulin-GFP; Histone-RFP embryo injected with TD60 antibody shows no time delay between chromosomal alignment and chromosomal separation. For control embryo: each frame is made up of 5 slices/stacks taken every 5 seconds. When converting to AVI the speed set was 5 frames per second. Each frame = 5 seconds x 5 frames per second = 25 seconds real time per second of AVI. For injected embryo: Each frame is made up of 5 slices/stacks taken every 2 seconds. When converting to AVI the speed set was 15 frames per second. Each frame = 2 seconds x 15 frames per second = 30 seconds real time per second of AVI.

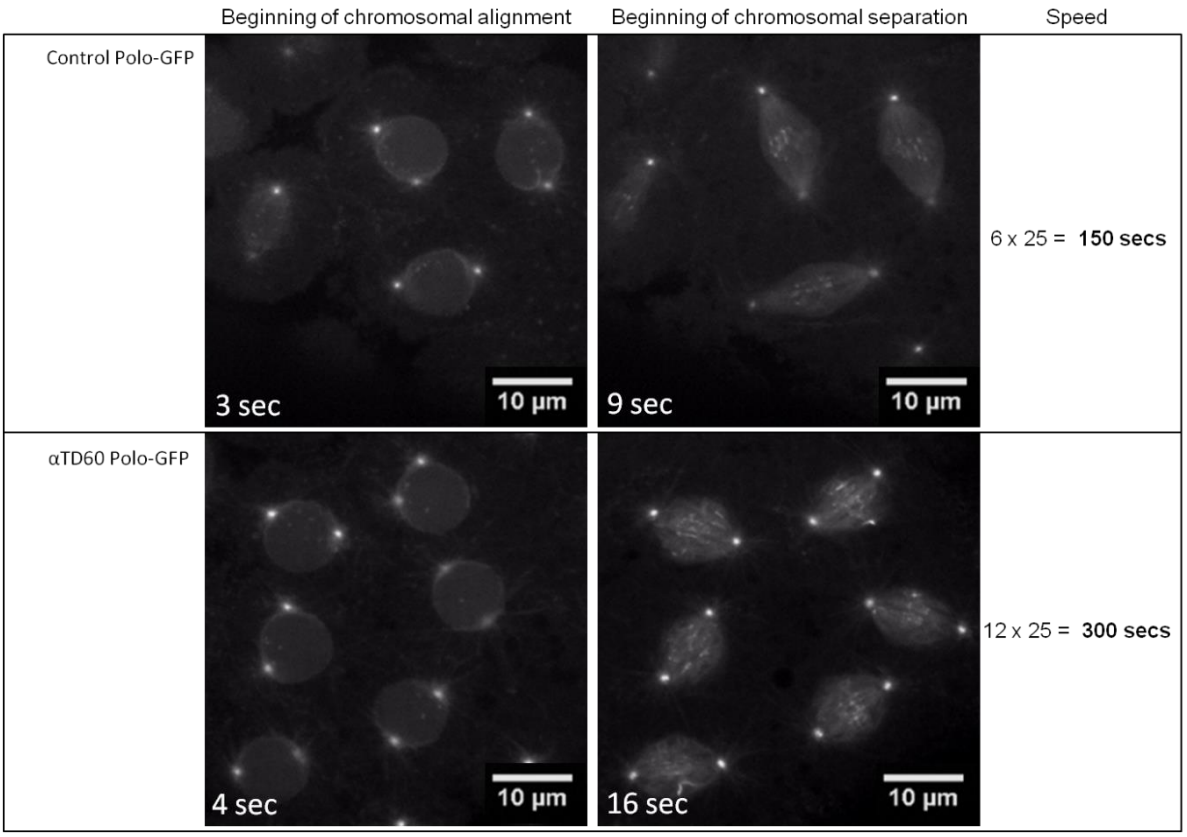

S3. Polo-GFP embryo injected with TD60 antibody shows a time delay between chromosomal alignment and chromosomal separation twice that of the time it takes in a control embryo.. Each frame is made up of 5 slices/stacks taken every 5 seconds. When converting to AVI the speed set was 5 frames per second. Each frame = 5 seconds x 5 frames per second = 25 seconds real time per second of AVI.

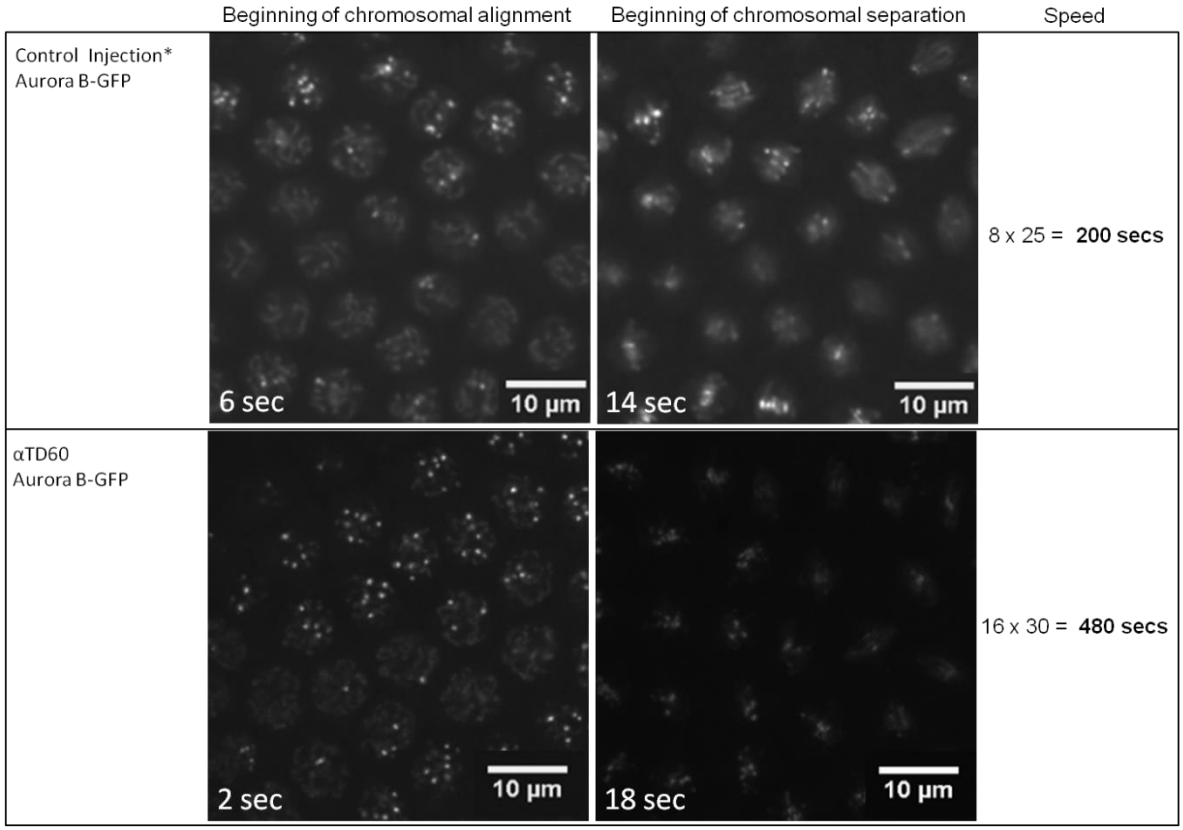

S4. Aurora B-GFP embryo injected with TD60 antibody shows a time delay between chromosomal alignment and chromosomal separation, more than twice the time it takes in a control embryo.. * = Injected with IgG Antibody 10 mg/ml in Interphase. For control embryo: each frame is made up of 5 slices/stacks taken every 5 seconds. When converting to AVI the speed set was 5 frames per second. Each frame = 5 seconds x 5 frames per second = 25 seconds real time per second of AVI. For injected embryo: Each frame is made up of 5 slices/stacks taken every 2 seconds. When converting to AVI the speed set was 15 frames per second. Each frame = 2 seconds x 15 frames per second = 30 seconds real time per second of AVI.

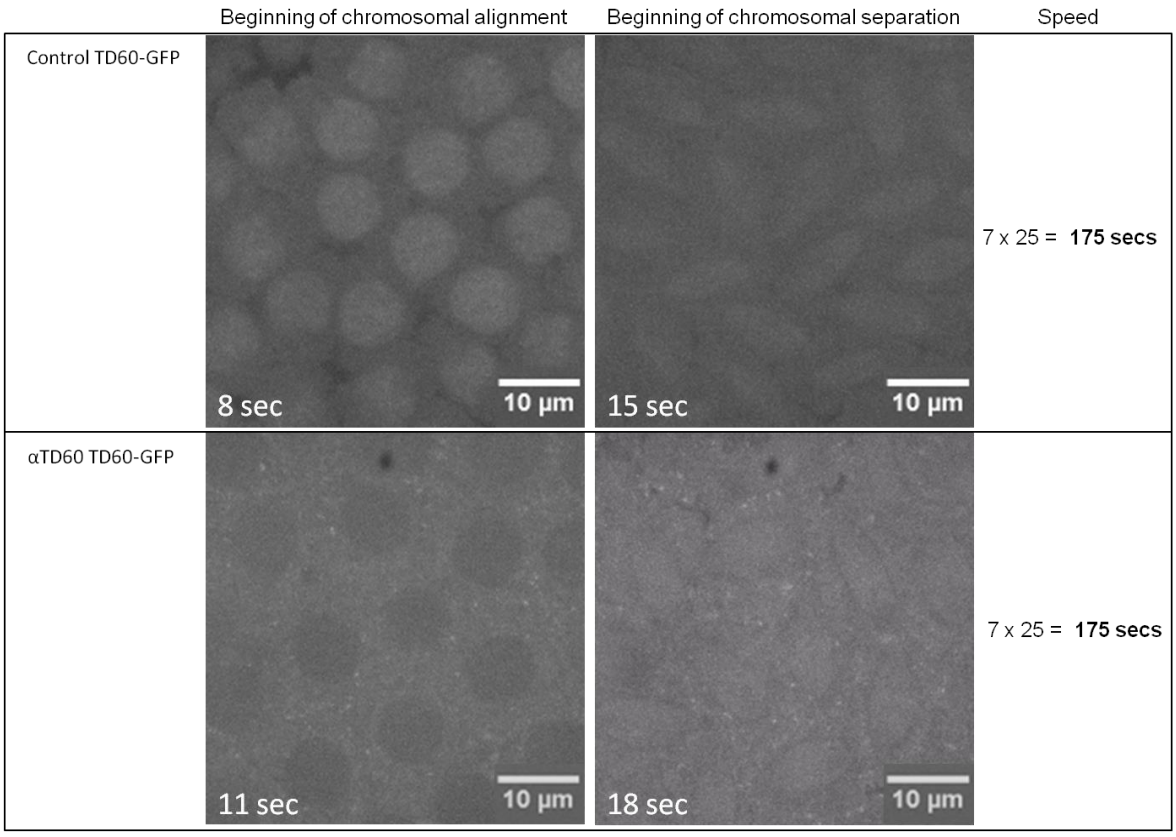

S5. TD60-GFP embryo injected with TD60 antibody shows no time delay between chromosomal alignment and chromosomal separation. Each frame is made up of 5 slices/stacks taken every 5 seconds. When converting to AVI the speed set was 5 frames per second. Each frame = 5 seconds x 5 frames per second = 25 seconds real time per second of AVI.

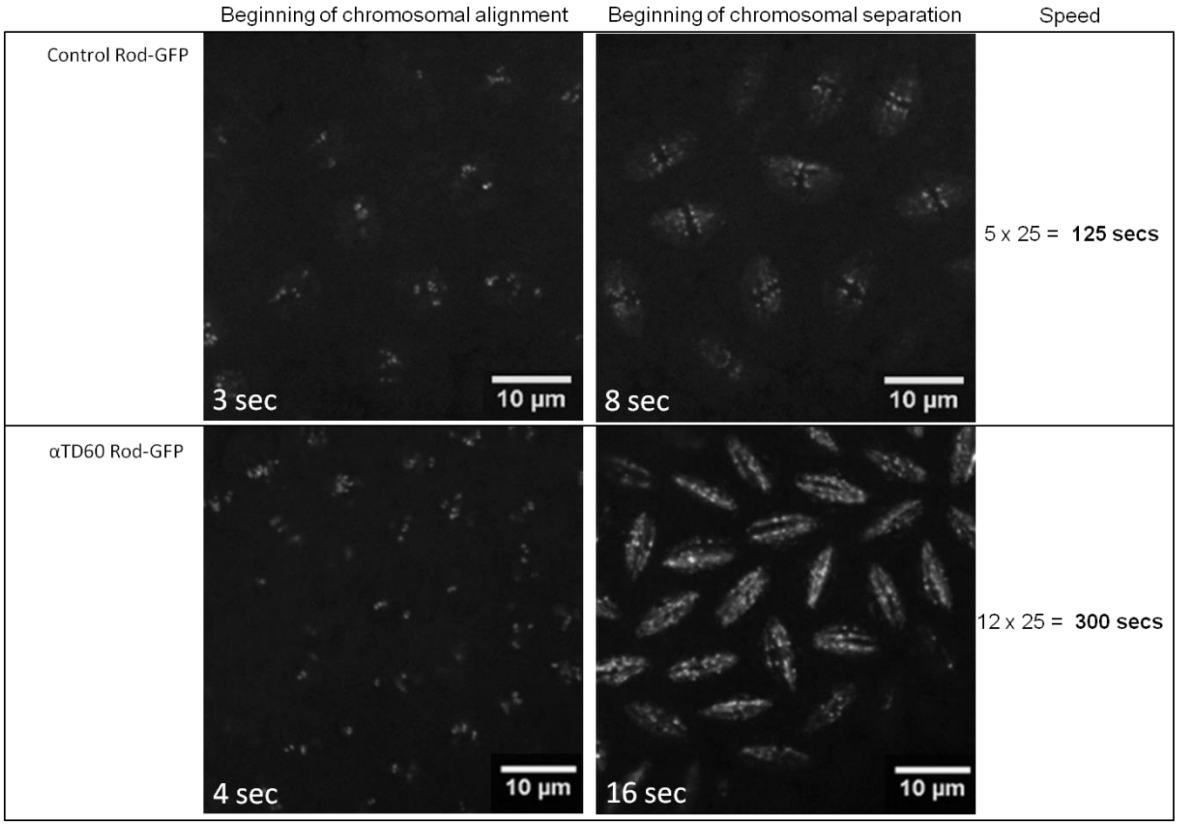

S6. Rod-GFP embryo injected with TD60 antibody shows a time delay between chromosomal alignment and chromosomal separation more than twice that of the time it takes in a control embryo. Each frame is made up of 5 slices/stacks taken every 5 seconds. When converting to AVI the speed set was 5 frames per second. Each frame = 5 seconds x 5 frames per second = 25 seconds real time per second of AVI.

6. References

Adams, M.D., Celniker, S.E., Holt, R.A., Evans, C.A., Gocayne, J.D., Amanatides, P.G., Scherer, S.E., Li, P.W., Hoskins, R.A., Galle, R.F., et al. (2000) The genome sequence of *Drosophila melanogaster*. *Science, 287,* 2185-2195. DOI: 10.1126/science.287.5461.2185.

Adams, R.R., Maiato, H., Earnshaw, W.C., & Carmena, M. (2001) Essential roles of *Drosophila* inner centromere protein (INCENP) and aurora B in histone H3 phosphorylation, metaphase chromosome alignment, kinetochore disjunction, and chromosome segregation. *The Journal of Cell Biology, 153* (4), 865–80.

Adams, R.R., Wheatley, S.P., Gouldsworthy, A.M., Kandels-Lewis, S.E., Carmena, M., Smythe, C., Gerloff, D. L., et al. (2000) INCENP binds the Aurora-related kinase AIRK2 and is required to target it to chromosomes, the central spindle and cleavage furrow. *Current Biology*, *10* (17), 1075–8.

Adams, R.R., Tavares, A.A., Salzberg, A., Bellen, H.J., & Glover, D.M. (1998) pavarotti encodes a kinesin-like protein required to organize the central spindle and contractile ring for cytokinesis. *Genes & Development, 15*, 1483-1494.

Ahonen, L.J., Kukkonen, A.M., Pouwels, J., Bolton, M.A, Jingle, C.D., Stukenberg, P.T., & Kallio, M.J. (2009) Perturbation of Incenp function impedes anaphase chromatid movements and chromosomal passenger protein flux at centromeres. *Chromosoma, 118* (1), 71–84. DOI: 10.1007/s00412-008-0178-0.

Andreassen, P.R., Palmer, D.K., Wener, M.H., & Margolis, R.L. (1991) Telophase disc: a new mammalian mitotic organelle that bisects telophase cells with a possible function in cytokinesis. *Journal of Cell Science, 99* (3), 523–34.

Baena-lo, L.A., Alonso, J., Rodriguez, J., & Santare, J.F. (2008) The Expression of Heat Shock Protein HSP60A Reveals a Dynamic Mitochondrial Pattern in *Drosophila melanogaster. Embryos research articles,* 2780–2788.

Basto, R., Lau, J., Vinogradova, T., Gardiol, A., Woods, C.G., Khodjakov, A., & Raff, J.W. (2006) Flies without centrioles. *Cell, 125*, 1375-1386. DOI: 10.1016/j.cell.2006.05.025.

Basto, R., Scaerou, F., Mische, S., Wojcik, E., Lefebvre, C., Gomes, R., & Karess, R. (2004) In Vivo Dynamics of the Rough Deal Checkpoint Protein during *Drosophila* Mitosis. *Current Biology, 14* (1), 56–61. DOI: 10.1016/j.cub.2003.12.025.

Bonaccorsi, S., Giansanti, M.G., & Gatti, M. (1998) Spindle self-organization and cytokinesis during male meiosis in *asterless* mutants of *Drosophila melanogaster*. *The Journal of Cell Biology, 142,* 751-761. DOI: 10.1083/jcb.142.3.751.

Bonaccorsi, S., Giansanti, M.G., Cenci, G., & Gatti, M. (2000) Cytological analysis of spermatocyte growth and male meiosis in *Drosophila melanogaster*. In *Drosophila Protocols* (ed. W. Sullivan, M. Ashburner and R. S. Hawley), pp. 87-97. Cold Spring Harbor, NY: Cold Spring Harbor Laboratory Press.

Buffin, E., Lefebvre, C., Huang, J., Gagou, M. E., & Karess, R. E. (2005) Recruitment of Mad2 to the kinetochore requires the Rod/Zw10 complex. *Current Biology, 15* (9), 856–61. DOI: 10.1016/j.cub.2005.03.052.

Carmena, M., Pinson, X., Platani, M., Salloum, Z., Xu, Z., Clark, A., Earnshaw, W. C., et al. (2012a) The chromosomal passenger complex activates Polo kinase at centromeres. *PLoS Biology, 10* (1), e1001250. DOI: 10.1371/journal.pbio.1001250.

Carmena, M., Riparbelli, M.G., Minestrini, G., Tavares, Á.M., Adams, R., Callaini, G., & Glover, D. M. (1998) Polo Kinase Is Required for Cytokinesis. *The Journal of Cell Biology*, *143* (3), 659–671. DOI: 10.1083/jcb.143.3.659.

Carmena, M., Wheelock, M., Funabiki, H., & Earnshaw, W.C. (2012b) The chromosomal passenger complex (CPC): from easy rider to the godfather of mitosis. *Nature Reviews Molecular Cell Biology*, *13* (12), 789-803. DOI: 10.1038/nrm3474.

Cesario, J.M., Jang, J.K., Redding, B., Shah, N., Rahman, T., & McKim, K.S. (2006) Kinesin 6 family member Subito participates in mitotic spindle assembly and interacts with mitotic regulators. *Journal of Cell Science*, *119* (22), 4770–80. DOI: 10.1242/jcs.03235.

Cheeseman, I.M., Chappie, J.S., Wilson-Kubalek, E.M., & Desai, A. (2006) The conserved KMN network constitutes the core MT-binding site of the kinetochore. *Cell, 127* (5), 983–97. DOI: 10.1016/j.cell.2006.09.039.

Dean, S.O., & Spudich, J. A. (2006) Rho kinase's role in myosin recruitment to the equatorial cortex of mitotic *Drosophila* S2 cells is for myosin regulatory light chain phosphorylation. *PloS One, 1* (1), e131. DOI: 10.1371/journal.pone.0000131.

Dean, S.O., Rogers, S.L., Stuurman, N., Vale, R.D., & Spudich, J.A. (2005) Distinct pathways control recruitment and maintenance of myosin II at the cleavage furrow during cytokinesis. *Proceedings of the National Academy of Sciences of the United States of America, 102* (38), 13473–8. DOI: 10.1073/pnas.0506810102.

Douglas, M.E., Davies, T., Joseph, N., & Mishima, M. (2010) Aurora B and 14-3-3 coordinately regulate clustering of centralspindlin during cytokinesis. *Current Biology, 20* (10), 927–33. DOI: 10.1016/j.cub.2010.03.055.

Duncan, T. (2011). Investigating the function of *Drosophila* MAPs Msd1 and dTD-60 in mitotic spindle assembly. DPhil. University of Oxford.

Duncan, T., & Wakefield, J.G. (2011) 50 ways to build a spindle: the complexity of MT generation during mitosis. *Chromosome Research, 19,* 321-333. DOI: 10.1007/s10577-011-9205-8.

Echard, A., Hickson, G.R.X., Foley, E., Farrell, P.H.O., Francisco, S., & Recherche, M. De. (2004) Terminal Cytokinesis Events Uncovered after an RNAi Screen. *Current Biology, 14,* 1685–1693. DOI: 10.1016/j.cub.2004.08.063.

Forer, A., & Pickett-Heaps, J. (1998) Cytochalasin D and latrunculin affect chromosome behaviour during meiosis in crane-fly spermatocytes. *Chromosome Research, 6* (7), 533-550. DOI: http://dx.doi.org/10.1023/A:1009224322399.

Forer, A., & Pickett-Heaps, J. (2005) Fibrin clots keep non-adhering living cells in place on glass for perfusion or fixation. *Cell Biology International*, *29* (9), 721–30. DOI: 10.1016/j.cellbi.2005.04.010.

Fortini, M.E., Skupski, M.P., Boguski, M.S., & Hariharan, I.K. (2000) A survey of human disease gene counterparts in the *Drosophila* genome. *The Journal of Cell Biology, 150,* 23-30. DOI: 10.1083/jcb.150.2.F23.

Fujiwara, T., Bandi, M., Nitta, M., Ivanova, E.V, Bronson, R.T., & Pellman, D. (2005) Cytokinesis failure generating tetraploids promotes tumorigenesis in p53-null cells. *Nature*, *437* (7061), 1043–7. DOI: 10.1038/nature04217.

Gao, S., Giansanti, M.G., Buttrick, G.J., Ramasubramanyan, S., Auton, A., Gatti, M., & Wakefield, J.G. (2008) Australin: a chromosomal passenger protein required specifically for *Drosophila melanogaster* male meiosis. *The Journal of Cell Biology*, *180* (3), 521–35. DOI: 10.1083/jcb.200708072.

Gassmann, R., Carvalho, A., Henzing, A.J., Ruchaud, S., Hudson, D.F., Honda, R., Nigg, E.A., et al. (2004) Borealin: a novel chromosomal passenger required for stability of the bipolar mitotic spindle. *The Journal of Cell Biology*, *166* (2), 179–91. DOI: 10.1083/jcb.200404001.

Gatti, M., Giansanti, M.G., & Bonaccorsi, S. (2000) Relationships between the central spindle and the contractile ring during cytokinesis in animal cells. *Microscopy Research and Technique, 49* (2), 202–8.

Giansanti, M.G., Bucciarelli, E., Bonaccorsi, S., & Gatti, M. (2008) *Drosophila* SPD-2 is an essential centriole component required for PCM recruitment and astral-MT nucleation. *Current Biology, 18* (4), 303–9. DOI: 10.1016/j.cub.2008.01.058.

Giansanti, M.G., Bonaccorsi, S., Bucciarelli, E., & Gatti, M. (2001) *Drosophila* male meiosis as a model system for the study of cytokinesis in animal cells. *Cell Structure and Function, 26,* 609-617. DOI: 10.1247/csf.26.609.

Giansanti, M.G., Bonaccorsi, S., Williams, B., Williams, E.V., Santolamazza, C., Goldberg, M.L., & Gatti, M. (1998) Cooperative interactions between the central spindle and the contractile ring during *Drosophila* cytokinesis. *Genes & Development, 12,* 396-410.

Giansanti, M.G., Farkas, R.M., Bonaccorsi, S., Lindsley, D.L., Wakimoto, B.T., Fuller, M.T., & Gatti, M. (2004) Genetic dissection of meiotic cytokinesis in *Drosophila* males*. Molecular Biology of the Cell, 15,* 2509–2522. DOI: 10.1091/mbc.E03-08-0603.

Giet, R., & Glover, D.M. (2001) *Drosophila* aurora B kinase is required for histone H3 phosphorylation and condensin recruitment during chromosome condensation and to organize the central spindle during cytokinesis. *The Journal of Cell Biology, 152* (4), 669–82.

Glotzer, M. (2009) The 3Ms of central spindle assembly: MTs, motors and MAPs. *Nature Reviews Molecular Cell Biology, 10,* 9-20. DOI: 10.1038/nrm2609.

Goshima, G., Mayer, M., Zhang, N., Stuurman, N., & Vale, R.D. (2008) Augmin: a protein complex required for centrosome-independent MT generation within the spindle. *The Journal of Cell Biology, 181,* 421-429. DOI: 10.1083/jcb.200711053.

Goshima, G., Wollman, R., Goodwin, S.S., Zhang, N., Scholey, J.M., Vale, R.D., & Stuurman, N. (2007) Genes required for mitotic spindle assembly in *Drosophila* S2 cells. *Science*, *316,* 417-421. DOI: 10.1126/science.1141314.

Greenspan, R.J. (2004) *Fly Pushing: The theory and practice of Drosophila genetics*. 2nd edn. New York: Cold Spring Harbor.

Griffis, E.R., Stuurman, N., & Vale, R.D. (2007) Spindly, a novel protein essential for silencing the spindle assembly checkpoint, recruits dynein to the kinetochore. *The Journal of Cell Biology, 177* (6), 1005–15. DOI: 10.1083/jcb.200702062.

Gruneberg, U., Neef, R., Honda, R., Nigg, E.A., & Barr, F.A. (2004) Relocation of Aurora B from centromeres to the central spindle at the metaphase to anaphase transition requires MKlp2. *The Journal of Cell Biology, 166* (2), 167–72. DOI: 10.1083/jcb.200403084.

Gruss, O.J., Carazo-Salas, R.E., Schatz, C.A, Guarguaglini, G., Kast, J., Wilm, M., & Mattaj, I.W. (2001) Ran induces spindle assembly by reversing the inhibitory effect of importin alpha on TPX2 activity. *Cell, 104* (1), 83–93.

Guse, A., Mishima, M., & Glotzer, M. (2005) Phosphorylation of ZEN-4/MKLP1 by aurora B regulates completion of cytokinesis. *Current Biology, 15* (8), 778–86. DOI: 10.1016/j.cub.2005.03.041.

Hales, K.G., & Fuller, M.T. (1997) Developmentally regulated mitochondrial fusion mediated by a conserved, novel, predicted GTPase. *Cell, 90,* 121-129. DOI: 10.1016/S0092-8674(00)80319-0.

Handler, D., Olivieri, D., Novatchkova, M., Gruber, F.S., Meixner, K., Mechtler, K., & Brennecke, J. (2011) A systematic analysis of Drosophila TUDOR domain-containing proteins identifies Vreteno and the Tdrd12 family as essential primary piRNA pathway factors. *The EMBO Journal, 30* (19), 3977–93. DOI: 10.1038/emboj.2011.308.

Hardwicke, M.A., Oleykowski, C.A, Plant, R., Wang, J., Liao, Q., Moss, K., & Patrick, D. (2009) GSK1070916, a potent Aurora B/C kinase inhibitor with broad antitumor activity in tissue culture cells and human tumor xenograft models. *Molecular Cancer Therapeutics, 8* (7), 1808–17. DOI: 10.1158/1535-7163.MCT-09-0041.

Hayward, D. (2014) The spindle assembly pathways of the *Drosophila* syncytial embryo. PhD thesis, University of Exeter.

Hayward, D., Metz, J., Pellacani, C., & Wakefield, J.G. (2014) Synergy between Multiple MT-Generating Pathways Confers Robustness to Centrosome-Driven Mitotic Spindle Formation. *Developmental Cell, 28* (1), 81–93. DOI: http://dx.doi.org/10.1016/j.devcel.2013.12.001.

Hickson, G.R.X., Echard, A., & O'Farrell, P.H. (2006) Rho-kinase controls cell shape changes during cytokinesis*. Current Biology, 16* (4), 359–70. DOI: 10.1016/j.cub.2005.12.043.

Inoue, Y.H., Savoian, M.S., Suzuki, T., Mathe, E., Yamamoto, M.T., & Glover, D.M. (2004) Mutations in orbit/mast reveal that the central spindle is comprised of two MT populations, those that initiate cleavage and those that propagate furrow ingression. *The Journal of Cell Biology, 166*, 49-60. DOI: 10.1083/jcb.200402052.

Jang, J.K., Rahman, T., & Mckim, K.S. (2005) The Kinesin like Protein Subito Contributes to Central Spindle Assembly and Organization of the Meiotic Spindle in *Drosophila* Oocytes. *Molecular Biology of the Cell*, *16,* 4684–4694. DOI: 10.1091/mbc.E04.

Jang, J.K., Rahman, T., Kober, V.S., Cesario, J., & McKim, K.S. (2007) Misregulation of the kinesin-like protein Subito induces meiotic spindle formation in the absence of chromosomes and centrosomes. *Genetics, 177* (1), 267–80. DOI: 10.1534/genetics.107.076091.

Jensen, L.J., Kuhn, M., Stark, M., Chaffron, S., Creevey, C., Muller, J., & Von Mering, C. (2009) STRING 8--a global view on proteins and their functional interactions in 630 organisms. *Nucleic Acids Research*, *37*, D412–6. DOI: 10.1093/nar/gkn760.

Job, D., Valiron, O., & Oakley, B. (2003) MT nucleation. *Current Opinion in Cell Biology, 15,* 111-117. DOI: 10.1016/S0955-0674(02)00003-0.

Kallio, M.J., McCleland, M.L., Stukenberg, P.T., & Gorbsky, G.J. (2002) Inhibition of aurora B kinase blocks chromosome segregation, overrides the spindle checkpoint, and perturbs MT dynamics in mitosis. *Current Biology*, *12* (11), 900–5.

Karess, R. (2005) Rod-Zw10-Zwilch: a key player in the spindle checkpoint. *Trends in Cell Biology, 15* (7), 386–92. DOI: 10.1016/j.tcb.2005.05.003.

Kerssemakers, J.W.J., Munteanu, E.L., Laan, L., Noetzel, T.L., Janson, M.E., & Dogterom, M. (2006) Assembly dynamics of MTs at molecular resolution. *Nature, 442*, 709-712. DOI: 10.1038/nature04928.

Kline-Smith, S.L., & Walczak, C.E. (2002) The MT-destabilizing kinesin XKCM1 regulates MT dynamic instability in cells. *Molecular Biology of the Cell, 13*, 2718-2731. DOI: 10.1091/mbc.E01-12-0143.

Laflamme, C., Assaker, G., Ramel, D., Dorn, J.F., She, D., Maddox, P.S., & Emery, G. (2012) Evi5 promotes collective cell migration through its Rab-GAP activity*. The Journal of Cell Biology, 198* (1), 57-67.

Li, J.J., & Li, S.A. (2006) Mitotic kinases: The key to duplication, segregation, and cytokinesis errors, chromosomal instability, and oncogenesis. *Pharmacology & Therapeutics, 111*, 974-984. DOI:10.1016/j.pharmthera.2006.02.006.

Liddell, S., & Bownes, M. (1991) Characterization, molecular cloning and sequencing of YP3s1, a fertile yolk protein 3 mutant in *Drosophila*. *Molecular Genetics and Genomics, 228* (1-2):81-8.

Maiato, H., Sampaio, P., Lemos, C.L., Findlay, J., Carmena, M., Earnshaw, W.G., & Sunkel, C.E. (2002) MAST/orbit has a role in MT-kinetochore attachment and is essential for chromosome alignment and maintenance of spindle bipolarity. *The Journal of Cell Biology*, *157*, 749-760. DOI: 10.1083/jcb.200201101.

Mandelkow, E., & Mandelkow, E-M. (1995) MTs and MT-associated proteins. *Current Opinion in Cell Biology*, *7*, 72-81. DOI: 10.1016/0955 0674(95)80047-6.

Martineau-Thuillier, S., Andreassen, P.R., & Margolis, R.L. (1998) Colocalization of TD-60 and INCENP throughout G2 and mitosis: evidence for their possible interaction in signalling cytokinesis. *Chromosoma, 107* (6-7), 461–70.

McKee, B.D., Yan, R., & Tsai, J.H. (2012) Meiosis in male *Drosophila*. *Spermatogenesis, 2* (3), 167–184. DOI:10.4161/spmg.21800.

Mitchison, T., & Kirschner, M. (1984) Dynamic instability of MT growth. *Nature, 312*, 237-242. DOI: 10.1038/312237a0.

Mollinari, C., Reynaud, C., Martineau-Thuillier, S., Monier, S., Kieffer, S., Garin, J., Andreassen, P. R., et al. (2003) The mammalian passenger protein TD-60 is an RCC1 family member with an essential role in prometaphase to metaphase progression. *Developmental Cell, 5* (2), 295–307.

Mosby's Medical Dictionary, 8th edition, (2009) Elsevier.

Müller, H., Schmidt, D., Steinbrink, S., Mirgorodskaya, E., Lehmann, V., Habermann, K., & Lange, B.M H. (2010) Proteomic and functional analysis of the mitotic *Drosophila* centrosome. *The EMBO Journal, 29* (19), 3344–57. DOI: 10.1038/emboj.2010.210.

Reis, R., Feijão, T., Gouveia, S., Pereira, A.J., Matos, I., Sampaio, P., & Sunkel, C.E. (2009) Dynein and mast/orbit/CLASP have antagonistic roles in regulating kinetochore-MT plus-end dynamics. *Journal of Cell Science, 122* (14), 2543–53. DOI: 10.1242/jcs.044818.

Rosasco-Nitcher, S.E., Lan, W., Khorasanizadeh, S., & Stukenberg, P.T. (2008) Centromeric Aurora-B activation requires TD-60, MTs, and substrate priming phosphorylation. *Science*, *319* (5862), 469–72. DOI: 10.1126/science.1148980.

Ruchaud, S., Carmena, M., & Earnshaw, W.C. (2007) Chromosomal passengers: conducting cell division. *Nature Reviews Molecular Cell Biology*, *8* (10), 798–812. DOI: 10.1038/nrm2257.

Salmon, E.D., Leslie, R.J., Saxton, W.M., Karow. M.L., & McIntosh, J.R. (1984) Spindle MT dynamics in sea urchin embryos: analysis using a fluorescein-labeled tubulin and measurements of fluorescence redistribution after laser photobleaching. *The Journal of Cell Biology, 99,* 2165-74.

Sampath, S.C., Ohi, R., Leismann, O., Salic, A., Pozniakovski, A., & Funabiki, H. (2004) The chromosomal passenger complex is required for chromatin-induced MT stabilization and spindle assembly. *Cell, 118* (2), 187–202. DOI: 10.1016/j.cell.2004.06.026.

Saul, D., Fabian, L., Forer, A., & Brill, J.A. (2004) Continuous phosphatidylinositol metabolism is required for cleavage of crane fly spermatocytes. *Journal of Cell Science*, *117* (17), 3887–96. DOI: 10.1242/jcs.01236.

Saxton, W.M. & McIntosh, J.R. (1987) Interzone MT behavior in late anaphase and telophase spindles. *The Journal of Cell Biology, 105,* 875-886.

Saxton, W.M., Stemple, D.L., Leslie, R.J., Salmon, E.D., Zavortink, M., & McIntosh, J.R. (1984) Tubulin dynamics in cultured mammalian cells. *The Journal of Cell Biology, 99*, 2175-86.

Scaërou, F., Starr, D.A, Piano, F., Papoulas, O., Karess, R.E., & Goldberg, M.L. (2001) The ZW10 and Rough Deal checkpoint proteins function together in a large, evolutionarily conserved complex targeted to the kinetochore. *Journal of Cell Science, 114* (17), 3103–14.

Steigemann, P., Wurzenberger, C., Schmitz, M.H.A, Held, M., Guizetti, J., Maar, S., & Gerlich, D.W. (2009) Aurora B-mediated abscission checkpoint protects against tetraploidization. *Cell, 136* (3), 473–84. DOI: 10.1016/j.cell.2008.12.020.

Szafer-Glusman, E., Fuller, M.T., & Giansanti, M.G. (2011) Role of Survivin in cytokinesis revealed by a separation-of-function allele. *Molecular Biology of the Cell, 22* (20), 3779–90. DOI:10.1091/mbc.E11-06-0569.

Terada, Y., Tatsuka, M., Suzuki, F., Yasuda, Y., Fujita, S., & Otsu, M. (1998) AIM-1: a mammalian midbody-associated protein required for cytokinesis. *The EMBO Journal*, *17* (3), 667–76. DOI: 10.1093/emboj/17.3.667.

Tulu, U.S., Fagerstrom, C., Ferenz, N.P., & Wadsworth, P. (2006) Molecular requirements for kinetochore-associated microtubule formation in mammalian cells. *Current Biology, 16* (5): 536–541. DOI: 10.1016/j.cub.2006.01.060.

Uehara, R., Nozawa, R.S., Tomioka, A., Petry, S., Vale, R.D., Obuse, C., & Goshima, G. (2009) The augmin complex plays a critical role in spindle MT generation for mitotic progression and cytokinesis in human cells. *Proceedings of the National Academy of Sciences of the United States of America, 106*, 6998-7003. DOI: 10.1073/pnas.0901587106.

Vagnarelli, P., & Earnshaw, W.C. (2004) Chromosomal passengers: the four-dimensional regulation of mitotic events. *Chromosoma*, *113* (5), 211–22. DOI: 10.1007/s00412-004-0307-3.

Von Mering, C., Jensen, L. J., Snel, B., Hooper, S.D., Krupp, M., Foglierini, M., & Bork, P. (2005) STRING: known and predicted protein-protein associations, integrated and transferred across organisms. *Nucleic Acids Research, 33*, D433–7. DOI: 10.1093/nar/gki005.

Wittmann, T., Hyman, A., & Desai, A. (2001) The spindle: a dynamic assembly of MTs and motors. *Nature Cell Biology, 3,* E28-34. DOI: 10.1038/35050669.

Yang, J., Ikezoe, T., Nishioka, C., Tasaka, T., Taniguchi, A., Kuwayama, Y., & Yokoyama, A. (2007) AZD1152, a novel and selective aurora B kinase inhibitor, induces growth arrest, apoptosis, and sensitization for tubulin depolymerizing agent or topoisomerase II inhibitor in human acute leukemia cells in vitro and in vivo. *Blood, 110* (6), 2034–40. DOI: 10.1182/blood-2007-02-073700.

Zhao, W., & Fang, G. (2005) MgcRacGAP controls the assembly of the contractile ring and the initiation of cytokinesis. *Proceedings of the National Academy of Sciences of the United States of America, 102* (37), 13158–63. DOI: 10.1073/pnas.0504145102.